

**MODELLING THE POTENTIAL IMPACTS OF CLIMATE CHANGE
AND VARIABILITY ON ELECTRICITY DEMAND IN REPUBLIC
OF NIGER**

BY

Bonkaney, Abdou Latif

MET/15/5744

September, 2019

**MODELLING THE POTENTIAL IMPACTS OF CLIMATE CHANGE
AND VARIABILITY ON ELECTRICITY DEMAND IN REPUBLIC
OF NIGER**

BY

**Bonkaney, Abdou Latif
BSc, MSc, (MET/15/5744)**

A Thesis in the Department of Meteorology and Climate Science, School of Earth and Mineral Science in partnership with the West African Science Service Centre on Climate Change and Adapted Land Use (WASCAL) submitted to the School of Postgraduate Studies in partial fulfillment of the requirements for the award of Doctor of Philosophy in Meteorology of the Federal University of Technology, Akure, Nigeria.

September, 2019

DECLARATION

I hereby declare that this Thesis was written by me and is a correct record of my own research work. It has not been presented in any previous application for any degree of this or any other University. All citations or sources of information are clearly acknowledged by means of references.

Candidate's Name:

Bonkaney, Abdou Latif

Signature

Date

CERTIFICATION

We certify that this Thesis entitled “Modelling the Potential Impacts of Climate Change and Variability on Electricity Demand in Republic of Niger” is the outcome of the research carried out by Bonkaney, Abdou Latif in the Department of Meteorology and Climate Science, The Federal University of Technology, Akure.

Major Supervisor’s Name:

Prof. A. A. Balogun

Signature

Date

Co-Supervisor’s Name:

Dr. I. S. Sanda

Signature

Date

Advisor’s Name:

Prof B.J. Abiodun

Signature

Date

ACKNOWLEDGMENT

This PhD programme is fully sponsored by The German Ministry of Education and Research (BMBF) through the West African Science Centre on Climate Change and Adapted Land Use (WASCAL). I am therefore thankful to BMBF and WASCAL for providing the full financial support during this programme. I would also like to express my sincere gratitude to the Executive Director, Dr M. Savadogo and the staff of the WASCAL Headquarter in Accra, Ghana, and the Director, Prof K.O. Ogunjobi and the staff of the WASCAL DRP-WACS, FUTA, Nigeria for their efforts in making this programme a success. My thanks also go Prof J.A. Omotosho, the first Director of the programme for encouragement throughout the study period.

I am sincerely grateful to Prof A.A. Balogun, Head, Department of Meteorology and Climate Science, FUTA, Nigeria, for supervising this work. He was also kind enough and available to guide and undertake the editing work despite of his busy timetable, and I acknowledge and appreciate his efforts. Thank you Sir. I am also grateful to Dr I. Seidou Sanda for co-supervising this work. He has always made himself available to clarify my doubts despite his busy schedules, and also helped to get most of the data used in this study. I sincerely appreciate his efforts and contributions.

I am also grateful to the staff of the Department of Meteorology and Climate Science, FUTA, Nigeria for their cooperation. Special thanks to Dr V.O. Vincent, Dr A. Akinbobola, Dr I.A. Balogun, Dr A. Oluleye and Dr E.A Adefisan.

I am extremely grateful to Prof B.J. Abiodun for guiding this work at University of Cape Town despite of his busy schedule. His contributions have been determinant in achieving

most of the objectives of this work. I am also grateful to all the CSAG staff at UCT, especially Mr P. Mukwhena, Romaric O., Sabina Abba Omar, Myra Naik, Mariam Nguvava, and Koketso Molepo for their availability and assistance.

Mr regards also go to the AGRHYMET Regional Centre (CRA) of Niamey for accommodating me for 12 months and giving me access to their HPC. My research work greatly benefited for the short time spent there.

Mr regards also go to my fellow WASCAL comrades, mainly to those in the third batch of the DRP-WACS: Akamah Kokouvi Abel, Sawadogo Windmanagda, Ballo Abdoulaye, Kumi Naomi, Faye, Aissatou, Dajuma, Alima, Quenum Mayeul, Gbode I., and Achugbu, I for the shared moment, memories and frustrations. I have gained a lot from them, through their personal and scholarly interactions and their suggestions at various points of my research programme.

My family has been a pillar of this work and constant source of inspiration. Special thanks to my mother, Hassane Hourey, my father Bonkaney, Issaka and my brothers, Usama, Zourkaleini and Moubarak, and my sister Amoudiyatou for their encouragements, support, and best wishes.

Above this, I owe it all to the ALLAH Soubhanahou Wa Tahala for granting me wisdom, health, and the strength to undertake this research and enabling me to its completion.

DEDICATION

This Thesis is dedicated:

To my family for their sincere love;

To my friends and colleagues for their support and encouragement;

In Memory of Late Prof. A. ABDOULAYE, the former director of WASCAL MRP-CCE,
whose knowledge I have gained from. May your soul rest in peace and happiness in
Paradise. Amine.

ABSTRACT

This study investigates the potential impact of climate change and variability on electricity demand under different Global Warming Levels (GWL1.5, GWL2.0, GWL2.5, and GWL3.0). First, to assess the sensitivity of electricity demand to climate variables, the Wavelet Transform Coherence (WTC) as well as Principal Component Analysis (PCA) were used. Secondly, to establish the relationship between electricity demand and climate variables, Multiple Linear Regression (MLR) and Artificial Neural Network (ANN) models have been used. Prior to the model development, the electricity demand data was de-trended to isolate only the influence of climate variables. Thirdly, to project the impact of climate change at specific GWL, the climate data from the reference period (1971-2000) was subtracted from that of GWL period. Results show that the electricity demand (DED) in Niger is positively correlated to Temperatures (T_{mean} , T_{max} , T_{min}), Cooling Degree-Days (CDD), and Heat Index (HI) and negatively correlated with Wind Speed (WSP) and Solar Radiation (SR). However, the electricity demand is more sensitive to temperatures, CDD, HI than SR and WSP. The regression models are able to adequately predict the electricity demand with a high coefficient of determination R^2 (>0.8) and a relatively low Root Mean Square Error ($\text{RMSE} < 150 \text{MWh/day}$). In addition, the residual analysis reveals that the models comply with the basics assumptions of regression models. Furthermore, the results also show that the CORDEX simulations give a realistic representation of all the necessary climate variables used to model the electricity demand in Niger. The simulations project a robust increase in electricity demand at all the GWLs over Niger and indicate that the magnitude of the projection grows with increasing GWLs. Indeed, an increase of 4-16% of DED is projected depending on the magnitude of the warming. It is also worth noting that

the magnitude of changes also differs with season, with the highest increase observed in March-May (MAM) and June-August (JJA) while December-February (DJF) displayed the lowest increase. For instance, the Regional Climate Models (RCMs) ensemble median project an increase of about 18% increase in DED for MAM and JJA while for DJF season, it only projects about 5% increase at GWL3.0. In addition to the increase in mean DED, simulations also project an increase in extreme electricity demand due to the increase of extreme temperatures and heatwaves over the country at all the GWLs. The study showed that climate change will affect both mean and peak DED at all the GWLs, with the magnitude of change growing with increasing GWLs. However, the study suggests the investigation of the roles of other factors to further the research, such as population change, future energy policy, urbanization, and economic growth that may also determine the future electricity demand for more robust projections.

RESUME

Cette étude examine l'impact potentiel du changement climatique et de la variabilité sur la demande d'électricité selon différents niveaux de réchauffement de la planète (NRP1.5, NRP2.0, NRP2.5 et NRP3.0). Tout d'abord, pour évaluer la sensibilité de la demande d'électricité aux variables climatiques, on a utilisé la transformée cohérente en ondelettes (TCO) et l'analyse en composantes principales (ACP). Deuxièmement, pour établir la relation entre la demande d'électricité et les variables climatiques, des modèles de régression linéaire multiple (RLM) et de réseau de neurones artificiels (RNA) ont été utilisés. Avant le développement du modèle, la tendance croissante de la demande en électricité due aux développements socio-économiques a été supprimée pour isoler les impacts des variables climatiques. Troisièmement, pour projeter l'impact du changement climatique pour un NRP spécifique, les données climatiques de la période de référence (1971-2000) ont été soustraites de celles de la période du NRP. Les résultats montrent que la demande en électricité au Niger est positivement corrélée aux températures (T_{mean} , T_{min} , et T_{max}), aux degrés-jours de refroidissement (DJR) et à l'indice de chaleur (IC) et en corrélation négative à la vitesse du vent (VV) et au rayonnement solaire (RS). Cependant, la demande en électricité est plus sensible aux températures, DJR, IC que RS et VV. Les modèles de régression permettent de prédire de manière adéquate la demande en électricité avec un coefficient de détermination élevé $R^2 (> 0,8)$ et une erreur quadratique moyenne relativement faible ($\text{RMSE} < 150 \text{ MWh / jour}$). En outre, l'analyse des résidus révèle que les modèles sont conformes aux hypothèses de base des modèles de régression. De plus, les résultats montrent également que les simulations CORDEX donnent une représentation

réaliste de toutes les variables climatiques nécessaires pour modéliser la demande en électricité au Niger. Les simulations prévoient une forte augmentation de la demande en électricité pour tous les NRP au Niger et indiquent que l'ampleur de la projection augmente avec l'augmentation des NRP. En effet, une augmentation de 4 à 16% de la demande en électricité est projetée en fonction de l'ampleur du réchauffement. Il convient également de noter que l'ampleur des changements diffère également d'une saison à l'autre. L'augmentation la plus forte a été observée en Mars-Mai (MAM) et en Juin-Août (JJA), tandis que celle de Décembre-Février (DJF) a été la plus faible. Par exemple, la médiane de l'ensemble des modèles climatiques régionaux (MCR) prévoit une augmentation d'environ 18% de la demande pour MAM et JJA, tandis que pour la saison DJF, elle ne prévoit qu'une augmentation d'environ 5% pour le NRP3.0. Outre l'augmentation de l'électricité moyenne, les simulations prévoient également une augmentation de la demande extrême en électricité en raison de l'augmentation des températures extrêmes et des vagues de chaleur sur le pays, pour tous les NRP. L'étude a conclu que le changement climatique affectera à la fois la demande moyenne et extrême pour tous les NRP, l'ampleur du changement augmentant avec l'augmentation des NRP. Cependant, l'étude suggère d'utiliser d'autres facteurs qui pourraient également déterminer la demande future en électricité pour des projections plus robustes.

TABLE OF CONTENTS

DECLARATION	i
CERTIFICATION	ii
ACKNOWLEDGMENT	iii
DEDICATION	v
ABSTRACT	vi
RESUME	viii
TABLE OF CONTENTS	x
LIST OF TABLES	xiv
LIST OF FIGURES	xv
ACRONYMS	xix
CHAPTER ONE	1
INTRODUCTION	1
1.1 Introduction	1
1.2 Background to the Study	2
1.2.1.....Energy situation in West Africa	7
1.2.2.....Current and Future Energy Situation in Niger	10

1.2.3.....Climate Driven Electricity Consumption	15
1.3 Justification of the Study	16
1.4 Research Questions	17
1.5 Aim and Objectives	18
1.6 Thesis Structure	19
CHAPTER TWO	20
LITERATURE REVIEW	20
2.1. Introduction	20
2.2 Energy Climate Nexus	20
2.2.1 Definitions Degree Days (DD)	21
2.2.2 Definitions of Extreme Climate Events	25
2.2.3 Heat Waves Events	26
2.2.4 Temperature Humidity Indices	28
2.3 West African Climate System	28
2.4 Overview of Statistical forecasting models used to predict the electricity based on climate variables	30
2.4.1 Multiple Linear Regression (MLR) Model	32
2.4.2 Machines Learning Techniques	33
2.5 Global and Regional Climate Models	37
2.5.1 Emissions Scenarios used as input to GCMs	37

2.5.2 Statistical Downscaling Techniques	39
2.5.3 Dynamical Downscaling Techniques	44
CHAPTER THREE	46
RESEARCH METHODOLOGY	46
3.1 Introduction	46
3.2 Study Area	46
3.3 Data and Methods	48
3.3.1 Electricity Data	48
3.3.2 Climate Data	51
3.3.3 Calculation of Degree Days (DD)	55
3.3.4 Calculation of Heat Indices	57
3.3.5 Extreme Temperature and Heat Waves Characteristics and Measurements	57
3.3.6 Relationship between the Electricity Demand and Climate Variables	59
3.3.7 Modelling the Influence of Climate on Electricity Demand	62
3.3.8 Predicting the Impact of Climate Change on Electricity Demand	63
CHAPTER FOUR	65
RESULTS AND DISCUSSIONS	65
4.1 Introduction	65
4.2 Relationship Between Electricity Demand and Climate Variables	65

4.2.1 Seasonal fluctuations of Electricity demand in Niger	65
4.2.2 Correlation between Electricity demand and Climate Variables	72
4.3 Modelling the Influence of Climate Variables on Electricity Demand	76
4.3.1 Selection of Independent Variables	76
4.3.2 Evaluation of Regression Models	79
4.4 Evaluation of CORDEX RCMs Simulations	86
4.5 Future Projection of Daily Electricity Demand and Different Predictors	92
4.5.1 Mean Changes in Daily Electricity Demand and Relevant Predictors at specific Global Warming Levels	92
4.5.2 Seasonal Changes in DED, CDD and HI	97
4.5.3 Temporal Pattern of Changes in Predictors	105
4.5.4 Projected Changes in near (2021-2050) and far (2070-2099) future	107
4.6 Influence of Extreme Heat and Heat waves on Electricity Demand	114
4.6.1 Influence of Extreme Temperatures on Peak Electricity Demand	114
4.6.2 Projected Changes of Climate Change on Heat Waves Characteristics	117
CHAPTER FIVE	121
CONCLUSIONS AND RECOMMENDATIONS	121
5.1 CONCLUSIONS	121
5.2 RECOMMENDATIONS	124
REFERENCES	126

LIST OF TABLES

Title	Page
2.1 Base Temperature Values used in Selected Studies the list is not Exhaustive)	23
2.2 Summary of Selected Studies That Used Machine learning Techniques to Predict The Electricity Consumption	36
2.3 Summary of Selected Studies that Have used The Morphing Methods	41
3.1 Average Annual Climate Variables (2015) and Electricity Consumption of Selected Cities used in this study	50
3.2 Names of GCMs and Downscaled RCMs Used	54
3.3 Phase Differences and Their Interpretations	61
4.1 Principal Components Analysis Loadings of Climate Variables and Electricity Demand	77
4.2 Correlation Between Electricity Demand and Climate Variables	78
4.3 Regression Statistics of the Five Models Considered in This Study	80
4.4 Regressions Coefficients and Their Corresponding P-Values	85

LIST OF FIGURES

	Title	Page
1.1	Global Greenhouse Gas Emissions by sector	5
1.2	Green House Gases Emissions by Sector for Different Economies in the World	6
1.3	Electricity Access Rate (in %) of West African Countries for 1990, 2000 and 2010	9
1.4	Times Series Evolution of Electricity Consumption and GDP per capita From 1992 to 2016 in Niger	11
1.5	Percentage of Population having Access to Electricity in Rural (blue) and Urban are in Niger from 1990-2016 (data from the World Bank)	14
2.1	Artificial Neural Networks Structure	35
3.1	West African Domain Showing the Study Area (Red Box)	47
3.2	Time Series Evolution of Monthly Electricity Consumption for the Main Cities in Niger	49
3.3	Time Series Evolution of Monthly Electricity Consumption for the Main Cities in Niger after De-trending	50
3.4	Scatter of Temperature Against Electricity Demand. The red curve Shows the Best Fit and R is Correlation	56
4.1	Seasonal Variation Index of Electricity Demand	67
4.2	Weekly Variation Index of Daily Electricity Demand	69
4.3	Diurnal variation Index of Electricity Load for Different Season; DJF: December January February, MAM: March April May, SON: September	

	October November, Annual: January-December	71
4.4	WTC and Phase Difference of Climate Variables & DED. The 5% Significance level against red noise is shown as a thick contour. The relative phase Relationship is shown as arrows (with in-phase pointing right, anti-phase Pointing left)	75
4.5	Validation of Regression Models using (a): time series plot of observed and Predicted values, (b): Coefficient of Variation and (c): Taylor Diagram	81
4.6	Scatter Plots of Actual Against Predicted Values for (a): MLR, (b): ANN(4,2,1), (c): ANN(4,4,1), (d): ANN(4, (2,1),1), and (e): ANN(4,(3,2),1)	82
4.7	Scatter plots of Standardized Residuals Against Predicted Values (Left Panel) And the Histogram of the Standardized Residuals (Right Panel)for Different Regression Models	84
4.8	Spatial Distribution of Climate Variables over Niger as Depicted by PGFD And CORDEX RCMs Ensemble Mean in Reference period (1971-2000). r Denotes the Spatial Correlation and Asterisk (*) Denotes Significance at 99% Confidence Level	89
4.9	Spatial Distribution of Climate Variables over Niger as Depicted by PGFD And CORDEX RCMs Ensemble Mean in Reference period (1971-2000). r Denotes the Spatial Correlation and Asterisk (*) Denotes Significant at 95% Confidence Level.	90
4.10	Annual Cycle of Daily Energy Demand and the Relevant Climate Variables Used to Build the Multiple Linear Regression Model in Niamey as Depicted By Observation and CORDEX RCMs	91
4.11	Projected Changes in DED (panel: a-d), CDD (e-h), RH (i-l), Radiation (m-p)	

	(m-p), and Wind (q-t) at different global Warming Level (GWL1.5, GWL2.0, GWL2.5, and GWL3.0).	94
4.12	Projected changes in a-) DED, b-) CDD, c-) HI, d-) Tmax, e-) RH, f-) Radiation, and g-) Wind at specific GWLs in Niger	96
4.13	Projected changes of DED at different GWL for different seasons: DJF: December-February, MAM: March-May, JJA: June-August and SON: September-November.	98
4.14	Projected changes of CDD at different GWL for different seasons: DJF: December-February, MAM: March-May, JJA: June-August and SON: September-November.	100
4.15	Projected Changes of HI at Different GWL for Different Seasons: DJF: December-February, MAM: March-May, JJA: June-August and SON: September-November.	102
4.16	Projected changes in Discomfort Index at different Global Warming Levels For different seasons: DJF: December-February, MAM: March-May, JJA: June-July August and SON: September-November.	104
4.17	Long-Term Time Series Evolution of Climate Variables Displayed as Anomalies from the Reference(1971-2000) and Averaged Over The Entire Country (Niger)	106
4.18	Projected changes in Daily Energy Demand expressed in Percentage (%) With Respect to the Reference Period 1971-2000 and Averaged over Two Time Periods as simulated by the RCMs for the Two RCP Scenarios	108
4.19	Projected Changes in Daily CDD with Respect to the Reference Period	

	1971-2000 and Averaged Over Two Time Periods as Simulated by the CORDEX RCMs for the two RCP scenarios.	110
4.20	Projected Changes of HI with Respect to the Reference Period 1971- 2000 and Averaged Over Two Time Periods as Simulated by the CORDEX RCMs For the two RCP scenarios.	111
4.21	Projected Changes of DI with Respect to the Reference Period 1971-2000 and Averaged Over Two Time Periods as Simulated by CORDEX RCMS for the two RCP scenarios.	113
4.22	Frequency Distribution in (%) of days Peak Load > E90 (90th Percentile of Electricity Load) with (a) $T > 40$, (b) > 29 , and (c) > 39 . R Denotes the Correlation Between the Extreme Load and Extreme Heat Indices	115
4.23	Heatwave Events Distribution in (%) of at least three successive Days Where Peak Load > E90 (90th percentile of electricity load) with (a) (a) $T > 40$, (b) $DI > 29$, (c) $HI > 39$. R Denotes the Correlation Between the Extreme Load and Extreme Heat Indices	116
4.24	Projected Changes in Heat Waves Frequency (a-d), Heat Waves Number (HWN) (e)-(h), and Heat Waves Duration (HWD; (i)-(l)). The Boxplots ((m)-(o)) Indicates the Agreement Among the RCMs Simulation using Tmax	119
4.25	Projected Changes in Heat Waves Frequency (a-d), Heat Waves Number (HWN); (e)-(h), and Heat Waves Duration (HWD; (i)-(l)). The Boxplots ((m)-(o)) Indicate the Agreement among the RCMs Simulation Using Excess Heat Factor (EHF)	120

ACRONYMS

AGRHYMET	Agro-Hydro-Meteorology
ALADIN	Aire Limitee Adaptation Dynamique Development International
ANN	Artificial Neural Networks
AR4	Fourth Assessment Report of IPCC
CCCMA	Canadian Center for Climate Modelling and Analysis
CDD	Cooling Degree-Days
CLMcom	Climate Limited-Area Modelling Community
CNRM	Centre National de Recherches Meteorologiques
COP	Conference of Party
CORDEX	Coordinated Regional Downscaling Experiments
CSIRO	Australian Commonwealth Scientific and Industrial Research Organization
DD	Degree Days
DED	Daily Electricity Demand
DI	Discomfort Index
ECOWAS	Economic Community of West African States
EHF	Excess Heat Factor
ENSO	El Nino Southern Oscillation, 33
EVT	Extreme Value Theory
GCMs	Global Climate Models
GHGs	Greenhouse Gases
GW	Gigawatt
GWh	Gigawatt-hour
GWL	Global Warming Level
Had GEM	Hadley Center Global Environment Model

HDD	Heating Degree-Days
HI	Heat Index
HW	Heat Waves
HWD	Heat Wave Duration
HWF	Heat Wave Frequency
HWN	Heat Wave Number
ICHEC	Irish Center of High-End Computing
IPCC	International Panel on Climate Change
IPSL	Institut Pierre-Simon Laplace
ITCZ	Inter Tropical Convergence Zone
ITD	Intertropical Discontinuity
LULCC	Land Use Land Cover Change
MBE	Mean Bias Error
MIROC	Agency for Marine-Earth Science and Technology, Japan
MPI	Max Planck Institute for Meteorology
NCC	National Climate Center of Norwege
NCEP-NCAR	National Center for Environmental Prediction-National Center For Atmospheric Research
NIGELEC	Electricity Company of Niger
PCA	Principal Component Analysis
PGF	Princeton Global Forecasting
RACMO	Regional Atmospheric Climate Model
RCA	Rosby Center Regional Atmospheric Model
RCMs	Regional Climate Models
RCPs	Representative Concentrations Pathways
SRES	Special Report on Emissions Scenarios
SST	Sea Surface Temperature
SSTA	Sea Surface Temperature Anomalies

SVM	Support Vector Machine
SVR	Support Vector Regression
TAR	Third Assessment Report of IPCC
THI	Thermo-Hygrometric Index
Tmax	Maximum Temperature
Tmean	Mean Temperature
Tmin	Minimum Temperature
TPES	Total Primary Energy Supply
WAM	West African Monsoon
WAPP	West African Power Pool
WTC	Wavelet Transform Coherency

CHAPTER ONE

INTRODUCTION

1.1 Introduction

The recent anthropogenic emissions of Greenhouse gases (GHGs) into the atmosphere have contributed to increase the global temperature for the last decades and every of the last three decades has been in turn hotter at the Earth's surface than any preceding decade since 1850 (*IPCC, 2013*). This has generated a lot of interest regarding the potential impacts of global warming on many socio economic sectors. One of the key economic sectors that would be affected by global climate change is the energy sector owing to the observed correlation between the energy consumption and climate variables chiefly air temperature throughout hot periods. For instance, Previous studies have shown the influence of climate variables on electricity demand and thereby demonstrated that demand might get altered with changing climate (*Aldl and Waris, 2014; Kaufmann et al., 2013; Jovanović et al., 2015; Valor et al., 2001; Guan et al., 2017; Pardo et al., 2002*). This means the potential impacts of climate driven future electricity demand as a result of global climate change.

Higher temperature from global temperature rise will change the energy demand patterns over the world resulting to an increase of the cooling demand and a decrease of the heating demand. Hence, depending on the dominance of cooling or heating demand for a specific country, the net future electricity demand will increase or decrease as a result of climate change. Therefore, it is necessary to quantify the impacts of global climate change on energy demand for a particular location. This could facilitate to enhance the adaptive

capability of the energy sector to the impacts of climate change, to lower the unwanted power shortages as a result of extreme temperatures.

Moreover, the demand in most African countries have experienced a continuous growth as a result of socio economic development. For example, the electricity demand in Niger has increased by more than 150% since 2001 with the largest increase in the residential and commercial sectors. Hence, a changing climate is not the only factor that could affect future electricity demand; population change, Gross Domestic Product (GDP) growth, energy efficiency measures, urbanization among others might additionally play a part. However, it is important to quantify the contribution from climate change. Therefore, this present study aims to provide a detailed projection of the potential impacts of climate change on electricity demand in Niger at specific Global Warming Levels (GWL1.5, GWL2.0, GWL2.5, and GWL3.0). The study uses fourteen (14) ensemble mean Regional Climate Models (RCMs) that participated in the Coordinated Regional Climate Downscaling Experiments (CORDEX) to project the potential impacts of climate change on electricity demand.

1.2 Background to the Study

The energy climate relationship has gained a great deal of interest within the scientific community because **it could** be a great example of feedback impact. The existing causal link from emissions due to combustion of fossil fuels to deliver energy is well established. For instance, many studies on global climate change have traditionally focused on Greenhouse Gas (GHG) emissions arising from the energy systems and related human activities and the associated contributions of these activities to global warming. However, warmer climate will change the energy consumption and production patterns. Indeed, there

are many ways climate may affect the energy consumption. For instance, in the residential and the commercial sectors, one could expect in a warmer climate, higher cooling demand to maintain a reasonable comfort level during summer and less heating demand during winter.

With regards to changes in energy pattern as a result of climate change, several studies have been interested in the potential impacts of climate change on energy demand in recent years. This to provide detailed analysis of cooling and heating energy demand to better understand the impacts of climate change on the energy sector.

Furthermore, the recent reports of the International Panel on Climate Change (IPCC) have identified possible solutions regarding the issues of energy and climate through adaptation and mitigation policies. Indeed, the energy sector is the most important contributor to the anthropogenic Greenhouse Gases (GHGs) emissions into the atmosphere (Figure 1.1). For this reason, the energy sector could be identified as one of the potential sector for mitigating climate change. In addition to that, about 65% of the World electricity produced come from the fossil fuel resources. Burning of these fossil fuels emit the GHGs into the atmosphere which leads to global warming. On the other hand, increased air temperature will require more energy for cooling and consequently increase the rate of fossil fuels burning. So, understanding the feedback between the energy and climate is an important step in dealing with the issues of climate change and energy use.

While in the developed economies, both adaptation and mitigation policies are needed to tackle the issues of climate change, in low income economies (most of West African countries), only adaptation measures are more relevant to tackle climate change and energy issues. Indeed, the contributions to the global GHGs in low economy countries from the

energy sector is very insignificant (Figure 1.2). However, climate change is expected to highly influence the energy sector because of the projected changes in climate variables as well as high vulnerability of these countries as a result of their low adaptive capacity. Hence, in order to deal with the issues of climate change and energy over West Africa, it is worth to understand how changes in the climate variables will affect the energy sector.

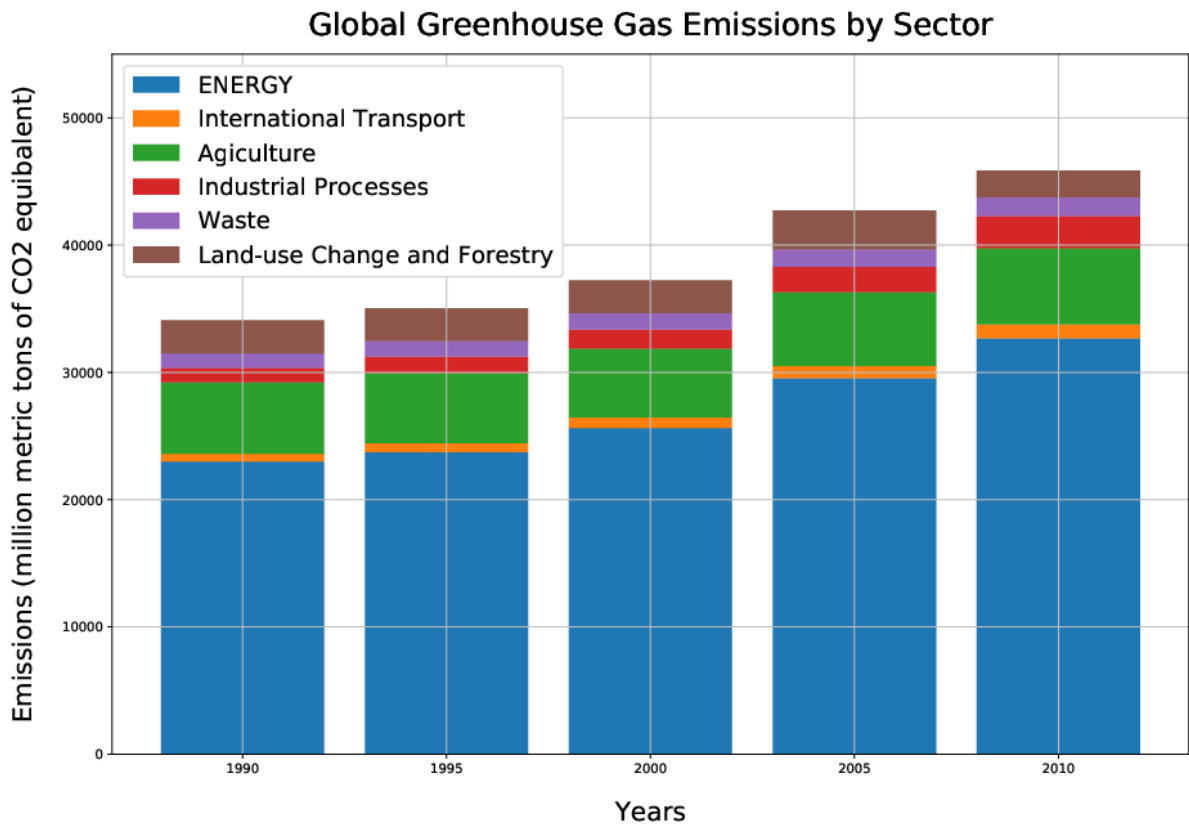


Figure 1.1: Global Greenhouse Gas Emissions by sector (source: data from WRI, 2014 and FAO, 2014)

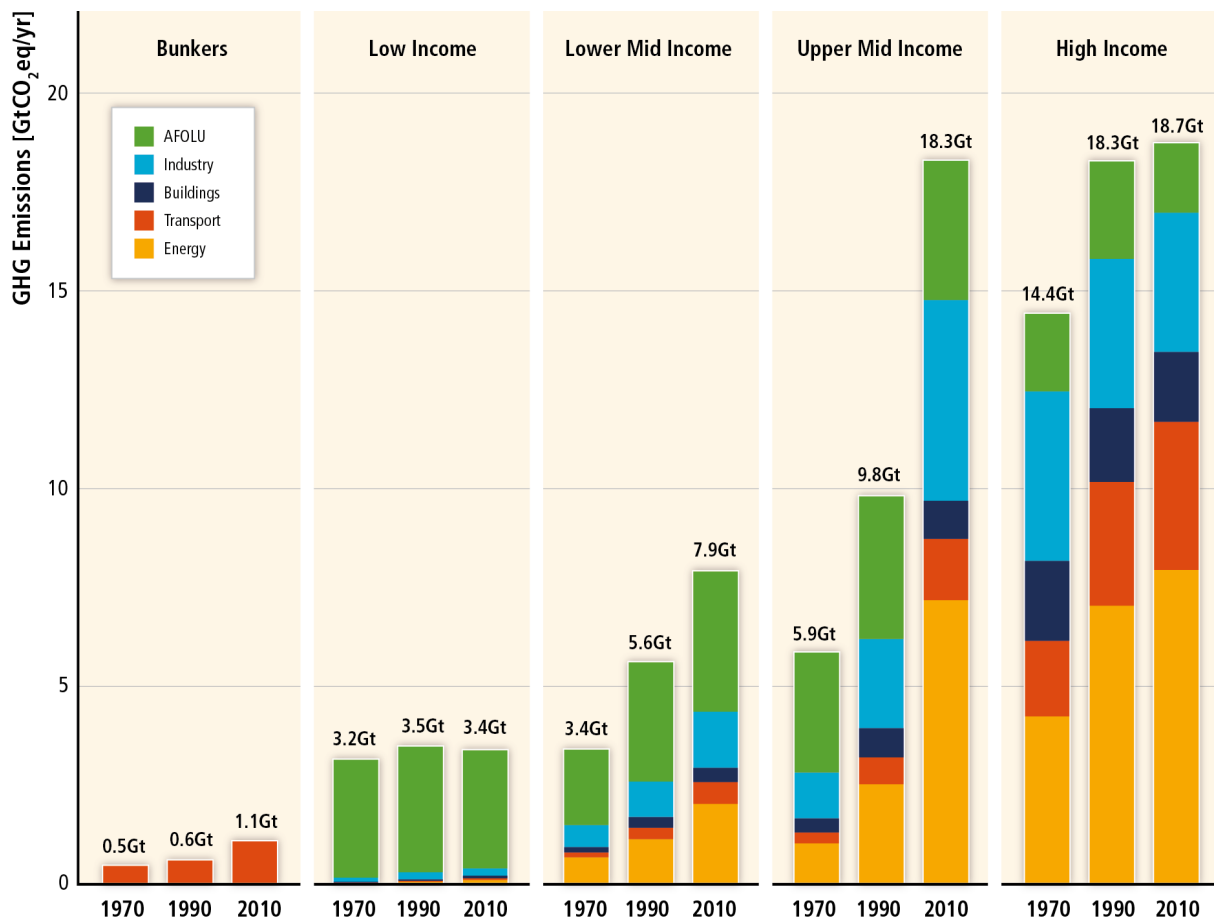


Figure 1.2: Green House Gases Emissions by Sector for Different Economies in the World

(Source: WRI, 2014)

1.2.1 Energy situation in West Africa

The energy sector in Sub-Saharan Africa particularly in West Africa is characterized by low access to modern energy systems and dominated by the inefficient and traditional systems. Indeed, the Total Primary Energy Supply (TPES) estimated to 189 million toe in 2013 was mainly from biomass with 78%, followed by fossil fuels and renewable, which account respectively 21% and 1% respectively (*ECREEE, 2015*).

Moreover, the number of people without access to electricity in Sub-Saharan Africa was estimated in 2012 to about 57% with 30% living in West Africa (*IEA, 2017*). This makes this region one of the largest concentration of people without access to electricity in the world. The electricity access over the region is only 34% with high discrepancies among countries with high access in Cape Verde (67%) and Ghana (61% in 2010) and low access in Liberia and Niger (Figure 1.3). The total installed capacity is 16.1GW with the main source of production being mainly Gas (52% of total production) followed by hydropower with 30% and petroleum with 18% (*ECREEE, 2015*).

However, due to the fact that any socio-economic development should be underpinned by access to modern energy systems, the West African countries have taken a number of measures to address this challenge. Hence, Despite the rapidly growth of population over the region, the number of people without access to electricity has been stable, if not improved since 2010; owing to the efforts of various countries in struggling to keep pace with the continuous increase of demand. For instance, between 2000 and 2016, many efforts have been carried out by some of the West African countries, especially in Ghana where the electricity access rate has increased from 45% to 84% between 2000 and 2016 (*IEA, 2017*).

Nevertheless, many efforts still remain to be done in many West African countries to meet the targeted goals of sustainable development. So, in order to better coordinate the electricity access over the Region, the Economic Community of West African States (ECOWAS) has established the West African Power Pool (WAPP) to coordinate the power generation, distribution and transmission among the member states. This to achieve a universal access to modern energy by increasing the electrification rate from 34% in 2012 to 88% in 2030 (*IEA, 2017*). Thus, many projects are ongoing to meet these targets. For example, it is expected that renewable energy share in the total energy production by 2030 will be 48%. However, in a context of socio-economic development and climate change, the success of these action plans require a better understanding of the factors that influence the energy consumption in the different member's states.

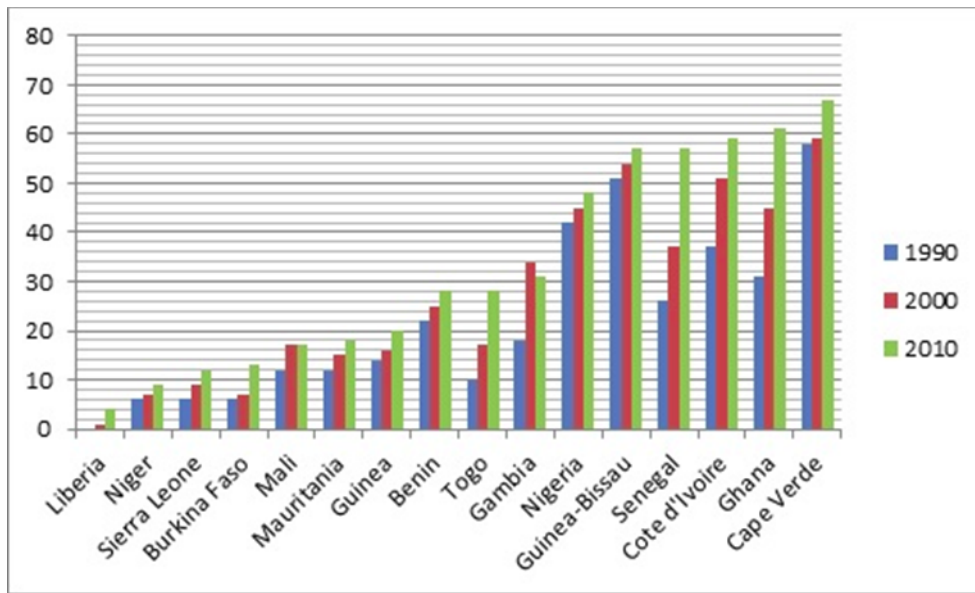


Figure 1.3: Electricity Access Rate (in %) of West African Countries for 1990, 2000 and 2010

[https://energypedia.info/images/c/c7/Trends in electrification rates in West Africa from 1990 to 2010.jpg](https://energypedia.info/images/c/c7/Trends_in_electrification_rates_in_West_Africa_from_1990_to_2010.jpg)

1.2.2 Current and Future Energy Situation in Niger

The current energy situation in Niger is characterized by a dual energy systems containing co-existing traditional and modernized energy systems and practices (*IRENA,2013*). As a matter of fact, 79% of the Total Primary Energy System (TPES) is from biomass, which meets 83% of the total household energy needs. The household sector is the main end user of energy consumption in Niger and represents 90% of the total energy consumption, followed by transport with 8% and industry which accounts for 2%. This poses a critical barrier to the development of the country. On the other hand, the electricity as well as modern energy appliances are also used in Niger mainly in urban areas (*IRENA, 2013*).

With the rapid growth of population and national economy, Niger's energy demand particularly the electricity consumption has tremendously increased in the last decade. Indeed, since 1992, the country's GDP shows a rapid growth and the total electricity consumption has sharply increased (Figure 1.4). As shown in Figure 1.4, the total electricity consumption rose from 330 GWh in 2005 to 821GWh in 2015, corresponding to about 150% increase in ten years. This trend will continue to increase as the energy planners are targeting 100% of electricity access in urban areas and 30% in rural areas by 2030.

Energy & GDP per Capita evolution

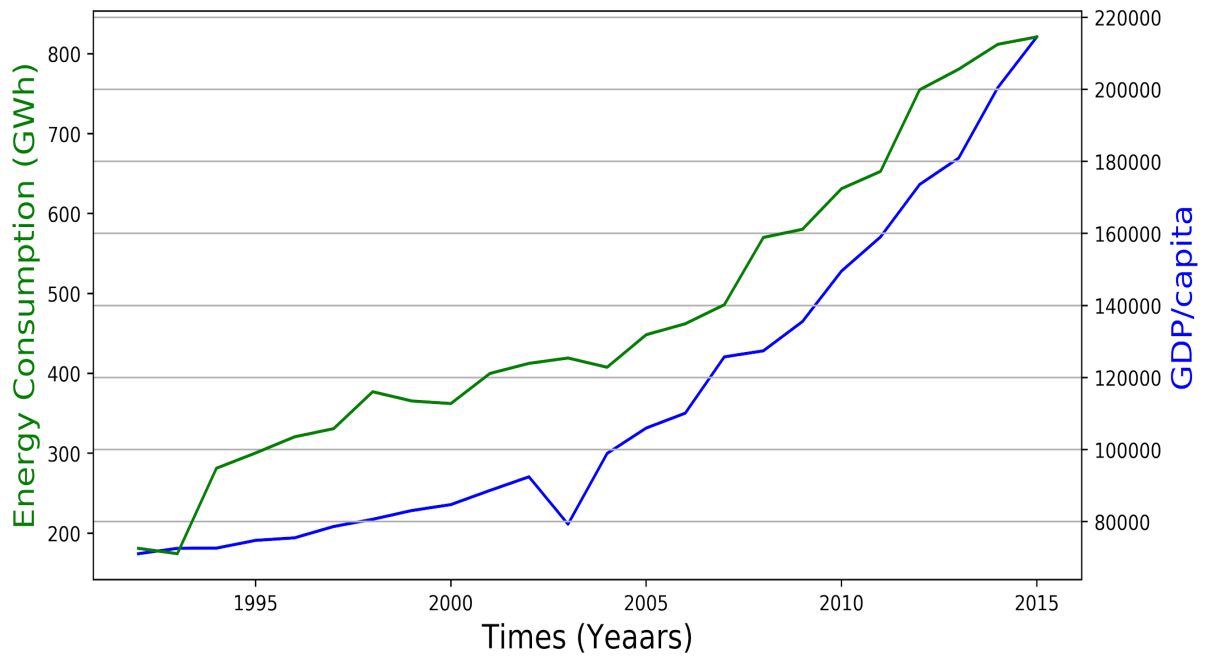


Figure 1.4: Times Series Evolution of Electricity Consumption and GDP per capita from 1992 to 2016 in Niger (World Bank, 2018)

Despite the rapid growth of the total energy consumption observed in this last decade, several challenges are still remaining to overcome. As a matter of fact, the country has relied on the electricity imported from Nigeria since 1977, which represents more than 60% of its total electricity consumption. This heavy reliance on electricity imported from Nigeria has undermined the electricity supply systems and contributed to insecure electricity supply observed these last years. This has prompted the government to gradually reduce its reliance on Nigeria by implementing additional power generation plants. In addition to heavy reliance on electricity imported from Nigeria, the increasing gap between the demand and the supply as a result of socio-economic development (population, GDP, and urbanization) is also a serious challenge that the energy sector is facing. However, during the last decade tremendous efforts have been made by the government of Niger to improve the electricity access over the country. In fact, despite the continuous growth of the population, and GDP, the percentage of people having access to electricity has improved (Figure 1.5). Owing to the fact that access to modern energy is the pillar of any socio-economic development, the government have taken number of measures to reach 100% and 30% of electricity access in urban and rural areas respectively by 2030.

In addition to the increase in electricity demand, significant increase in mean and extreme temperatures is also projected to result from climate change (*IPCC, 2013*). The observed correlation between temperature and peak demand during extreme hot days and nights suggests potential temperature driven electricity demand across many localities. Several works over West Africa are projecting an increase of mean and extreme temperature to result from global warming (e.g. *IPCC, 2013, Klutse et al., 2018; Nikulin et al. 2018*). Yet, the electricity supply system has not been able to adequately keep up with the peaks demand

during the hot periods when the demand exceeds the available generating capacity, resulting to blackouts in several localities. For example, during the hot periods in 2016, the power company in Niger (NIGELEC) was not able to meet half of the demand resulting to blackout in many areas. This problem will be compounded in the future with a combined effect of climate change, population growth, urbanization and economic development. Hence, providing information about future climate and its possible impacts on electricity demand will help the energy planners to take informed decisions.

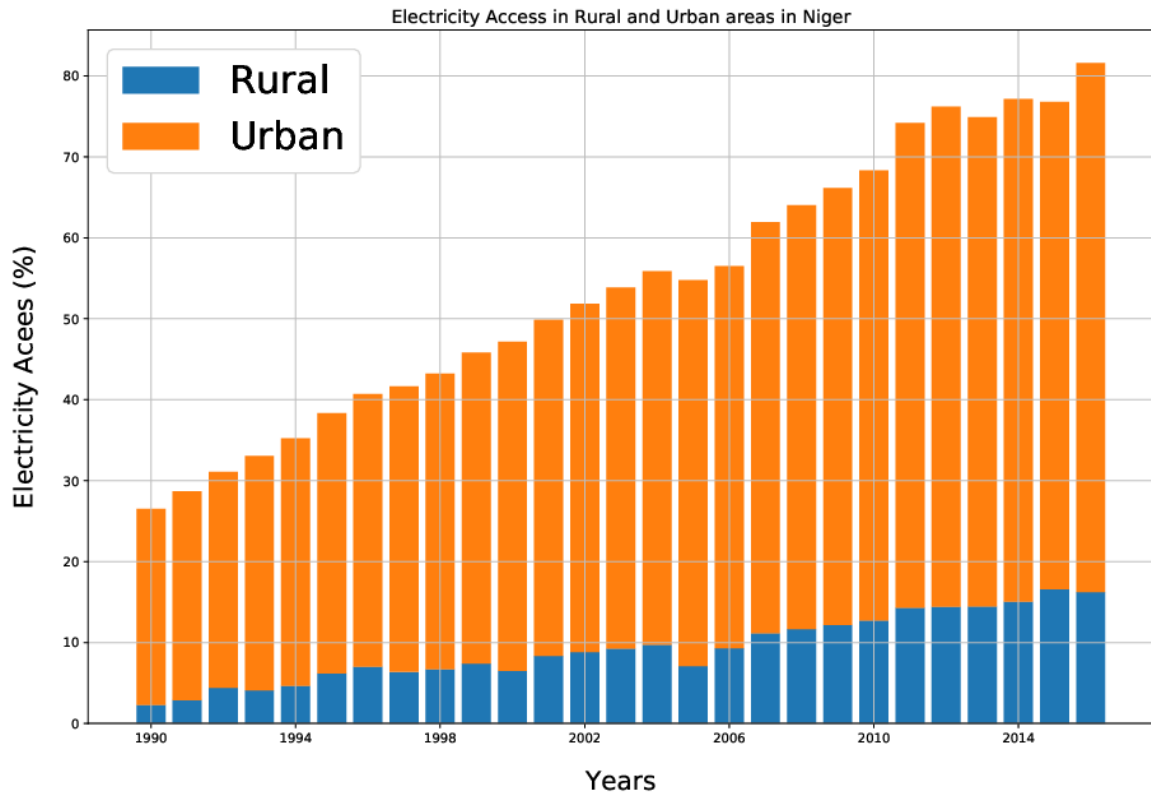


Figure 1.5: Percentage of Population having Access to Electricity in Rural (blue) and Urban are in Niger from 1990-2016 (data from the World Bank)

1.2.3 Climate Driven Electricity Consumption

The impacts of energy use on GHG emissions have drawn the attention of climate change research community for many years since the adoption of the IPCC (*Fearnside, 2002; Huo et al., 2012; Lu, 2017; Pao et al., 2011; Soytas et al., 2007; Van Vliet et al., 2011*). However, in recent years, researchers have also started to be interested on the impacts of climate change on energy demand because of the observed correlation between the electricity consumption and climate variables. Previous studies have shown the relation between electricity demand and climate variables and demonstrated that demand might get altered with changing climate (*Aldl and Waris, 2014; Kaufmann et al., 2013; Jovanović et al., 2015; Valor et al., 2001; Guan et al., 2017; Pardo et al., 2002*). Hence, for a better management of future electricity supply, there is a need to quantify the potential impacts of climate change on electricity demand. The present study intends to provide more information in this area.

Many studies have addressed the impacts of climate change on electricity demand in several countries across the world, and showed that the impacts differ from one climate zone to another, and from one city to the other. For instance, in cold climate, it is projected that climate change would decrease the energy demand since less energy will be required for heating the buildings during winter. In Finland, *Jylhä et al. (2015)* reported a decrease of 20-35% in total energy consumption by 2100 depending on the magnitude of climate change. *Wan et al. (2012)* shows that the reduction heating may be up to 22.3% in Harbin, 23.6% Hong Kong, 26.6% in Beijing, and 55.7% in Shanghai (55.7%). On the other hand, the energy demand is projected to increase in tropical countries where more electricity will be required for cooling the buildings. *Shourav et al. (2018)* revealed that climate change

would increase the daily electricity and peak demand in Dhaka City by up to 5.9-15.6% and 5.1-16.7% respectively toward the end of this century under different climate change scenarios. *Ahmed et al. (2012)* reported that an increase in temperature alone may lead to 1.36, 2.72 and 6.34 % rise in per capita demand during summer season and 2.09, 4.5, and 11.3% rise in per capita demand during the spring of 2030, 2050, and 2100 respectively. In Brazil, *Invidiata et al. (2015)* reported that climate change would induce an increase in the annual energy demand from 19-65% in 2020, 56-112% in 2050, and 112%-185% in 2080. While, it could be speculated that the electricity demand in Niger would also increase because of climate change, no such study has been quantifying the percentage of increase in West African country. Since the impacts of climate change may differ from one geographic location to another, it is worth to investigate the potential impact of climate change at specific location. Indeed, according to IPCC, the effects of climate change should be carried out at a location where the impacts are felt and the responses are implemented. Hence, given the heterogeneity of climate change impacts, carrying out such study will provide reliable information to the policymakers and electricity planners to take anticipated measures as far as the energy sector is concerned.

1.3 Justification of the Study

The increasing threats of climate change and global warming have generated a lot of interest to better understand the influence of climate variables and variability on energy demand. In Africa, especially West Africa, many studies project an increase of mean and extreme temperatures as well as changes in other climatic variables (Relative Humidity, Wind Speed, Solar Radiation) to result from climate change. This will have serious implications on energy demand, which already is facing many challenges such as insecure supply,

recurrent power shortage leading to blackouts because of the increasing gap between the demand and supply. Owing to the high vulnerability of West Africa region to global climate change (*IPCC, 2013*) because of its low adaptive capacity, climate change impacts will further foster these challenges. Hence, given the magnitude of the problem and the undesirability of such situations to continue in the future, there is a need to find a way out to solve these challenges. Therefore, for a better future management of the energy sector and a sustainable supply of electricity, it is necessary to investigate the potential impacts of climate change on electricity demand, thereby providing relevant information to the policy makers in the energy sector to take informed decisions to tackle the issues of climate change.

While it is projected that climate change will increase the mean and extreme temperature over West African region, increasing thereby the vulnerability of power sector to the impacts of climate change, no previous studies on the impacts of climate change on electricity demand over the region has been carried out. Hence, this study aims at investigating the potential impacts of climate change on electricity demand at different Global Warming Levels (GWL1.5, GWL2.0, GWL2.5, and GWL3.0) in Niger Republic.

1.4 Research Questions

The study considers the influence of climate variables on electricity demand in Niger and the potential impacts of climate change on future electricity demand. To achieve this, the following research questions are addressed:

- a. What is the sensitivity of electricity demand to climate variables in Niger?

- b. What is the historical relationship between the electricity demand and climate variables in Niger?
- c. How well do the Regional Climate Models (RCMs) reproduce the observed climate over the study area?
- d. What are the potential changes in future electricity demand as a result of climate change at specific Global Warming Levels?

1.5 Aim and Objectives

This study aims at investigating the potential impacts of climate variability and change on electricity demand in Niger using an ensemble Regional Climate Models (RCMs) that have participated to the CORDEX project.

To achieve this aim, the specific objectives will be carried:

- a. determine the sensitivity of electricity demand to climate variables in Niger;
- b. establish the historical relationship between the electricity demand and climate variables;
- c. assess the ability of the CORDEX Regional Climate Models (RCMs) in simulating the observed climate over the study area; and
- d. project the potential impacts of climate change on electricity demand in Niger at specific Global Warming Levels (GWL1.5, GWL2.0, GWL2.5 and GWL3.0)

1.6 Thesis Structure

This thesis is organized into five chapters. Chapter 2 presents the literature relevant to the research areas. It defines some climate variables, discuss the different methods used to develop the electricity models based on climate variables, as well as the various downscaling techniques used to predict the impact of climate change on electricity demand over the world. Chapter 3 presents the methodology used in the study; discuss the regional climate models, the different climate indices, as well as the methods used to build the relationship between the electricity demand and climate variables. Chapter 4 presents and discusses the findings of the study relative to the sensitivity electricity demand to climate variables as well as the potential impacts of climate change on electricity demand. The chapter also discusses the ability of RCMs in reproducing the observed climate variables used to build the electricity models. Chapter 5 presents the conclusions of the research, its limitations, and provide some suggestions.

CHAPTER TWO

LITERATURE REVIEW

2.1. Introduction

This chapter presents a comprehensive review of previous studies on the sensitivity of electricity demand to climate variables, and the potential impacts of climate change on electricity demand. The review discusses the different forecasting models used to build the electricity model as well as the climate indices used. Moreover, the review discusses also the different climate change scenarios, as well as the Global Climate Models and Regional Climate Models.

2.2 Energy Climate Nexus

Relationship between electricity consumption and climate variables became an area of interest because of the existing feedback between electricity and climate. Indeed, electricity generation through the combustion of fossil fuels contributes to increase in GHG emissions into the atmosphere thereby increasing the global temperature. On the other hand, high temperature will lead to high cooling demand to maintain a reasonable comfort level. For instance, many studies have shown the influence of climate variables on electricity consumption with the temperature, the most influential climate parameter that influences the electricity demand (*Colombo et al., 1999; Akbari et al., 2005; Yi-Ling et al., 2014; Fung et al., 2006*). Both mean and extreme temperatures have potential impacts on energy consumption. In fact, *Colombo et al. (1999)* analysed the frequency of extreme heat and energy demand over nine sites in Canada and their results suggested that an increase in the mean daily maximum temperature by 3°C in Toronto during the summer would increase

the average and standard deviation of the peak load by 7% and 22% respectively. *Akbari et al. (2005)* found that increases in air temperature can explain 5-10% of urban peak electric demand, with a typical rise of 2-4% for every 1°C rise in daily maximum temperature over 15-20°C. In Shanghai, *Yi-Ling et al. (2014)* analysed the influence of urban temperature represented by the cooling degree-days (CDD) and heating degree-days (HDD) on electricity consumption. Their results indicated that winter and summer are the two peaks of the consumption due to urban residential heating and cooling demand. Similarly, *Fung et al. (2006)* reported that a 1°C rise of temperature would result in 9.2%, 3% and 2.4% of an increase in electricity consumption for domestic, commercial and industrial sectors respectively in Hong Kong. *Jovanovich et al. (2015)* in analysing the impacts of daily mean temperature on electricity consumption, pointed out that deviations in power consumption depend on the deviations in air temperature. However, in West Africa especially in Niger, there is no study regarding the impacts of climate variables on electricity demand.

2.2.1 Definitions Degree Days (DD)

Because of the non-linear relationship between the electricity demand and temperature, the concept of degree-days was introduced in many works to study the relationship between the electricity demand and air temperature. The degree-days can be defined as the difference between the mean daily temperatures from the base temperature (*Valor et al., 2001*). Hence, the Heating (Cooling) Degree-Days is an indication of the sensible heating (cooling) requirements for a particular location (*Giannakopoulos and Psiloglou, 2006*). Ordinarily, the standard base temperature commonly used in the literature is 18°C for the calculation of heating and cooling degree-days (*Badescu and Zamfir, 1999; Valor et al., 2001; Sivak, 2008; Hekkenberg et al., 2009; Semmler et al., 2010; Xu et al., 2012*). However, other

climatic areas could require different base temperatures. Indeed, *Sailor and Pavlova (2003)* used a unique base temperature of 18.3°C to estimate the HDD and the CDD over 39 cities in USA. In Greece, *Matzarakis and Balafoutis (2004)* after they have conducted an experimental and empirical methods of trial and error, have fixed the value of 14°C as based temperature. In United Kingdom, *Kolokotroni et al. (2010)* proposed a unique value of 15.5°C as base temperature. Moreover, *Taseska et al. (2012)* in their study of climate change impacts on energy demand in Macedonia used a base temperature of 20°C to calculate both heating and cooling degree-days.

Another way of selecting the base temperature could be to use two different base temperatures for heating and cooling indices because of the non-sensitivity temperature zone observed around the base value. For instance, *Kadioğlu et al. (2001)* used a base temperature of 15°C and 24°C for heating and cooling degree-days respectively in Turkey. Within these two limits, a comfort zone could be established, in which no heating and cooling is required. Furthermore, *Christenson et al. (2006)* employed 3 different base temperatures (8, 10, and 12°C) to calculate the HDD and 3 others (18.3, 20, and 22°C) for calculating CDD in Switzerland. Their approach was based on outdoor air temperature (for specified internal temperature) at which the total heat loss is equal to internal and solar gains. Moreover, *Papakostas al. (2010)* reported a value of 15°C for HDD and 24°C for CDD. *Cartalis et al. (2001)* in their study of climate change in the southern Mediterranean (especially the area of Greece) used the values of 15.5°C and 18°C to calculate HDD and CDD respectively. Table 2.1 presents the various base temperature values used in many but not exhaustive studies over the World.

Table 2.1:Base Temperature Values used in Selected Studies (The list is not Exhaustive)

Country and City	Base Temperature		Justification for Base Temperature	Reference
	HDD	CDD		
Spain	15°C	18°C	within these two limits, a comfort zone was establish and thereby no heating and cooling is required	Valor et al., (2001)
Macedonia	20°C	20°C	-	Taseska et al. (2012)
Netherlands	18°C	18°C	-	Hekkenberg et al. (2009)
Ireland	18°C	18°C	Thom (1954)	Semmler et al., (2010)
Greece	14°C	-	With experimental and empirical methods of trial and error, a value of 14 °C was fixed as the basic temperature base	Matzarakis and Balafoutis (2004)
Greece	15°C	24°C	These temperatures are the most common balance temperatures of normally insulated buildings without especially large heat gains from internal heat sources and solar radiation	Papakostas et al. (2010)
Switzerland (Lugano)	8, 10 and 12 °C	18.3, 20, and 22°C	Outdoor air temperature (for a specified internal temperature) at which the total heat loss is equal to the internal and solar heat gains.	Christenson et al. (2006)
USA (39 cities)	18.3°C	18.3°C	Base temperature selected after an optimization study revealed that alternative definitions would not improve upon the	Sailor and Pavlova (2003)

USA	18°C	18°C	models in a statistically significant way' 18°C is due to the additional heat generated by occupants and their activities, resulting in an average indoor temperature of 21°C.	Sivak, (2008)
Greece	18°C	26°C	The base temperature was based on the technical directive issued by the Technical Chamber of Greece, which is responsible for technical issues, including building's energy requirements	Moustris et al., (2010)
Shanghai	10°C	22°C	The base temperature is based on outdoor temperature for which the heating and cooling demand become obvious	Ying-Li et al., (2014)

2.2.2 Definitions of Extreme Climate Events

The definition of extreme climate events poses debate in the scientific community. There are various difficulties associated with the definition of extreme climate events. However, the two main definitions found in literature are based on either the probability of occurrence of given quantities or on thresholds exceedances generally defined for a given time frames with respect to reference time period. The latter used two different types of threshold to define extremes: the fixed absolute thresholds and the relative absolute thresholds while the former is based on Extreme Value Theory (EVT). The fixed absolute threshold indices used a threshold value appropriate to a specific area of interest to identify an extreme climate event. So, any event with a climate variable (temperature or precipitation) exceeding that threshold is identified as an extreme event and the threshold can differ from one geographical location to the other. For example, *Klutse et al. (2015)* used a fixed threshold of 20mm to identify heavy rainfall event in West Africa. In Taiwan, *Chen et al. (2007)* define a heavy rainfall event when the threshold of 50mm is exceeded in a day and a very extreme rainfall when the threshold of 130 mm is exceeded in one day. Moreover, *Vizy and Cook (2012)* used a fixed threshold of 41°C of daily maximum temperature to define extreme temperature. However, owing to the high spatial variability of West African climate, the use of fixed absolute is less adequate. Indeed, *Klein et al. (2009)* and *Zhang et al. (2011)* argued that over large area, the use of fixed thresholds is less suitable for spatial distribution of number of days exceeding the threshold than the percentile thresholds. Hence, many works on extreme climate events over West Africa commonly used the percentile thresholds. However, considerable variations could also be found in the percentiles used. For instance, *Abiodun et al. (2013)* defined an extreme rainfall day and

extreme temperature day for Nigeria as a day where rainfall or maximum temperature is above the 99.5 percentiles of daily rainfall or maximum temperature of the climatological base reference while *Sylla et al. (2012)*; *Vizy and Cook, (2012)* and *Klutse et al. (2015)* used 95th percentile threshold to define extreme rainfall events over West Africa. Nevertheless, unlike the fixed absolute thresholds, the percentiles threshold is more suitable for spatial comparisons of extreme climate events and meaningful for all regions.

Hence, in this study, we will use the percentile thresholds to define extreme temperature day for Niger using the 90th percentile threshold. So following *Miller et al. (2007)*, we defined a hot day as a day where the maximum temperature is above the 90 percentile of daily maximum temperature and a warm night as a day where minimum temperature is above the 90 percentile of minimum temperature in reference to 1971-2000 climatology.

2.2.3 Heat Waves Events

Predicting Heat Wave (HW) events in a changing climate has gained a lot of interest in the scientific community these recent years because of their associated impacts on human and natural systems. For instance, it has been reported that heat waves cause more deaths than any other natural hazards (*Peterson et al., 2013*; *Ravinesh and Chung, 2016*; *Son et al., 2012*; *Nairn and Fawcett, 2015*; *Kim et al., 2016*; *Chen et al., 2017*). In addition to their disastrous impact on human health, HW events also influence the electricity consumption by increasing the demand for cooling. Indeed, according to *IPCC (2013)*, HW are one of the most worrying climatic extremes due to the vulnerability of the society and the expected increase in their frequency and severity in the 21st century as a result of climate change.

Though there is no strict consensus on the definitions of HW, in general, a HW event is defined when for a few consecutive days, the maximum temperature is above a certain threshold. Thus, the disagreement among HW definitions arise from either the number of consecutive days used or the nature of the threshold (fixed or relative threshold). For example, *Vizy and Cook (2012)* and *Russo et al. (2014)* defined a HW event using a fixed threshold for temperature calculated over a given reference period. Then, a HW occurs as conditions above the defined threshold persist for a required number of days. The limitation of this definition of HW is the variation across different location in the threshold value and the minimum number of days above the threshold required to be considered as heat wave. For instance, *Perkins and alexander (2013)* demonstrated that the use of fixed-threshold based calculations to define HW is not appropriate for various climatic types and thereby suggest the use of percentile-based calculations, as long as the percentile is not set too low or too high. In the same view, *Keeling's and Waylen, (2014)* also suggested a HW definition as a sequence of consecutive days with air temperature exceeding a certain high percentile threshold, commonly between 90th and 99th. Also, the use of 5 consecutive days excludes shorter HW (less than 5 days), while it is reported that the impacts of HW (death rate as well as electricity demand increase due to heat) is generally higher during the first few days of a HW, and that the acclimatization factors seem to be important HW (*Kalkstein and Davis, 1989; Energy Networks, 2019*).

More recently, to help develop heatwave definition applicable to any location, *Nairm and Fawcett (2013)* have introduced a new heat index, named Excess Heat Factor (EHF). EHF is the combined effect of excess heat and heat stress calculated as an index that provides a comparative measure of intensity, load, duration and spatial distribution of HW event

(*Nairn and Fawcett, 2013*). This study employs the EHF as defined by *Nairn et Fawcett (2013)* as well as percentile based threshold to define heatwaves and to explore its influence on electricity demand in Niger.

2.2.4 Temperature Humidity Indices

Besides the temperature variable, other climate variables could also influence the electricity demand, such as relative humidity, solar radiation, wind speed, and precipitation. However, the impacts of relative humidity on electricity demand has been found to be relevant in conjunction with warm and hot temperature because the perceived temperature can be higher in such meteorological conditions and consequently the use of cooling appliances increases (*Apadula et al., 2012*). Hence several temperature-humidity indices can be found in the literature. The temperature-humidity indices widely used in literature include Heat Index (HI), Discomfort Index (DI), and the Thermo-Hygrometric Index (THI). However, the HI has been already used in investigating the impacts of climate variables on electricity demand (*Apadula et al., 2012*). Hence, in this study, both HI and DI will be used to investigate the impact of relative humidity in conjunction with high temperature on electricity demand in Niger.

2.3 West African Climate System

The climate of West Africa is influenced by West African Monsoon (WAM) which is characterized by summer rainfall and winter drought (*Cornforth, 2012*). Indeed, the WAM is an important feature of rainfall variability over the region. The contrast in temperature and atmospheric pressure between the landmass and the sea surface are responsible to the African monsoon circulations that originate from tropical East Atlantic and the West

Indians Ocean (*Lebel and Ali, 2009*). These seasonal circulations of winds bring moisture inland, and their variability in both strength and position is a contributing factor to the dry/wet episodes over tropical and equatorial Africa. During dry episode, hot and dusty tropical continental air mass from the Saharan region blowing from the northeast over most of the countries in West Africa and known as 'Harmattan'. On the other hand, the second is the wet episode, which is a warm and moist tropical maritime air mass blowing from southwest and transporting moisture over land from Atlantic Ocean and providing West Africa countries with rain. The tropical Atlantic air mass reaches its northernmost position about 22 °N August while the hot and dusty continental air masses reach its southernmost position of about 7 °N in January. The zone of convergence of the two air masses (tropical continental and tropical maritime) is referred to as the Intertropical Discontinuity (ITD) when it occurs over continental West Africa at the surface and the Inter tropical convergence zone (ITCZ) when it occurs over the Ocean.

In addition to the WAM, the West African Climate system is also influenced by other features/phenomenon such El Nino Southern Oscillation (ENSO), Sea Surface Temperature (SST), and Land Use Land Cover Change (LULCC). Indeed, ENSO, which is a climate phenomenon in the equatorial pacific, influences global atmospheric circulation and worldwide sea surface temperatures, which in turn affects the climate over most regions of the world including West Africa. Several studies have already investigated the role of ENSO in climate variability over West Africa and found that there is a signal between the ENSO and the rainfall over the region. Another feature that influences the climate of West Africa is the SST. Indeed, the Atlantic is the primary source of moisture for major landmass in West Africa. Results from various studies provided evidence that SST patterns in the

tropical Atlantic Ocean are the most prominent driving force for sub-Saharan African rainfall (*Giannini et al., 2003; Sarr, 2012*). Moreover, *Losada et al. (2010)* and *Rodriguez-Fonseca et al. (2011)* demonstrated that climate model forcing of warm sea surface temperature anomalies (SSTA) over the Gulf of Guinea increases the rainfall over the Guinea Coast and induces drought over Sahel. Finally, LULCC plays also an important part in the climate variability of West Africa. Indeed, land cover characteristics including surface roughness, albedo, moisture availability among others control land-atmosphere interactions, and their changes can alter the natural cycles and atmospheric circulation (*Taylor et al., 2002*). Hence, *Paeth et al. (2009)* argued that changing vegetation cover due to primarily population growth has led to changes in temperature and rainfall patterns. In recent years, several studies have investigated the impacts of land use land cover change on the climate variability over West Africa. *Abiodun et al. (2008)* showed that desertification has reduced rainfall amounts in the Sahel and increase it over the Guinea Coast regions, while deforestation reduces rainfall amounts over the entire Africa. Moreover, studies of the recent droughts have also suggested that land cover changes in tropical and subtropical Africa were responsible for the drought observed in these regions (*Lotsch et al., 2003*).

2.4 Overview of Statistical forecasting models used to predict the electricity based on climate variables

The existence of historical consumption data provides basic source of information for the application of the statistical techniques to establish the relationship between consumption and the relevant factors. Hence, many methods have been developed to model the electricity consumption based on climate and non-climate factors. These methods broadly include

observations based regression/prediction, global/regional energy modeling and individual building energy simulation methods.

The individual building energy simulation approach is mainly used to simulate high-frequency output (e.g. hourly) for specific building types. Hence the impacts of climate change on energy requirement is assessed using this approach. For instance, *Huang and Gurney (2016)* used this approach to quantitatively explore the impact of climate change on building energy consumption by focusing on the variations of the impact across different building types at multiple time scale (e.g. annual, monthly, and hourly) and spatial scales (e.g. national, climate zone, and location). Also, *Dirks et al. (2015)* used the same approach to examine the impact of climate change on peak and annual energy consumption over a portion of Eastern interconnection located in the United States. However, the use of this approach requires a detailed information of the building characteristics, which are often limited and hourly weather data to drive the simulation.

The second approach is the global/regional energy modeling, which aims to simulate the energy consumption in a numerical model composed of different variables such as energy demand/supply, population, policy, and climate. Hence, this approach can be used to assess the impact of climate change on energy consumption as well as the impacts of other socio-economic variables such as population, mitigation policy, land use change, carbon taxes etc... However, the complexity and flexibility of this approach comes at the expense of the output resolution. This approach has been already used to investigate the impacts of climate change on energy consumption at annual timescales and various spatial scales (e.g. global, regional, national, and state) (*Isaac and van Vuuren, 2009; Zhou et al., 2013; Zhou et al., 2014*).

Finally, the third approach, which is the observation-based regression/prediction approach takes the advantage of historical relationship between the energy consumption and climate variables to predict future energy consumption in a changing climate. The regression techniques widely used in forecasting the energy consumption include the Multiple Linear Regression (MLR), the Artificial Neural Networks (ANN) and the Support Vector Regression (SVR).

Because to their learning abilities from data and their use in computer algorithms, the ANN and the SVR are often called machine learning techniques.

Owing to the fact that the regression approach is based on historical data, it's self-calibrated when fitted to a model and the accuracy of the prediction is assessed using statistical criteria (e.g. R², RMSE: Root Mean Square Error, MAE: Mean absolute Error). The details description of the three regression models widely used in forecasting energy consumption is given below.

2.4.1 Multiple Linear Regression (MLR) Model

The MLR model is used to describe the historical relationship between the consumption and the influential parameters. This technique assumes that the electricity consumption at a particular period can be estimated by means of linear combination of some independent variables. In addition, the regression coefficients needed to build the model are determined using statistical techniques. Due to ease application and results explanation of the MLR model, this technique has been widely used to predict the energy consumption based on relevant independent variables. For example, *Ahmed et al. (2012)* used MLR model to analyze climate change induced future electricity demand in New South Wales, in Australia.

Also, *Zhang et al. (2012)* applied the regression model to two principal components to analyze the influence of major economic factors on electricity consumption in China. *Lam et al. (2010)* applied the MLR for building's office energy use in China and showed that the model was able to accurately predict the electricity consumption with an R^2 varies from 0.89 to 0.97 and thereby suggested that the use of MLR to estimate the likely energy savings /penalty. *Braun et al. (2014)* employed MLR analysis to predict the electricity consumption of a supermarket in UK and thereby proposed the regression models as a flexible tool for energy prediction.

2.4.2 Machines Learning Techniques

The machine learning techniques commonly used in modeling energy consumption include the Artificial Neural Networks (ANN) and the Support Vector Machine (SVM) methods. The latter is a supervised learning method developed by *Vapnik (1995)* that generates input-output mapping function from a set of training data and the former is a computational techniques modeled on the learning processes of the human cognitive systems and the neurological function of the brain. In ANNs, the function of artificial neurons is similar to that of real neurons; with the ability to communicate by sending signals to each other over a large number of weighted or biased connection. Each of these neurons has an activation function which describes how the weighted sum of its input is converted to an output (Figure 2.1). Different types of ANNs have been developed based on the neuron arrangement. However, the Multi-Layer Perceptron has been found to be most useful in engineering application.

On the other hand, in SVM the ultimate aim is to establish maximum margin of the separated classes, which will enable to have good classification performance on the training

data as well as to provide high predictive accuracy for the future data from the same distribution. The SVM applies to classification and output variables are restricted to take only binary values. However, the SVM models have been extended for general estimation and prediction problems, including a version of SVM for regression, which is known as support vector regression (SVR) technique. Usage of support vector regression (SVR) technique eliminates this restriction since SVR methodology allows use of nonlinear functions.

Both ANNs and SVR have been used in energy studies. Table 2.2 summarizes the previous studies that have used ANNs and SVR to forecast the energy consumption.

However, the goal of accurate modeling of consumption requires some extremely important points. The choice of the best model and the variables affecting the consumption should be well understood. Hence, in this study both the MLR and ANN models will be employed to establish the historical relationship between electricity demand and climate variables. This will permit to project the potential impact of climate change on electricity demand.

Biological Neuron versus Artificial Neural Network

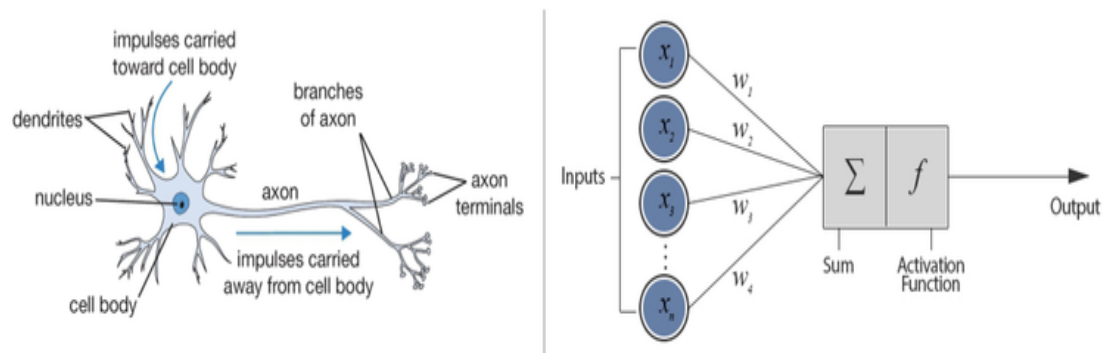


Figure 2.1: Artificial Neural Networks Structure (Keras tutorial, 2019)

https://s3.amazonaws.com/assets.datacamp.com/blog_assets/Keras+Python+Tutorial/content_content_neuron.png

Table 2.2: Summary of Selected Studies That Used Machine learning Techniques to Predict The Electricity Consumption

Forecasted countries	Models used	Independent variables	Forecasted energy types	Ref.
Turkey	ANN and SVR		Electricity consumption	Ogcu et al., (2012)
Greek	ANN	Temperature; installed capacity, yearly per resident electricity consumption, GDP	Energy consumption	Ekonomou, (2010)
South Korea	ANN	GDP, population, import, export	Energy demand	Geem and Roper (2011)
Turkey	ANN	Population, GNP, import, export	Electricity consumption	Kavaklioglu et al., (2009)
Turkey	SVR	Population, GNP, import, export	Electricity consumption	Kavaklioğlu (2011)
New York City (USA)	SVR	weather, time of day, previous consumption	Energy consumption	Jain et al., (2014)
China	SVM	Previous Electricity load	Electricity load	Yangyang Fu et al., ()
China	SVR	Temperature, humidity, radiation, GDP, urbanization	Energy consumption	Zhitong Ma et al., (2018)
Singapore	SVR	Temperature, Humidity, Radiation.	Energy consumption	Dong et al., (2005)
Hangzhou, China	SVM	Previous electricity Load	Electricity load	Li et al., (2009)
Brazil	ANN and SVR	Energy demand	Energy demand	Ruas et al., (2008)

2.5 Global and Regional Climate Models

To project the impacts of future global warming, information on how future climate projection under different emissions scenarios is needed. This information is provided by means of the Global Climate models (GCMs) also known as General Circulation Models. Indeed, the GCMs are essentially mathematical models of the general circulation of a planetary atmosphere, which describe the most important, components, processes and interactions in the climate system. Hence, GCMs are valuable research tools used for a range of application including investigating interactions between processes of global climate systems and their evolutions as well as providing projections of future climate characteristics under different emission scenarios that might alter the evolution of the climate system.

However, the spatial resolutions of the GCMs are still too coarse for impact assessments. Owing to the fact, running the GCMs at spatial resolution that is convenient for impact studies are very costly and resource consuming, the only alternative is to downscale the GCMs for a desired resolution for impact studies.

2.5.1 Emissions Scenarios used as input to GCMs

In 1990, The IPCC has published its first set of emissions scenarios, called SA90 used as input to GCMs that has been used in its first assessment report. Later, in 1995, a second set of emissions scenarios, called IS95 was released, and then followed by a third generation of emissions scenarios, called Special Report on Emissions Scenarios (SRES) released in 2000. The SRES were used in two subsequent reports, mainly the Third Assessment Report

(TAR) (IPCC, 2001) and the fourth assessment report (AR4) (IPCC, 2007). Furthermore, in 2007, taking into consideration the calls for improvements of the SRES, the IPCC developed four emissions scenarios (RCP2.6, RCP4.5, RCP6.0, and RCP8.5) defined as Representative Concentrations Pathways (RCPs). In contrast to their predecessors, the new emissions scenarios consider new and larger amount of data such as socio economic aspects, emerging technologies and land cover changes as well as providing more detailed spatial information at a grid level (60km grid resolution compared to 110km in the AR4). The name “representative concentration pathways” reflects thereby two important characteristics of the RCPs. The word “representative” means that each of the RCPs represents a large set of scenarios published in the literature while “concentration pathways” means that the RCPs are not a complete package of socio economic, emission, and climate projections but rather internally consistent sets of projections of the components of the radiative forcing. Based on the radiative forcing target level for the years spanning from 1850-2100, four RCPs can be identified:

- a. RCP2.6: a mitigation scenario leading to a very low forcing level with peak at 3W/m^2 (~490 ppm CO₂ equivalent before 2100) and then decline to 2.6W/m^2 by 2100.
- b. RCP4.5: a medium stabilization scenario without overshoot pathway to 4.5W/m^2 (~650 ppm equivalent by 2100)
- c. RCP6.0: a medium stabilization scenario without overshoot pathway to 6.0W/m^2 (~850 ppm CO₂ equivalent after 2100)
- d. RCP8.5: one very high baseline emission scenarios with radiative forcing leading to 8.5W/m^2 (1350 ppm of CO₂ equivalent by 2100).

It is worth noting that since the Conference of Party at Paris (COP21), researchers are becoming more interested in the target level of global warming instead of using different emissions scenarios. Indeed, The Paris Agreement aims to limit the global temperature at 1.5 and 2°C above the pre-industrial levels (*Hulme 2016; Schleussner et al. 2016; Rogelj et al. 2016*). Several studies have already discussed the consequences of reaching these targets on many sectors at global and regional scales (e.g. *Giannakopoulos et al., 2009; Abiodun et al., 2018, Kumi et al., 2018, Nikulin et al 2018; Klutse et al., 2018; Sawadogo et al.2019*). Among the few studies regarding the impacts of climate change at specific GWLs on energy demand, one could find the work of *Ying et al. (2018)* who investigated the changes of cooling and heating energy demand over China in response to GWL1.5, GWL2.0, GWL3.0, and GWL4.0. However, to our knowledge, no studies could be found over West Africa regarding the impacts of climate change at specific GWLs on the energy demand. Hence, in this study, the potential impact of climate change on energy demand in Niger is investigated under specific GWLs (GWL1.5, GWL2.0, GWL2.5, and GWL3.0).

2.5.2 Statistical Downscaling Techniques

The statistical Downscaling Techniques used statistical methods to downscale GCMs into a desired time and space resolutions for impact assessments. Hence, the statistical downscaling techniques by means of morphing approach have been widely used to assess the impacts of climate change on electricity consumptions in the previous works (*Wang et al., 2010; Shen, 2017; Wang et al., 2017; Cellura et al., 2018*). Table 2.3 presents some selected studies that have used the morphing methods to downscale the GCMs in predicting the impacts of climate change on electricity demand.

While the morphing technique only reflects changes in the average weather conditions and not possible to see changes in extreme climate conditions for the morphed data, the extreme climate conditions are projected to increase as a result of climate change (*IPCC, 2013*). Hence, the morphing technique might underestimate the impact of climate change on energy consumption. This shortcoming makes the morphing technique less relevant for assessing the impact of climate change on electricity consumption.

Table 2.3: Summary of Selected Studies that Have used The Morphing Methods

Country/ City	Scenarios	Findings	Model	Year	Ref.
25 locations throughout the world	IPCC TAR	In cold climates, the net change to annual energy use due to climate change will be positive reducing energy use on the order of 10% or more. For tropical climates, buildings will see an increase in overall energy use due to climate change, with some months increasing by >20% from current conditions. Temperate, mid-latitude climates will see the largest change but it will be a swapping from heating to cooling, including a significant reduction of 25% or more in heating energy and up to 15% increase in cooling energy.	HADCM3	2008	Crawley, (2008)
Southampton (UK)	UKCIP02	The results have shown that for UK climates the observed performance of a naturally ventilated building under current heat wave conditions can function as benchmark for its performance in a typical hot summer in the 2050s.	HADCM3	2008	Jentsch et al., (2008)
Alice Springs, Darwin, Hobart, Melbourne And Sydney (Australia)	IPCC TAR	The total heating and cooling energy requirements would vary significantly under different emissions scenarios. In the temperate climates of Sydney, for example, in 2100 the increase in the total heating and cooling energy consumption would be 120% and 530% when the global temperature increases by 2 °C and 5 °C, respectively.	CCCMA, CNRM, CSIRO- Mk3.5, GISS- AOM, GISS-EH, IAP- FGOALS, IPSL- CM4, MICRO- M, MRI- GCM232		Wang et al., (2010)

Table 2.3 (Continue)

Country/City	Scenarios	Findings	Model	Year	Ref.
Hong Kong (China)	IPCC TAR	The results indicate that there will be substantial increase in air-conditioning energy consumption under the impact of future climate change, ranging from 2.6% to 14.3% and from 3.7% to 24% for office building and residential flat, respectively.	MIROC3.2-MED	2011	Chan, 2011
Montréal and Massena (Canada)		Net Zero Energy Buildings should always be designed using multi-year simulations with weather data that take climate change into account	HadCM3	2012	Robert and Kummer t, (2012)
Miami, Houston, Phoenix, Memphis, San Francisco, Philadelphia, Albuquerque, Chicago, Burlington, Duluth (USA)	IPCC TAR	The results show that buildings with the present configurations of renewable energy systems will be losing their capability to meet the zero-energy goal in half of the considered climate zones.	HadCM3	2016	Shen and Lior, (2016)
Tokyo (Japan)	IPCC AR5	The results show that the total sensible heat load in August increased by 26% and the latent heat load increased by 10%.	MIROC4h	2016	Arima et al., (2016)
Macon (France)	IPCC AR5	Heating decreased from 24 to 44%, whereas cooling was multiplied by 4–8.	Not specified	2016	Roux et al., (2016)

Table 2.3 (Continue)

Country/City	Scenarios	Findings	Model	Year	Ref.
Guangzhou (China)	IPCC TAR	The indoor temperatures in 2020s, 2050s and 2080s will increase by 0.82 °C, 1.91 °C and 3.41 °C accordingly	HadCM3	2017	Song and Ye, (2017)
Taipei (Taiwan)	IPCC TAR	The simulations revealed increases in cooling energy of 31%, 59%, and 82% in the three time slices.	MIRCO3.2-MED	2017	Huang and Hwang, (2016)
Philadelphia, Chicago, Phoenix and Miami (USA)	IPCC TAR	The change of yearly energy use is predicted to be variable from -1.64% to 14.07% for residential building up to -3.27% for office building due to reduction of heating being much higher than increase in cooling needs.	HadCM3	2017	Shen, (2017)
Miami, Phoenix, Los Angeles, Washington DC and Akron (USA)	IPCC TAR and IPCC AR5	The results show discrepancies in the increases of annual average dry bulb temperature from future weather data predicted by the two groups of emissions scenarios.	HadCM3, CESM1 (CAM5)	2017	Wang et al., (2017)

2.5.3 Dynamical Downscaling Techniques

Unlike the statistical downscaling techniques, the dynamical downscaling technique by means of Regional Climate Models has the ability to generate physically consistent datasets across different variables. The RCMs have the advantage to provide the state of the atmosphere at each time step as well as in long integrations over a century. This provides a better representation of future climate compared to morphed data. Despite their ability to represent more accurately the future climate than the morphed data, very few studies have used the RCMs data to investigate the impact of climate change on energy demand all over the world and no study can be identified over West Africa. The rare studies found in literature include *Spinoni et al. (2018)* who used an ensemble 11 RCMs that have participated to EURO-CORDEX project to predict changes in HDD and CDD over Europe under RCP4.5 and RCP8.5 scenarios. In addition, *Damm et al. (2017)* also used the same datasets to project the impact of 2° warming on electricity demand in 26 European Countries.

Hence, in this study, the dynamical downscaling technique by means of RCMs is used to investigate the potential impact of climate change on electricity demand in a West African Country.

However, given a variety of RCMs, selecting a single RCM model with specific boundary conditions is not a trivial task. The IPCC suggests that given the strengths and weaknesses of various models, no single models can be considered as the best. To assist developing countries that lack computer infrastructure have access from multi-RCM projections, the Coordinated Regional Climate Downscaling Experiment (CORDEX) has made their datasets available publicly, and several studies have already used the CORDEX data to

assess the impacts of global warming on various sectors over the continent (*Abiodun et al., 2017; Kumi & Abiodun, 2018; Klutse et al., 2018, Nikulin et al., 2018; Maïre et al. 2018; Abiodun et al., 2018, Sawadogo et al., 2019*) . Nevertheless, none of these studies have investigated the impact of climate change on energy demand over West Africa. The present study intends to fill this gap.

CHAPTER THREE

RESEARCH METHODOLOGY

3.1 Introduction

This chapter provides a detailed description of both electricity demand and climate variables data used in this study as well as the methods used to describe the relationship between electricity demand and climate variables. Moreover, the statistical techniques used to establish the historical relationship between the electricity demand and climate variables are also provided. The chapter discusses also the definitions used to identify the extreme temperature and heat wave events over Niger, their influence on the electricity demand and the methods used to quantify their changes under a warming climate.

3.2 Study Area

The study domain on which the present study focuses is Niger Republic, a West African country, extending from 0 to 16 °E and 12 to 24 °N as indicated by the red box in Figure 3.1. Niger is a landlocked country limited in the North by Libya and Algeria, in the South by Nigeria and Benin Republic, in The East by Chad Republic and in the West by Mali and Burkina Faso. The country has a total land area of 1,267,000 km² with four different climate zones that can be identified including the Sudano-Sahelian zone (about 1% of the total land area), the Sahelian zone (about 10% of the total land area), the Sahelo-Saharan zone (about 12% of the total land land) and the Saharan zone (about 77% of the total land area).

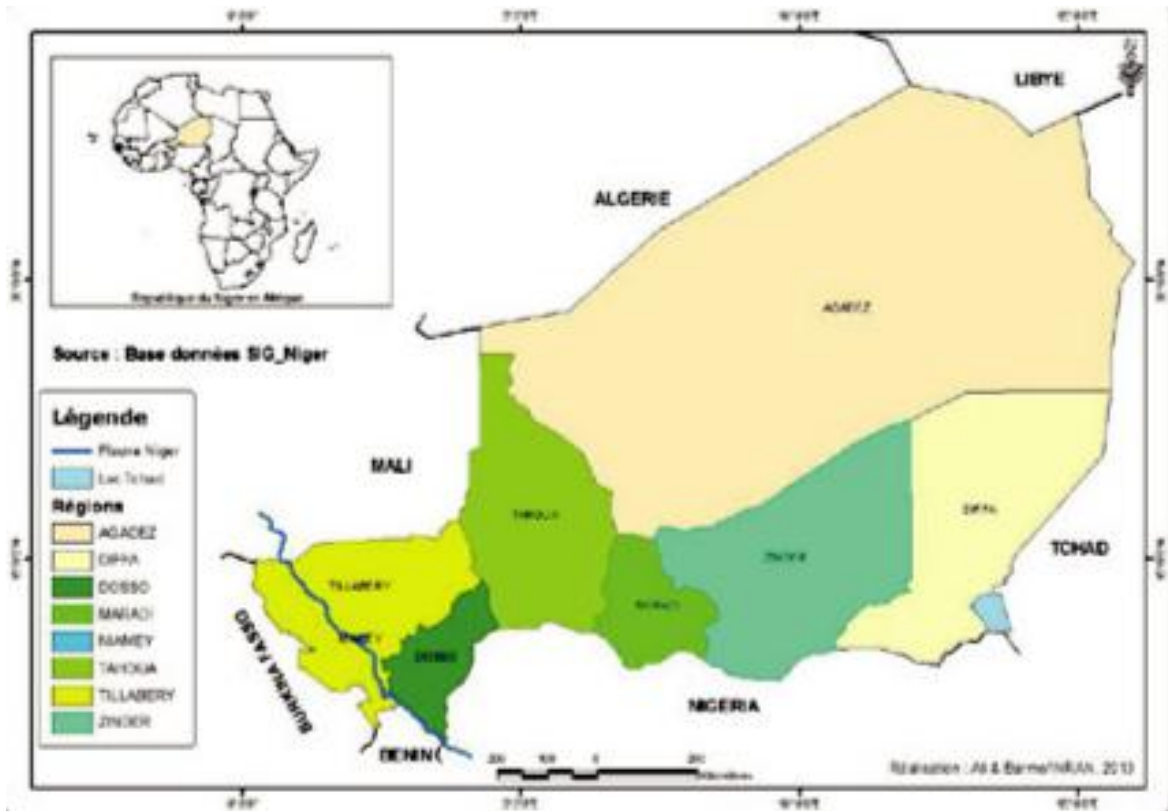


Figure 3.1: Map of the Study Area Showing the Main Cities (Salifou, 2015).

3.3 Data and Methods

3.3.1 Electricity Data

Electricity demand data used in this study was provided by The National Company of Electricity in Niger. The data comprises hourly electricity demand data spanning from 2001 to 2017 for Niamey. Then the daily peak demand was derived from the hourly data as well as the daily energy demand. In addition to these hourly data, monthly electricity consumption for the main cities spanning from 2003 to 2016 are also used. Figure 3.2 presents the monthly electricity consumption for the main cities used in this study. The electricity data comprises the aggregated demand for all the sectors, as disaggregated data are not available. From Figure 3.2, it can be assumed that the electricity consumption in Niger shows an increasing trend and seasonal variation. The latter is due to socio economic development while the former is a result of seasonal fluctuations. Since our interest solely depends on climate variables, it is important to isolate only the influence of climate on electricity consumption; thus the electricity data was de-trended following the procedure of *Moral-Carcedo and Vincent-Ocero (2005)* by removing the trend (due to socio economic development) and seasonality (due to holidays effects). The general regression model is given by the Equation 3.1

$$E_t = \beta_0 + \beta_1 * t + \beta_2 * t^2 + \beta_3 * I_w + DED \quad (3.1)$$

Where E_t is the aggregated electricity demand, T is the time variable ($t=0,1,2,3,\dots$), I_w is the dummy variable taking the value of 1 if the observation of the demand corresponds to holidays and 0 otherwise, DED is the electricity demand solely due to weather fluctuations, β_i are the coefficients.

Figure 3.3 shows the demand after removing the trend due to socio-economic development.

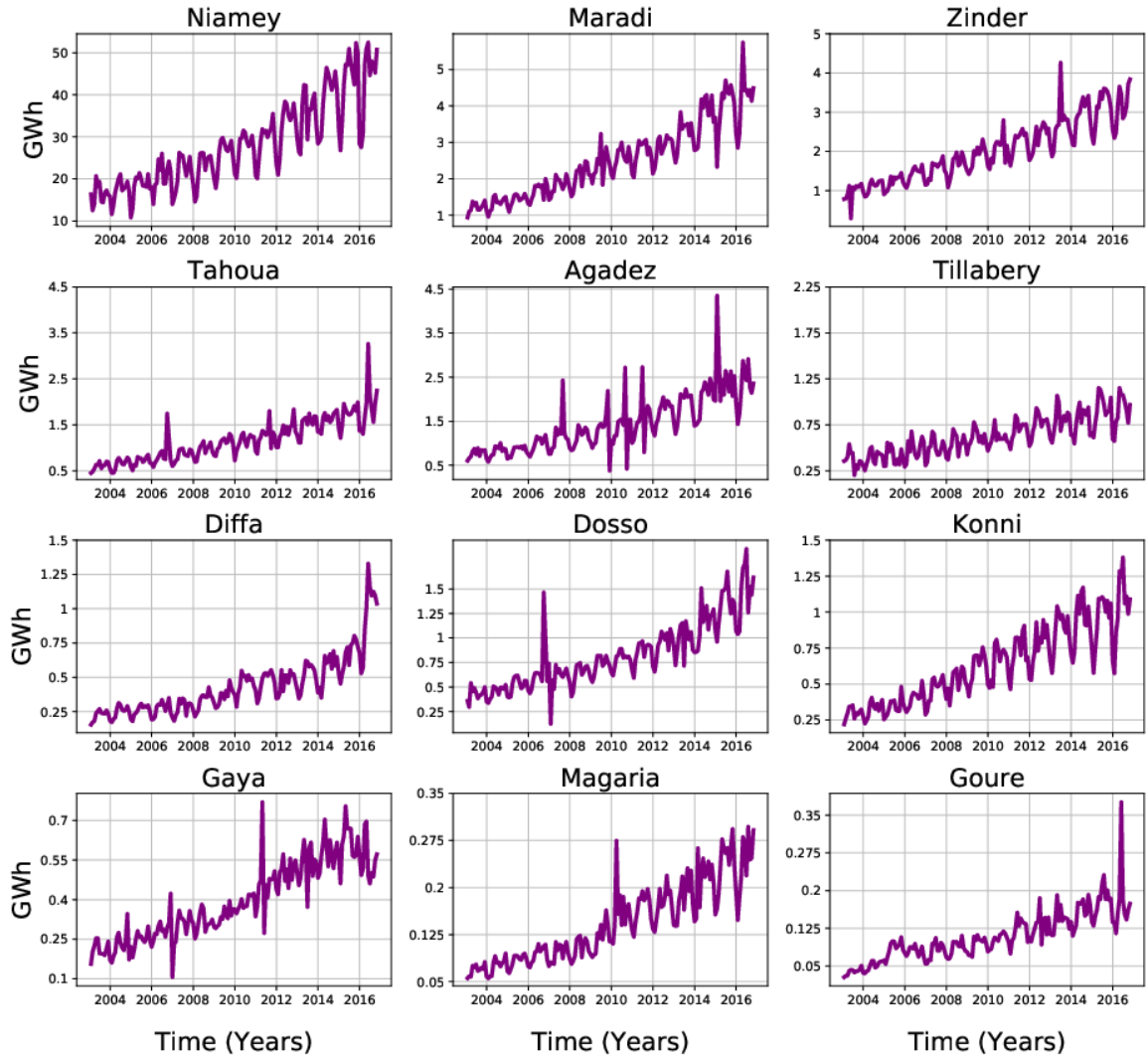


Figure 3.2: Time Series Evolution of Monthly Electricity Consumption for the Main Cities in Niger

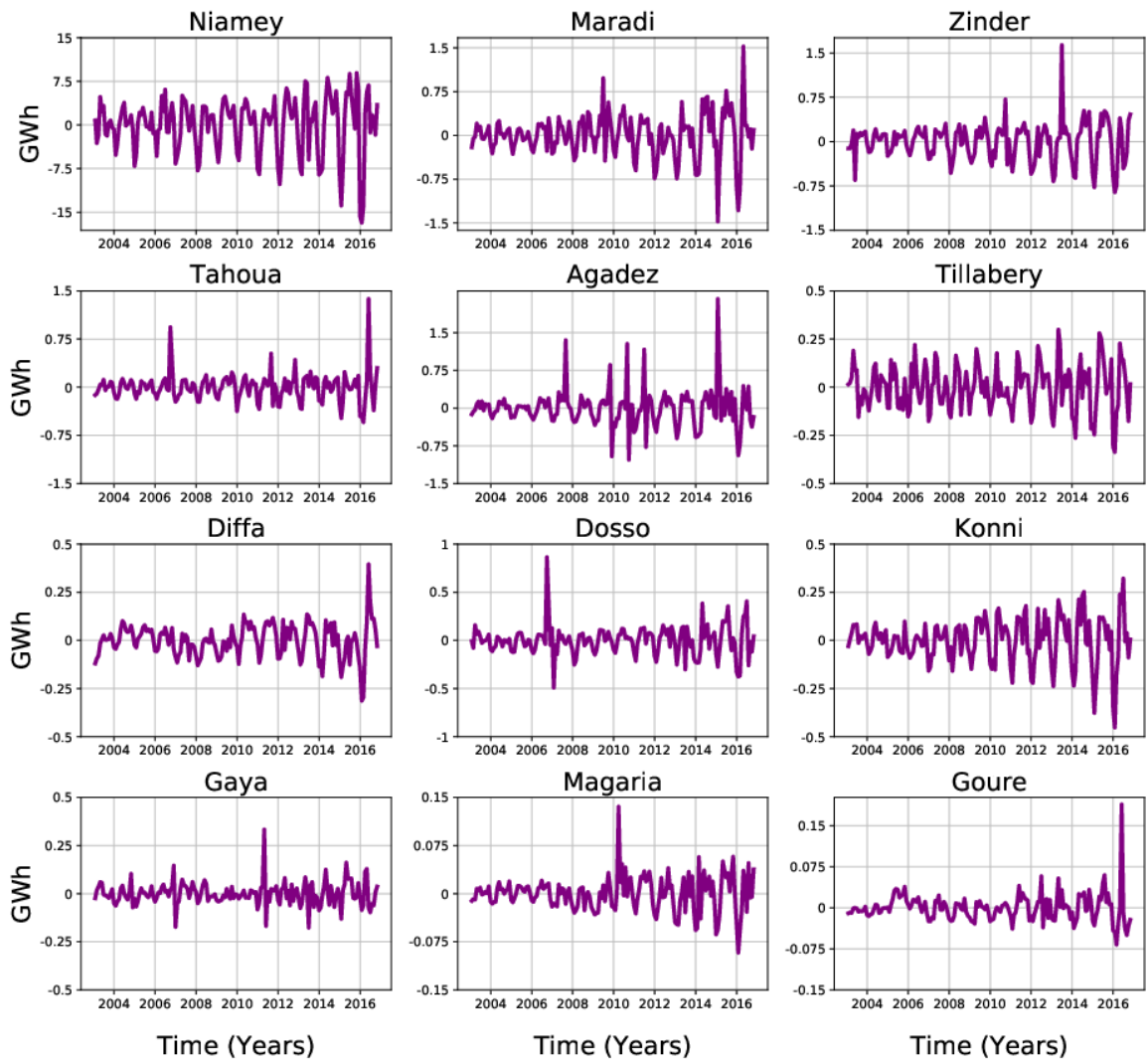


Figure 3.3: Time series Evolution Monthly Electricity Consumption for the main Cities in Niger after De-trending

3.3.2 Climate Data

Both observation and simulation data were analyzed in this study. The climate data comprises the variables such as temperatures (mean, maximum, and minimum), Relative Humidity (RH), Solar Radiation (SR) and Wind Speed (WSP). The observation datasets include the station data obtained from the meteorological office of Niger and Regional Centre in Niamey and the Princeton Global Forecasting (PGF) data. The PGF data is an observational-reanalysis hybrid dataset which provides near surface meteorological data for driving land surface models and other terrestrial modeling systems (Sheffield et al., 2006). PGF data consists of a global 50-years (1948-2008), 3 hourly at 1degx1deg resolution. It is constructed from reanalysis of the combination of a set of global observation datasets with the National Center for Environmental Prediction-National center for Atmospheric Research (NCEP-NCAR) (Sheffield et al., 2006). The biases in the precipitation and near surface meteorology reanalysis are corrected using observation-based datasets of precipitation, air temperature, and radiation (Sheffield et al., 2006). Table 3.1 provides the mean climatological values of the climate variables used while table 3.2 gives a brief summary of the contributing datasets used in the development of the PGFD.

On the other hand, simulation datasets were obtained from CORDEX. They consist of 14 regional climate simulation datasets from four Regional Climate Models (RCMs: RCA, CCLM, REMO, and ALADDIN). The RCMs and GCMs downscaled are given in Table 3.3. To assess the impacts of a warming level on climate variables, we calculated the difference between the projected future values (for the warming level) and the historical values (i.e. GWL minus historical). For more information on the definition of GWL period, we refer the readers to (Nikulin et al., 2018).

Table 3.1: Average Annual Climate Variables (2015) and Electricity Consumption of Selected Cities used in this study

Cities	Lon	Lat	Tmean (°C)	Tmax (°C)	Tmin (°C)	SR (Watt/m2)	WSP (m/s)	RH (%)	E (GWh) (in 2015)
Niamey	2.16	13.48	29.9	36.6	23.8	267	3.38	33.2	513
Maradi	7.10	13.28	29.3	35.3	21.8	272	2.36	36.8	47.6
Zinder	8.99	13.46	29.8	35.2	21.8	274	3.78	28.3	37.6
Tahoua	5.27	14.54	30.0	36.2	23.1	277	4.8	36	20.6
Tillabery	1.26	14.11	30.2	36.8	24.1	278	1.45	37.2	10.9
Agadez	7.98	16.96	31.4	36.7	21.9	322	6.11	22	30.44
Konni	5.25	13.79	29.2	36.3	22.8	269	1.37	39.4	11.33
Gaya	3.27	11.52	29.8	35.5	23.9	255	2.97	46.6	7.37
Diffa	12.78	13.41	28.3	36.2	21.2	274	2.72	42	8.01

Table 3.2: Summary of Datasets Used in the Construction of PGF Data

Dataset	Variables	Temporal coverage	Spatial Coverage
NCEP-NCAR Reanalysis	P,T, SW, LW, q, Ps, w	1948 present, 6 hourly	Global, ~2degx2deg
CRU TS2.0	P, T, Cld	1901-2000, monthly	Global land excluding antarctica, 0.5 x 0.5
GPCP	P	1997-present, daily	Global, 1x1
TRMM	P	Feb 2002,-present, 3 hourly	50S-50N, 0.25 x 0.25
NASA Langley SRB	LW, SW	1983-1995, monthly	Global, 1.0 lat x 1.0-120 lon

source: Sheffield et al., (2006). Note: Variables are precipitation (P), surface air temperature (T), downward shortwave radiation (SW), downward longwave radiation (LW), surface air pressure (Ps), specific humidity (q), wind speed (w), and cloud cover (Cld)

Table 3.3: Names of GCMs and Downscaled RCMs Used

RCMs	GCMs	Period of Global Warming Level			
		1.5	2.0	2.5	3.0
RCA	CCCMA	1999-2028	2012-2041	2024-2053	2044-2053
	CNRM	2015-2046	2029-2058	2041-2070	2052-2081
	CSIRO	2018-2047	2031-2059	2040-2069	2050-2079
	Had GEM	2010-2039	2033-2062	2042-2071	2051-2080
	IPSL	2002-2031	2016-2045	2027-2056	2036-2065
	MIROC	2019-2048	2034-2063	2047-2076	2058-2087
	MPI	2004-2033	2021-2050	2034-2063	2046-2075
	NCC	2019-2048	2034-2063	2047-2076	2059-2088
CCLM	CNRM	2015-2044	2029-2058	2041-2070	2052-2081
	HadGEM	2010-2039	2023-2052	2033-2062	2042-2071
	ICHEC	2005-2034	2021-2050	2034-2063	2047-2076
	MPI	2004-2033	2021-2050	2034-2063	2046-2075
ALADIN	CNRM	2015-2044	2029-2058	2041-2070	2052-2081
RACMO	ICHEC	2003-2032	2021-2050	2035-2064	2046-2075

3.3.3 Calculation of Degree Days (DD)

Degree-day is defined as the difference between the daily mean temperature and a given reference temperature called base temperature. For each day, we calculated the Heating and Cooling Degree Days (HDD/CDD) using the formula below:

$$HDD = \begin{cases} T_b - T & \text{if } T < T_b \\ 0 & \text{otherwise} \end{cases} \quad (3.2)$$

$$CDD = \begin{cases} T - T_b & \text{if } T > T_b \\ 0 & \text{otherwise} \end{cases} \quad (3.3)$$

with HDD/CDD the heating/cooling degree days, T is the average air temperature and T_b is the base temperature obtained in our case using the scatter plot (Figure 3.3) of electricity and temperature data. The equation of the best fit curve is given by equation 3.4.

$$DED = 0.03T^4 - 3.81T^3 + 172T^2 - 3326T + 22429 \quad (3.4)$$

Where T is the temperature (°C) and DED is the demand deviations (MWh/day)

Hence, the base temperature is identified as the temperature where the demand shows its minimum value.

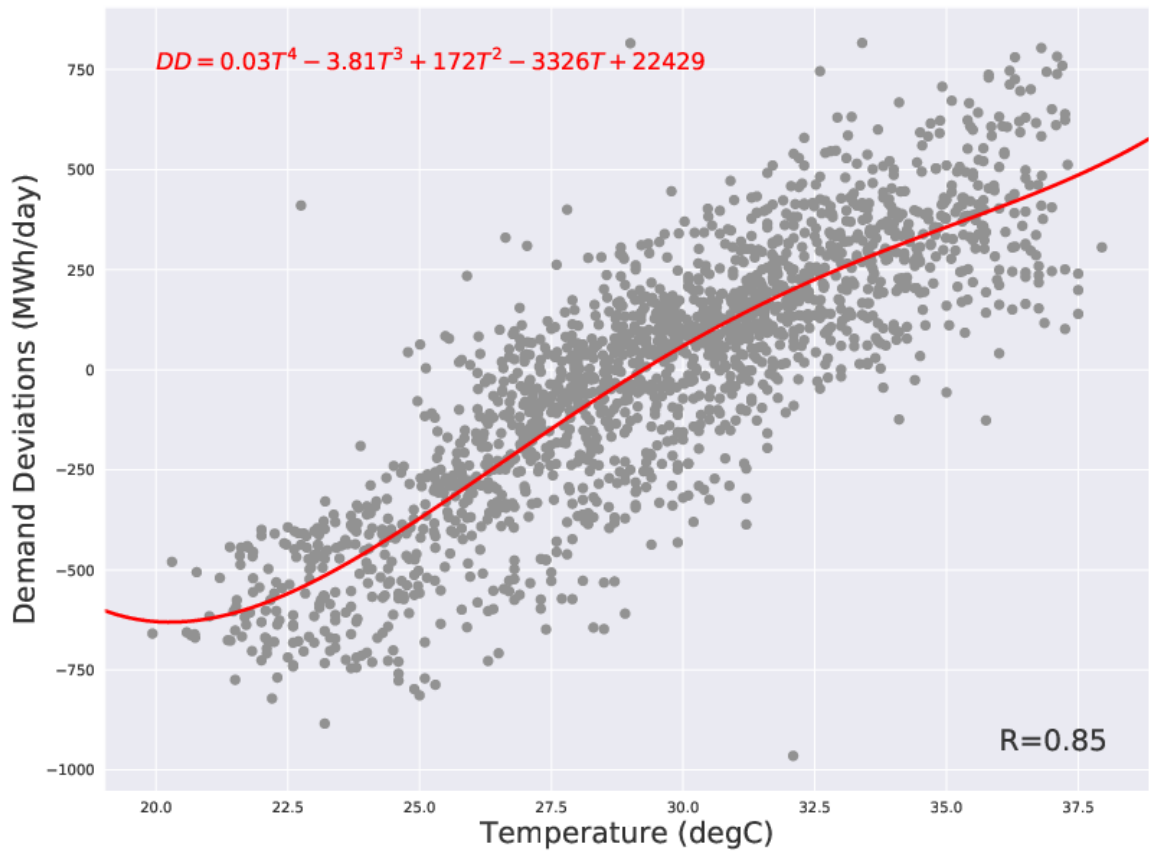


Figure 3..4: Scatter Plot of Temperature Against Electricity Demand. The red Curve Shows the Best Fit and R is the Correlation.

3.3.4 Calculation of Heat Indices

Two different heat indices are used in this study. The first is the Heat Index and the second one is the Discomfort Index (DI). The Equation 3.4 and 3.5 display the formula of HI and DI respectively.

$$HI = C_0 + C_1 * T + C_2 * H + C_3 * TH + C_4 * T^2 + C_5 * H^2 + C_6 * T^2 * H + C_7 * T * H^2 + C_8 * T^2 * H^2 \quad (3.5)$$

$$DI = T - (0.55 - 0.0055 * H) * (T - 14.5) \quad (3.6)$$

Where T is the temperature in Fahrenheit (for the calculation of HI) and °C (for calculation of DI), and H is the relative humidity in %.

3.3.5 Extreme Temperature and Heat Waves Characteristics and Measurements

The calculation of Extreme temperatures as well as heat waves is based on the 90th percentile threshold. Indeed, we defined a warm day, any day where the maximum temperature is above the 90th of the maximum temperature for the climate reference period 1971-2000. In the same way, a warm night is defined as a day when the minimum temperature is above the 90 percentile of the Tmin. The hot days and warm nights are calculated using the equation 3.7 and 3.8 respectively.

$$WD = \begin{cases} 1 & \text{if } Tmax > TX90 \\ 0 & \text{otherwise} \end{cases} \quad (3.7)$$

$$WN = \begin{cases} 1 & \text{if } Tmin > TN90 \\ 0 & \text{otherwise} \end{cases} \quad (3.8)$$

Where TX90 is the 90th percentile of the maximum temperature and TN90 that of the minimum temperature

However, for the definition of the heat wave events, we adopted two different definitions. The first one is based on the percentile threshold of the daily maximum temperature while the second definition is based on the Excess Heat Factor (EHF). For the first definition, the 90th percentile threshold (TX90) of daily maximum temperature is calculated for the period 1971-2000 using all days of the year. In the second definition, both excess heat and heat stress are calculated using the mean temperature. The former measures how hot a three-day period is in reference to long-term climatic reference (daily mean temperature) calculated for the period 1971-2000. The latter is a measure of how hot a three-day period is compared to the recent past (previous 30 days), to measure the short term acclimatization. Equation 3.8, 3.9 and 3.10 provides the formula of excess heat, heat stress and excess heat factor respectively.

$$EHI_{sig} = \frac{T_i + T_{i+1} + T_{i+2}}{3} - T95 \quad (3.9)$$

$$EHI_{accl} = \frac{T_i + T_{i+1} + T_{i+2}}{3} - \frac{T_{i-1} + \dots + T_{i-30}}{3} \quad (3.10)$$

$$EHF = EHI_{sig} * \max(1, EHI_{accl}) \quad (3.11)$$

Where T95 is the 95th, of mean daily temperature.

Hence, for each heat wave index, a heat wave event is defined, at any grid point, when the respective threshold value is exceeded ($T_{max} > 0$, $EHF > 0$) for at least three consecutive days. Furthermore, we define both indices using a framework of different characteristics following (*Perkins et al., 2012*) by focusing on Heatwave number (HWN), Heat average Wave Frequency (HWF) and the Heat Wave Duration. The HWN is defined as a total number of HW events for a given year while the HWF is the total number of days satisfying

the index criteria. The HWD is obtained by dividing the total number of heat wave days by the total number of heat wave events (HWF/HWN).

Moreover, to assess, the influence of extreme heat on electricity demand, the frequency distribution of peak demand higher than the 90th percentile as well as the frequency distribution of days with extreme heat (Temperature, DI, and HI) greater than a given threshold are calculated and compared. The temperature threshold is calculated by using the 90th percentile threshold of daily temperature for the climate reference period (1971-2000) while the DI and HI thresholds are respectively 29°C (values at which the whole population feels a heavy discomfort) and 39°C (value at which heat exhaustion is possible with prolonged exposure and physical activity)

3.3.6 Relationship between the Electricity Demand and Climate Variables

In order to understand the relationship between the electricity demand and climate variables, we used the Wavelet Transform Coherency (WTC) and phase analysis (PA) to explore the relationship between two-time series in a time-frequency space. Unlike the simple linear regression (LR) model, which gives an overview of the relationship between two-time series, the WTC allows to illustrate the correlation between two-time series in the time frequency space. In addition, the phase analysis provides information on the variables that is leading in the relationship. The following equations give the formula of WTC and phase difference.

$$WTC = \frac{|sWavex.y|^2}{sPowerx.sPowery} \quad (3.12)$$

$$Angle(\tau, s) = Phase_x - Phase_y \quad (3.13)$$

Where the prefix s indicates the need of smoothing, angle (τ, s) the phase difference between the two series.

The phase difference between the two series provides information on the delays of oscillations between these series.

An absolute value of the phase difference less (larger) than $\pi/2$ indicates that x and y are in phase (anti-phase respectively) referring to the instantaneous time as time origin and at period in question while the sign between the two phase difference shows which series is leading in the relationship. In this study, the x represents our influential factor while the y represents the electricity demand.

The R package “biwavelet” is used to carry out the WTC and phase analysis of between electricity demand and temperature

The phase differences and their interpretation are given in Table 3.4

Table 3.4: Phase Differences and Their Interpretations

PhaseX-PhaseY	X (Climate Variables)	Y (Electricity Demand)
$[0, \pi/2]$	Leading	Lagging
$[\pi/2, \pi]$	Lagging	Leading
$[-\pi, -\pi/2]$	Leading	Lagging
$[-\pi/2, 0]$	Lagging	Leading

In this study, the WTC is used to measure the intensity of the covariance of the two-time series (temperature and electricity demand) in time-frequency space. The WTC ranges from 0 to 1 and it can be interpreted as the correlation coefficient. The closer the value is to one the more correlated are the two series.

3.3.7 Modelling the Influence of Climate on Electricity Demand

Both Multiple Linear Regression (MLR) and Artificial Neural Network (ANN) were used in this study to model the influence of climate variables on the de-trended electricity demand using historical demand and weather variables. The general form of MLR is given in Equation below.

$$DED = \alpha_0 + \sum \alpha_i * X_i + \varepsilon \quad (3.14)$$

Where DED is the de-trended electricity demand, α_i the regression constants which are determined by the ordinary least square method (OLS); X_1, X_2, \dots, X_n are the independent variables (climate variables), and ε is the error term.

The MLR model is validated by splitting the dataset into training and testing data. Hence 80% of the data was used to train the model while 20% is used to test model. Moreover, we check the basics linear models assumptions using the residual plots (homogeneity of the variance, and histogram of residuals) to find out whether or not the model complies with the basics assumptions of linear models. Then, the accuracy of the model was assessed using the Root Mean Square Error (RMSE), the Mean Absolute Error (MAE) as well as the Coefficient of determination. The equations 3.15, 3.16 and 3.17 provide the formula of RMSE, MAE and R^2 .

$$RMSE = \sqrt{\frac{\sum(P_i - O_i)^2}{n}} \quad (3.15)$$

$$MAE = \sum_{i=1}^n \frac{|P_i - O_i|}{n} \quad (3.16)$$

$$R^2 = \frac{\sum_{i=1}^n (P_i - \bar{O})^2}{\sum_{i=1}^n (O_i - \bar{O})^2} \quad (3.17)$$

Where O_i is observation, P_i the predicted value, \bar{O} is the mean observation and n is the number of sample.

Finally, the significance of individual independent variables to the regression model used also assessed by means of t-test. The level of significance is set to 0.05. In other words, all the variables with p-value less than 0.05 will be considered as statistically significant.

3.3.8 Predicting the Impact of Climate Change on Electricity Demand

Before assessing the impacts of climate change, we evaluate the performance of the simulation datasets in reproducing the observed climate by comparing the RCMs datasets used to the PGF data. Then, to assess the impacts of climate change at various GWLs (GWL1.5, GWL2.0, GWL2.5, and GWL3.0), we calculated the difference between climate variables in the reference period (1971-2000) and the GWL period (i.e. GWL minus reference). Then based on the model developed, we project the potential impact of climate change on electricity demand in Niger. Finally, the robustness of climate change projections is assessed using the following criteria:

- at least 85% of the simulation must agree on the sign of the change

- at least 85% of the simulations must indicate that the changes are statistical significant (99% confidence level; using a t test, with respect to the climate variability of the reference period)

Hence, the climate signal is consistent if the above mentioned criteria are satisfied. The two methods have been previously used to assess the climate change signal (*Abiodun et al., 2018; Klutse et al., 2018; Nikulin et al., 2018; Maure et al., 2018*).

CHAPTER FOUR

RESULTS AND DISCUSSIONS

4.1 Introduction

In this chapter, the research findings are presented relative to the influence of climate variables on electricity demand and the potential impacts of climate change on future electricity demand. First, the electricity variation patterns were investigated by means of Seasonal Variation Index (SVI), Weekly Variation Index (WDI) and Diurnal Variation Index (DVI) as well as its relationship with climate variables. Secondly, the electricity demand model was developed for the study area by means of Multiple Linear Regression (MLR) and Artificial Neural Network (ANN). Then, the potential impacts of climate change on electricity demand based on the resulting electricity model was presented. Lastly, the robustness of the projections was assessed.

4.2 Relationship Between Electricity Demand and Climate Variables

This section explores the characteristics of electricity demand in Niger as well as its relationship with climate variables. The annual cycle, weekly cycle and diurnal cycle of the electricity demand are also investigated.

4.2.1 Seasonal fluctuations of Electricity demand in Niger

The average SVI shows a high demand of electricity in May due to high temperature values recorded in this month, which thereafter gradually decreases until August (Figure 4.1). The gradual decrease of electricity demand due to the onset of rainy season coincides with the decrease in ambient temperature and the increase in both relative humidity and wind speed

that contribute to reduce the electricity demand. Then, the electricity starts again to gradually increase to reach a second peak in October (Figure 4.1). This increase is due to a second temperature rise. As we move to winter, the demand starts decreasing again and reaches its minimum value in January. This is due to the fact that in winter, the demand for cooling and refrigeration is very low because of low temperature values in this particular season. In summary the electricity demand in Niamey is highly influenced by cooling appliances such as air conditioners and refrigerators.

Seasonal Variation Index

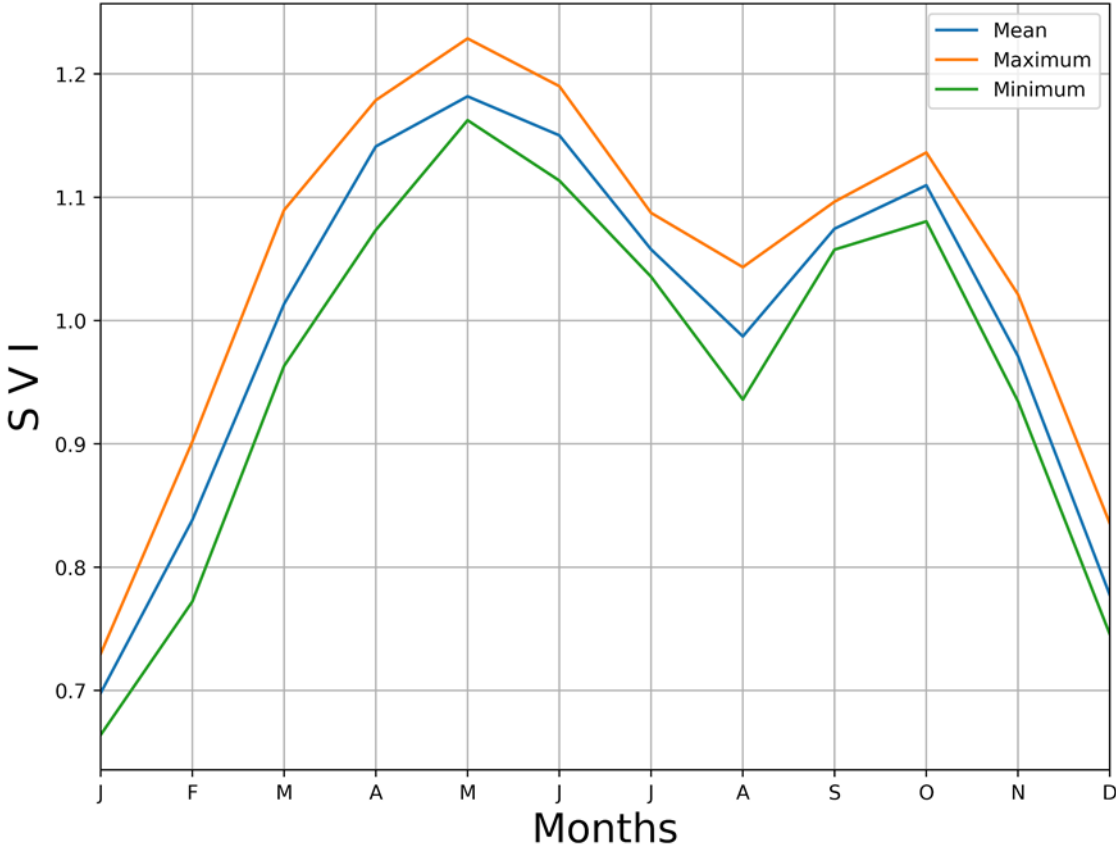


Figure 4.1: Seasonal Variation Index of Electricity Demand

Figure 4.2 depicts the variation of Weekly Variation Index (WDI) according to the day of the week. It is clearly noticeable that the electricity demand is lower during weekends (especially Sunday) due to the reduced of economic activities. Lower levels of demand are also observed on Friday compared to the other weekdays because on Friday, most of the services close earlier than the other working days. Moreover, electricity demand also decreases during holidays that fall between Monday and Friday. This effect is easily appreciable in Figure 4.2 where the minimum values of weekdays are comparable with the weekend average values.

Weekly Variation Index

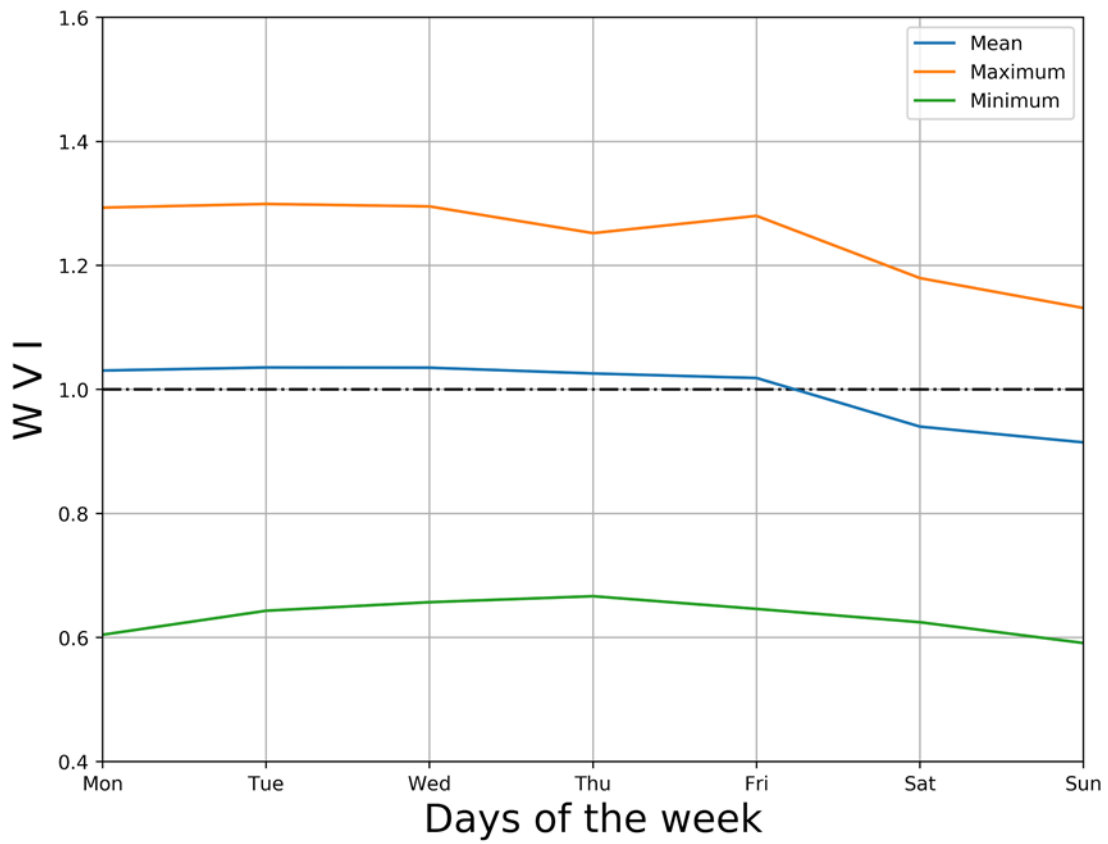


Figure 4.2: Weekly Variation Index of Daily Electricity Demand

In Figure 4.3, the hourly variation during a day (24H) is evident. In general, the Diurnal Variation Index (DVI) presents two peaks; one close to 3PM, which could be attributed to the extensive use of cooling devices mainly AC as the air temperature reaches its high maximum value around this time. The second maximum around 9 PM is due to the excessive use of lighting, fans and AC during the late afternoon and early evening hours as everybody resumes from services. Also, note that during weekends, the evening peak is much important than the afternoon peak for all the seasons.

However, differences exist among seasons regarding the peaks observed during weekdays. For instance, the afternoon peak is much more important for the season MAM and JJA while it less important for DJF compared to the evening one. Indeed, for MAM and JJA seasons, the electricity is predominantly used for cooling purposes because of the higher temperature values recorded in these seasons. On the other, during DJF seasons where low temperature values are observed, the electrical energy used is much more for lighting, TVs, and home entertainment.

Diurnal Variation Index

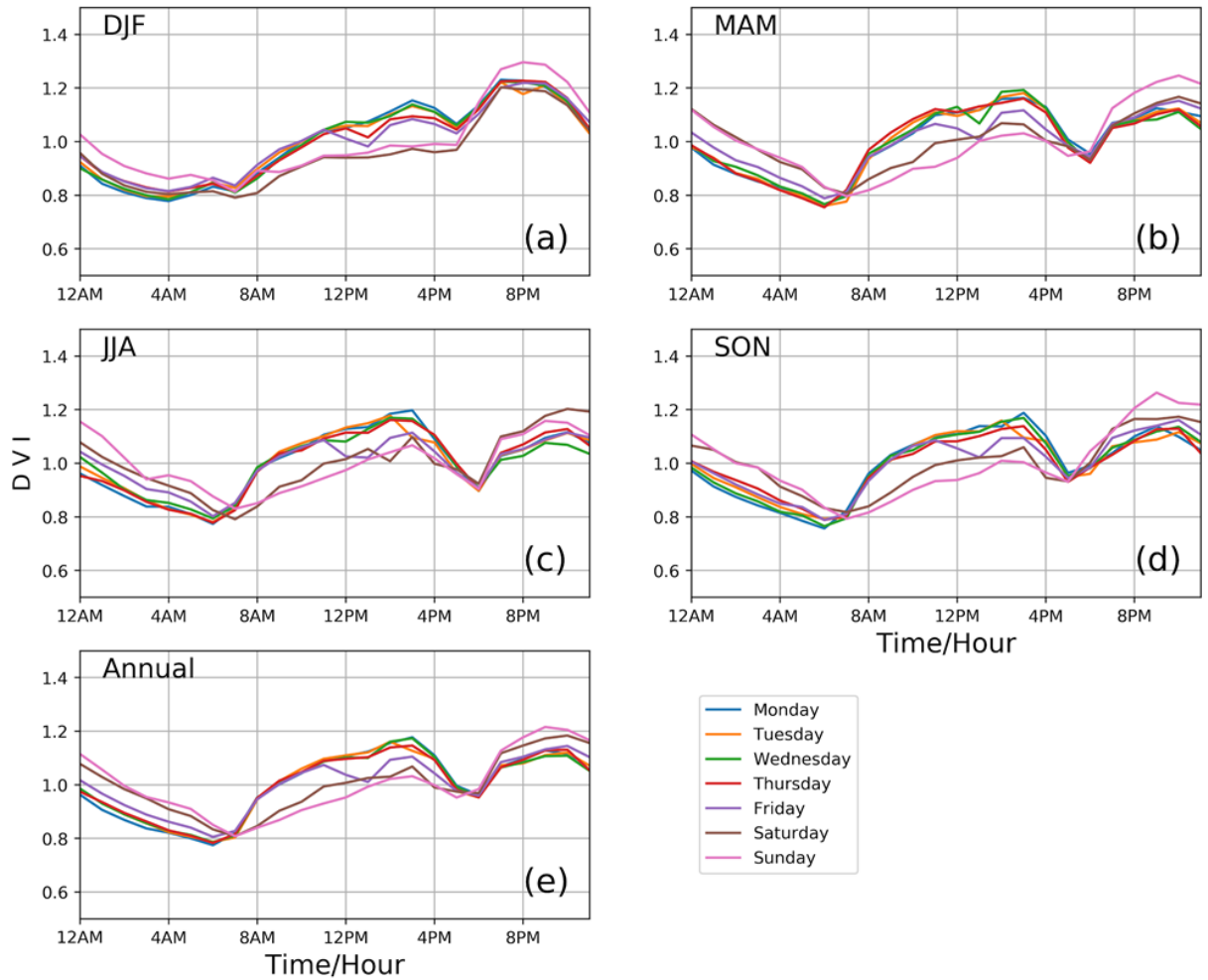


Figure 4.3: Diurnal variation Index of Electricity Load for Different Season; DJF: December January February, MAM: March April May, SON: September October November, Annual: January-December

4.2.2 Correlation between Electricity demand and Climate Variables

In this section, WTC and phase analysis are applied to illustrate the co-movement between the electricity demand and climate variables at different time-period space. The WTC indicates the regions in time-period space where the two-time series co-vary and the color code indicates different WTC ranges, ranging from blue (low correlation) to red (high correlation), adding to the significance of the regions while the phase difference between the two-time series is defined by arrows, which orientation indicates the level and type of correlation between the two series as well as the leading time series in the relationship. Hence significant coherence between air temperature and electricity demand for different periods throughout the time horizon can be identified (Figure 4.4-A)). The most significant and in phase region over the entire time horizon is observed for the period over 256 days' band indicating strong positive correlation between the temperature and electricity demand for this band period. With arrows pointing right and slightly up, the air temperature is leading the electricity demand in the relationship. This suggests a high dependence of electricity demand on air temperature as well as strong seasonal relationship between DED and temperature. In other words, high temperature during the summer period will result in higher demand for cooling purposes, while low temperature values during the winter period will decrease it. Finally, for the period band between 32-64 days' band, significant coherence between temperature and electricity demand could also be identified. This indicates the monthly relationship between the temperature and electricity demand.

Looking at Figure 4.4 B) showing the WTC and PA between the humidity and electricity demand, significant coherence can be identified for the two series. The most significant region can be identified in the 256 days' band and above with anti-phase relationship

indicating negative correlation between relative humidity and electricity demand. In other words, high humidity will lead to low energy demand. This is usually observed in July-August where the demand drops (Figure 4.1). With the phase difference in the quadrant $(-\pi/2, 0)$, the humidity is leading the electricity demand for this particular period band. However, around 128 days' period, particularly from August 2011 to 2017, significant correlation between the humidity and the electricity, with anti-phase correlation can also be observed. This also suggests negative correlation between humidity and electricity demand for this particular band. In other words, high humidity during the rainy season (June-September) will result to low energy demand.

Regarding the relationship between the radiation and electricity demand, the most significant in phase relationship is identified in the 64-256 days' period band, suggesting strong seasonal positive correlation between radiation and electricity demand. Indeed, high solar radiation will increase the temperature and thereby increase the energy requirement for cooling.

For the WTC and phase analysis between the wind and electricity demand, the most significant region can be identified around the 256 days' period with anti-phase relationship for the period 2011-2016. In other words, high wind speed will result to a decrease of the demand. With the phase difference between $(0, \pi/2)$, the wind is leading the electricity demand. The second significant region can also be identified around the 128 days' period, with anti-phase relationship for the time 2013-2014. This suggests the negative correlation between the wind and electricity demand for this period. Finally, in 2013 another significant region is observed around the period 32-64 days' band, with anti-phase relationship indicating also negative correlation between the two-time series.

Looking at WTC and phase difference between Heat Index (HI) and electricity demand, significant regions can also be identified (Figure 4.4-F)). The most significant region is identified in the 256-365 days' period band with in phase relationship for the entire time horizon. This suggests the strong seasonal relationship between the HI and electricity demand. With the phase difference between $(0, \pi/2)$, the HI is leading the electricity demand for this period. The second significant region can also be identified in the band 128-192 days, with in phase relationship, suggesting positive correlation between the two series. Moreover, some localized significant coherence can also be identified for several years across the time horizon in the period band 32-64 days, with in phase relationship.

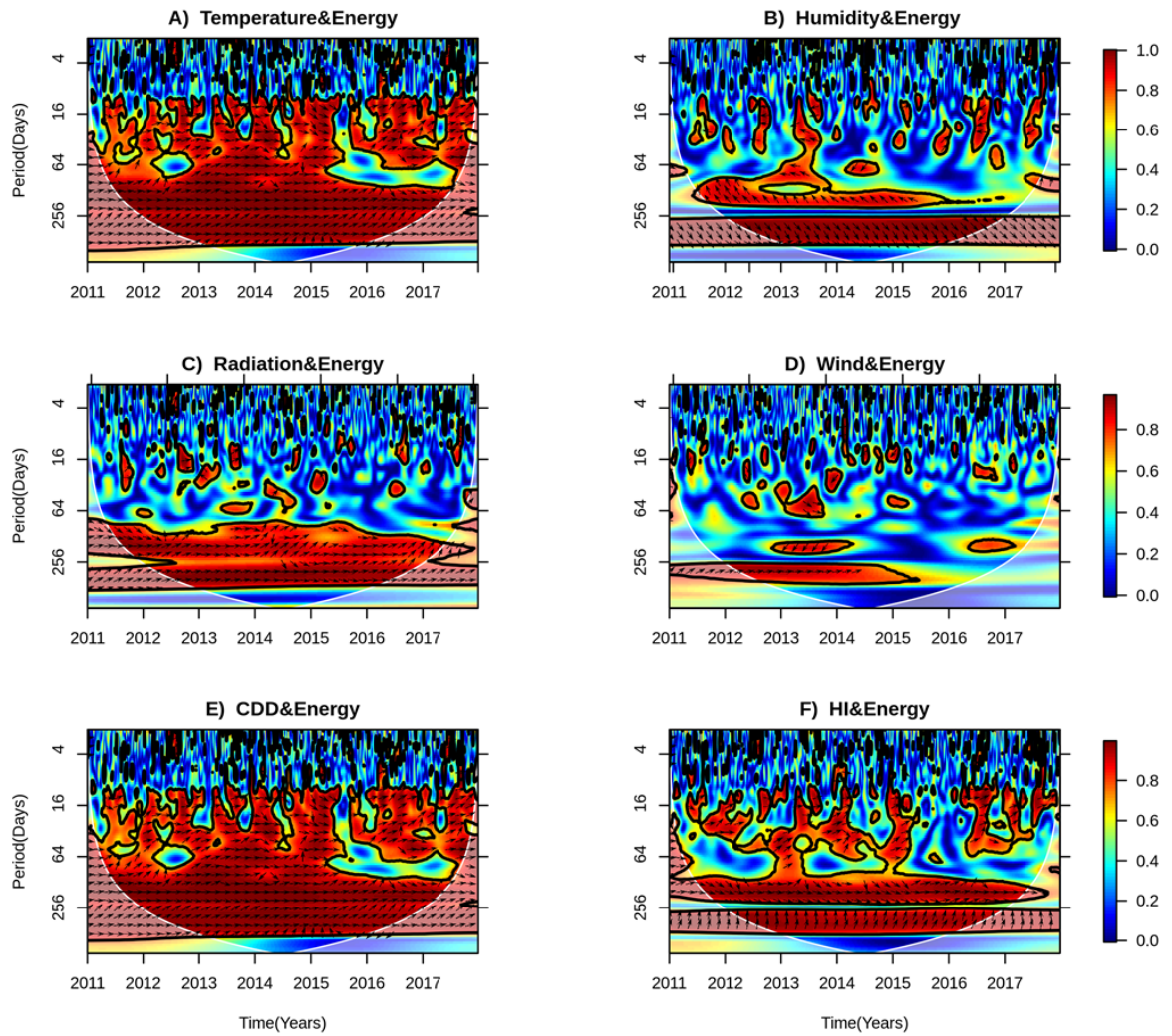


Figure 4.4: WTC and Phase Difference of Climate Variables & DED. The 5% significance level against red noise is shown as a thick contour. The relative phase relationship is shown as arrows (with in-phase pointing right, anti-phase pointing left)

4.3 Modelling the Influence of Climate Variables on Electricity Demand

4.3.1 Selection of Independent Variables

Before building the regression models, it is worth to examine the variables that are highly correlated with the electricity demand.

Table 4.1 provides the loading of the principal Component Analysis using PC1 and PC2. As stated earlier, the PCA is used in this study to group the key weather variables that are highly correlated with the electricity demand. From these results it is noticeable that the PC1 is highly correlated with the energy, Tmean, Tmin, Tmax, Radiation, and HI. In other words, there is a process that couples the increase of demand with these weather variables. Therefore, the PCA result suggests that the CDD, Tmax, Tmin, and HI are highly correlated with the electricity demand.

However, owing to the fact that the predictors should have little or no correlation with each other (i.e. the correlation coefficients should be less than 0.7) in a regression model, it is necessary to test the predictors for multi-collinearity by, for instance calculating their correlation coefficients R. Table 4.2 shows high correlations between some potential predictors. For instance, the temperature is highly correlated with the CDD, HI, Tmax, and Tmin. Hence, using either temperature or CDD with HDD, humidity, radiation, and wind could yield to acceptable equations.

Table 4.1: Principal Component Analysis Loadings of Climate Variables and Daily Electricity Demand

Variables	PC1	PC2
Energy	0.817	-0.363
CDD	0.970	-0.188
Temp	0.971	-0.190
Humidity		-0.851
Radiation	0.594	0.109
Tmax	0.928	0.324
Tmin	0.787	-0.580
HI	0.816	0.491
HDD	-0.277	0.100
Wind	0.161	-0.367
DTR		0.954
DI		
Proportion of variance	<i>0.469</i>	0.243
Cumulative variance	0.469	0.713

Table 4.2: Correlation Between Demand Energy Demand and Climate Variables

	ENE	Tmean	Tmax	Tmin	CDD	HDD	HI	WSP	Rad	RH
ENE	1									
Tmean	0.84*	1								
Tmax	0.65*	0.85*	1							
Tmin	0.82*	0.88*	0.55*	1						
CDD	0.84*	0.99*	0.85**	0.88**	1					
HDD	-	-	-0.21**	-	-	1				
	0.2**	0.25*		0.23**	0.22**					
HI	0.50	0.71*	0.9**	0.39**	0.71**	-	1			
		*				0.16**				
WSP	0.08*	0.49*	0.004	0.32**	0.24**	-	0.007	1		
	*	*				0.07**				
Rad	0.40*	0.24*	0.54**	0.36**	0.49**	-	0.43*	-0.02	1	
	*	*				0.09**	*			
RH	0.29*	0.05	-0.3**	0.36**	0.05	-	-	0.06*	0.001	1
	*					0.08**	0.50*			
							*			

ENE: Detrended Electricity Demand; Tmean: Mean Air Temperature, Tmax: Maximum Temperature; Tmin: Minimum Temperature; CDD: Cooling Degree Days; HDD: Heating Degree Days; HI: Heat Index; WSP: Wind Speed; Rad: Solar Radiation; RH: Relative Humidity

** Significant at 99% level of confidence

* Significant at 95% level of confidence

4.3.2 Evaluation of Regression Models

Regression models based on Multiple Linear Regression (MLR) and Artificial Neural Network (ANN) with different architectures were developed using the de-trended electricity data and climate variables that are highly correlated with the electricity demand. The actual and forecasted values of de-trended DED is plotted in Figure 4.5 along with the coefficient of variation as well as the Taylor diagram comparing the different forecasting techniques with the observed DED. It can be noted a close correspondence between the actual and forecasted values. However, all the forecasted techniques failed to predict the extreme values in the actual DED. In addition, all the models underestimate the standard deviation compared to the observed data. Nevertheless, the correlation between the actual and forecasted data for all the models are very high ($r > 0.9$).

Furthermore, Figure 4.6 shows the scatter plot of actual and forecasted models used in this study. It shows that most of the data points are aligned along the diagonal. This indicates that the models perform well in estimating the actual demand; confirming the ability of the selected climate variables to quantify the electricity demand.

The regression statistics (RMSE, MAE, and R^2) for the five models are summarized in Table 4.4. It can be noted that all the regression models achieve a high R^2 ($R^2 > 0.8$) and a very low RMSE ($< 140 \text{MWh/day}$) and MAE ($< 110 \text{MWh/day}$) compared to the mean observed values during the period considered (1630MWh/day). Hence, it can be safely concluded that the models are all performing well and thus the selected climate variables are able to accurately predict the electricity demand. However, the best regression model is given by the ANN (4, (3,2),1) with the highest R^2 ($R^2 = 0.86$) and lowest RMSE (RMSE=122.08) and MAE (MAE=91.79).

Table 4.3: Regression Statistics of the Five Models Considered in This Study

	RMSE (MWh)	MAE (MWh)	R ²
MLR	139.23	107.67	0.825
ANN(4,2,1)	132.13	101.15	0.842
ANN(4,4,1)	123.21	99.77	0.863
ANN(4,(2,1),1)	132.42	101.07	0.841
ANN(4,(3,2),1)	122.08	91.79	0.865

ANN (4,2,1): four input variables (CDD, RH, Rad, and WSP), one hidden layer with 2 neuros, and one output variable.

ANN (4,4,1): four input variables (CDD, RH, Rad, and WSP), one hidden layer with 2 neuros, and one output variable.

ANN (4, (2,1),1): four input variables (CDD, RH, Rad, and WSP), two hidden layer with 2 neuros in the first layer and one neuron in the second layer, and one output variable.

ANN (4, (3,2),1): four input variables (CDD, RH, Rad, and WSP), two hidden layer with 3 neuros in the first layer and 2 neurons in the second layer, and one output variable.

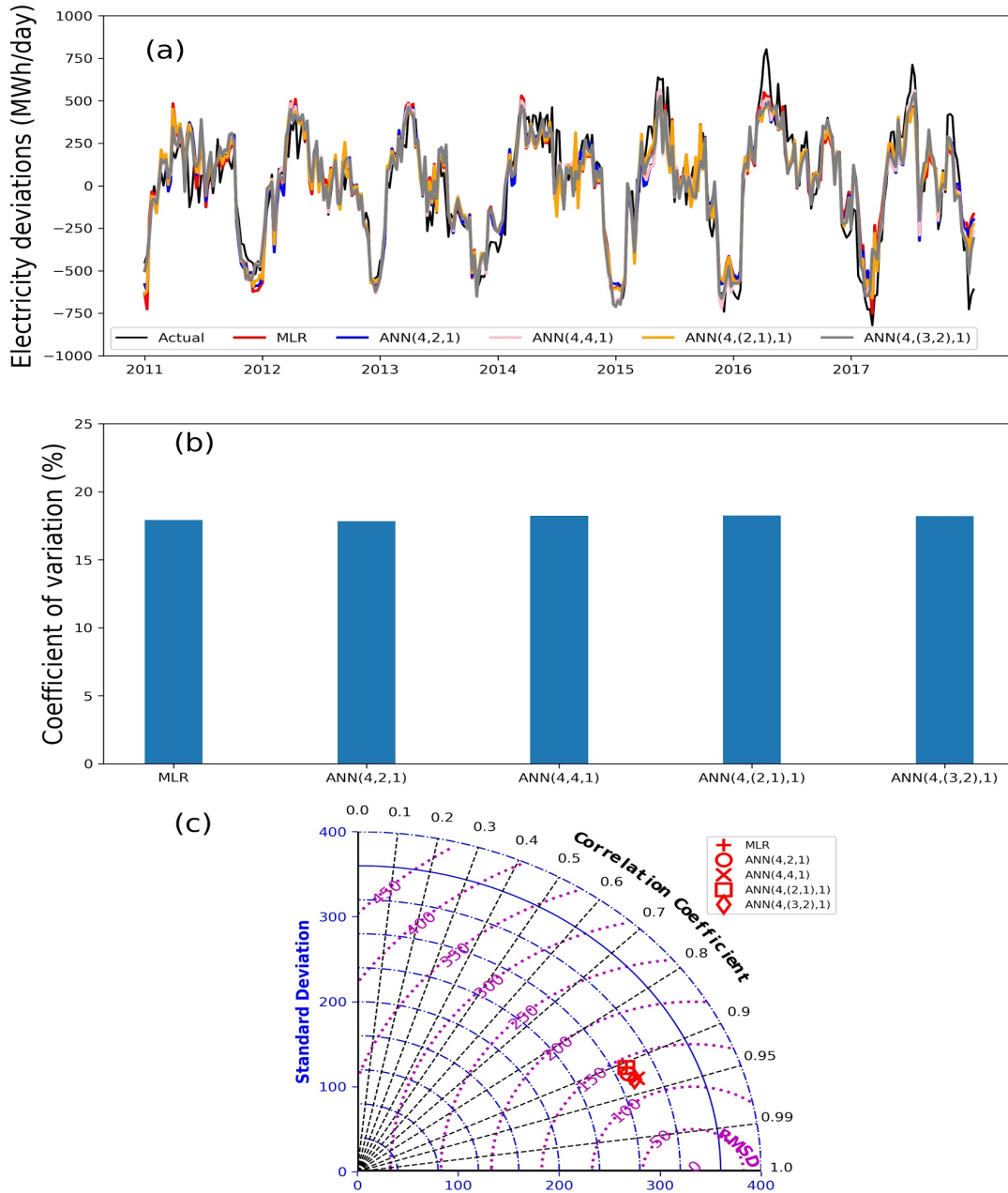


Figure 4.5: Validation of Regression Models using (a): time series plot of observed and predicted values, (b): Coefficient of Variation and (c): Taylor Diagram

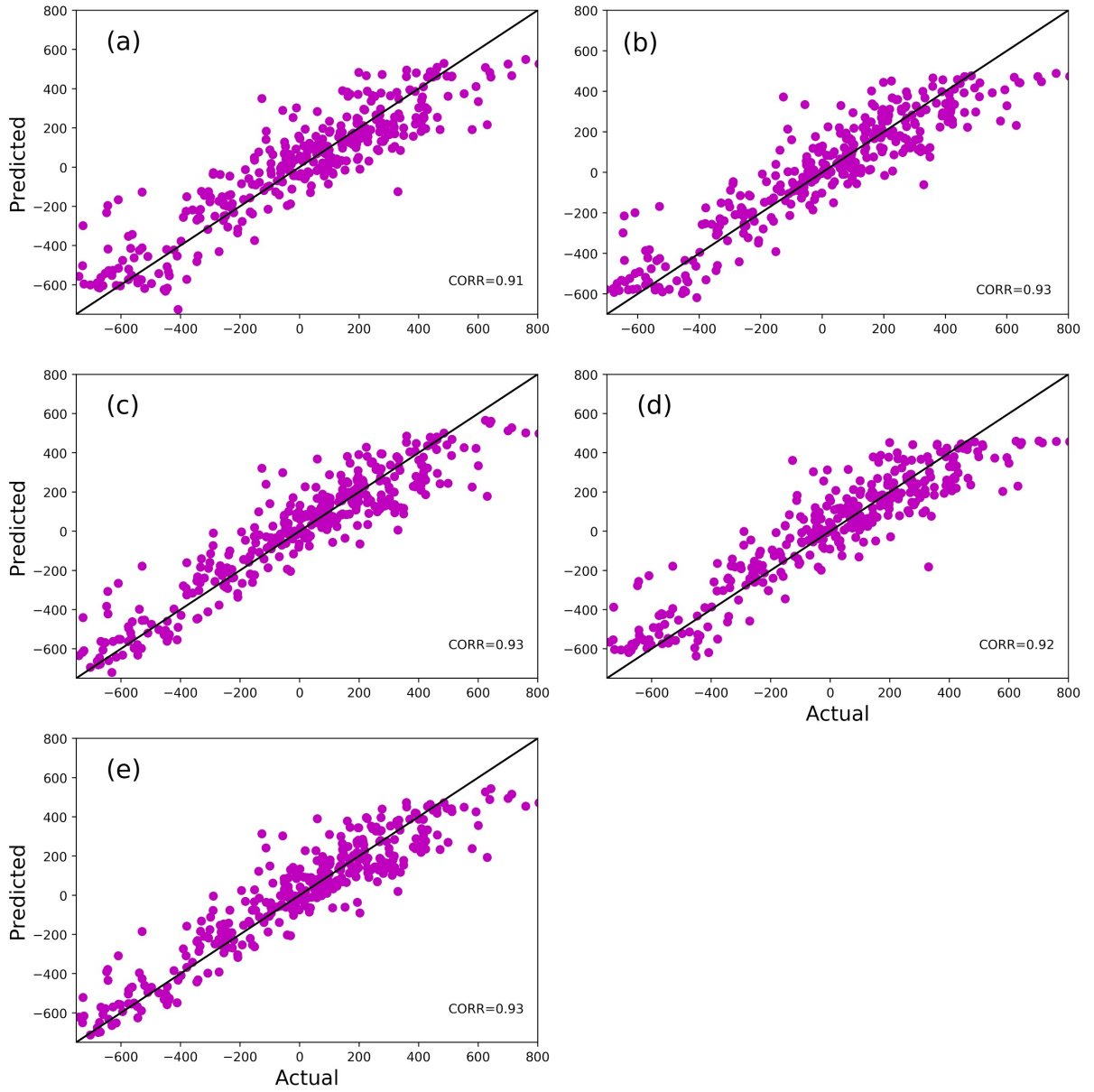


Figure 4.6: Scatter Plots of Actual Against Predicted Values for (a): MLR, (b): ANN(4,2,1), (c): ANN(4,4,1), (d): ANN(4, (2,1),1), and (e): ANN(4,(3,2),1)

Furthermore, the residual plots are also taken in to account when analyzing the homogeneity of the variance and the histogram of the standardized residuals of each model in order to find out whether the models comply with the basic assumptions of regression models. Figure 4.7 shows that the residuals are randomly distributed (no specific curvature or pattern can be identified) and follow normal distribution for all the models. Moreover, the standardized residuals are within $[-2, 2]$, indicating that the observations are within 95% confidence interval level. Consequently, it can be safely concluded that the models comply with the assumptions of the regression models and thus can be used to predict the impacts of climate change on energy demand.

Hence the resulting electricity consumption is given in equation 4.1:

$$DED = -588.28 + 79.22 * CDD + 3.79 * RH - 0.33 * Rad - 39.54 * WSP \quad (4.1)$$

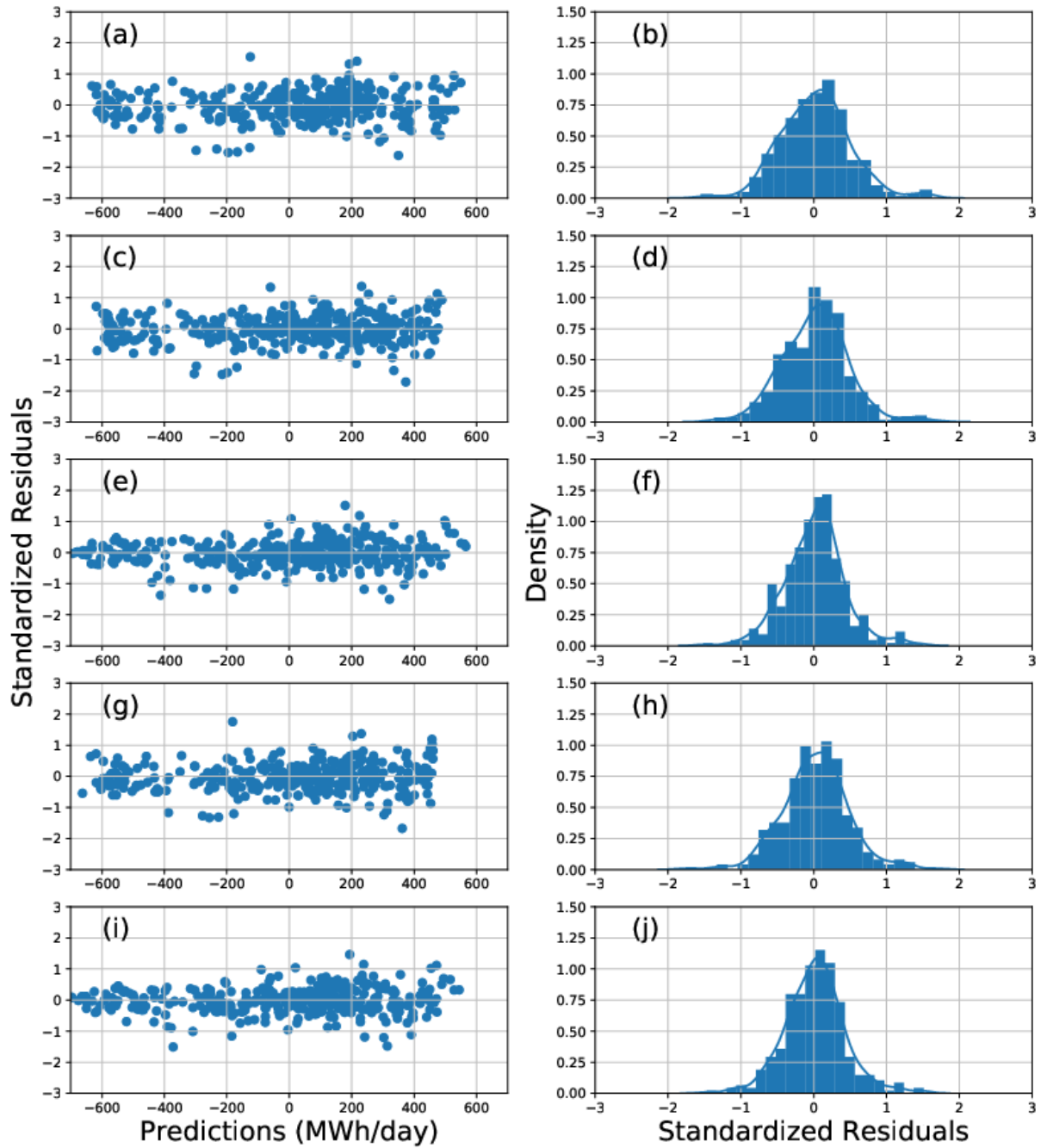


Figure 4.7: Scatter Plots of Residual Against Predicted Values (Left Panel) and the Histogram of Standardized Residuals (Right Panel) for the Different Regression Models

Table 4.4: Regressions Coefficients and Their Corresponding P-Values

Variables	Coefficients	P values
Intercept	-588.28	0.000
CDD	79.22	0.000
RH	3.79	0.000
Rad	-0.33	0.000
WSP	-39.54	0.000

4.4 Evaluation of CORDEX RCMs Simulations

To predict the impacts of climate change on electricity demand using the simulated RCMs data, it is mandatory to assess the ability of these RCMs in reproducing the present climate. Hence, the selected climate variables used to build the electricity model were evaluated by comparing the CORDEX RCMs data with the Princeton Global Forecasting Data (PGFD). The RCMs give a realistic simulation of all the necessary variables used to develop the electricity model (Figure 4.8, 4.9 and 4.10). The models adequately reproduce the spatial distribution of temperatures (T_{mean} , T_{max} , and T_{min}), Relative Humidity (RH), Solar Radiation (SR), and Wind Speed (WSP) (Figure 4.8). For all the variables, the correlation between the simulated and observed field is high ($r > 0.8$) and significant (at 99% confidence level) except for the RH and WSP where the correlation is respectively 0.69 and 0.55. Nonetheless, noticeable biases are observed between simulated and observed fields (Figure 4.8). For instance, the RCMs ensemble mean features a cold bias over the entire country (up to $-6\text{ }^{\circ}\text{C}$ in T_{min} and T_{max} and up to $-10\text{ }^{\circ}\text{C}$ in T_{mean}). The cold bias translates to an underestimation of temperatures (T_{mean} , T_{max} , and T_{min}) over the country. The RCMs also underestimate the SR over the entire country. Indeed, While the observation features a maximum SR over the Northern part of up to $300\text{W}/\text{m}^2$, the RCMs ensemble mean shows a maximum value of about $280\text{W}/\text{m}^2$ over a narrower area. The associated bias is up to $-50\text{W}/\text{m}^2$, suggesting that the models highly underestimate the SR. Contrary, the models overestimate the WSP and RH with a bias up to $1.5\text{m}/\text{s}$ and up to 10% respectively.

While these biases might result from the deficiency of RCMs, they may also come from the deficiency of the PGF data used for the validation. For instance, PGF data is a hybrid

observation-reanalysis datasets created by combining global observation datasets and reanalysis datasets (NCEP-NCAR) (Sheffield et al. 2006). Hence because of the very low density of the observational network over the country, the PGF data might not be able to capture the spatial variability of the climate variables. Notwithstanding, it may capture the day-to-day variation of most of the climate variables used in this study.

The RCMs ensemble mean also adequately reproduce the spatial distribution of Cooling Degree Day (CDD) and heat indices (HI and DI) (Figure 4.9). Indeed, the correlation is very high ($r > 0.9$) for CDD and DI except for HI where the correlation is 0.62. In both cases, the correlation is significant (at 99% confidence level). However, some biases are also observed between the observed and simulated datasets. The RCMs ensemble mean overestimate the CDD over the entire country with a bias of up to 10 °C, with the highest in the Northern part of the Country. This might be due to low density of the observational network. While for the HI, the RCMs ensemble mean underestimate the Heat Index (HI) over the Southern part of the country (up to 3 °C), it overestimates it in the Northern part (also up to 3°C). For the Discomfort Index (DI), the RCMs underestimate this variable over the entire country with a bias up to 3°C.

Figure 4.10 also shows that the RCMs reproduce well the annual cycle of daily electricity demand and the climate variables (CDD, Tmean, Tmin, Tmax, HI, DI, RH radiation, and WSP). In most cases the observed annual cycles lie within the RCMs ensemble spread except for CDD for which the RCMs models fail in reproducing the peak value observed in May and October and also for WSP where the RCMs fail in reproducing the minimum values of wind speed observed in April. Furthermore, both observed and simulated cycles show high values of DED, CDD, HI, DI, and Tmax in April-June and October, and high

values of WSP in June-July, reflecting the seasonal movement of the Intertropical Discontinuity (ITD) and December-February, reflecting the prevailing harmattan conditions. In both the observed and simulated curves, the minimum values of solar radiation occur in August while the maximum values occur in March-April. However, significant discrepancies can be observed between the RCMs in simulating the observed climate variables. This is translated by the models ensemble spread observed for many variables. Hence, the use of the ensemble mean simulations is crucial in projecting the future climate.

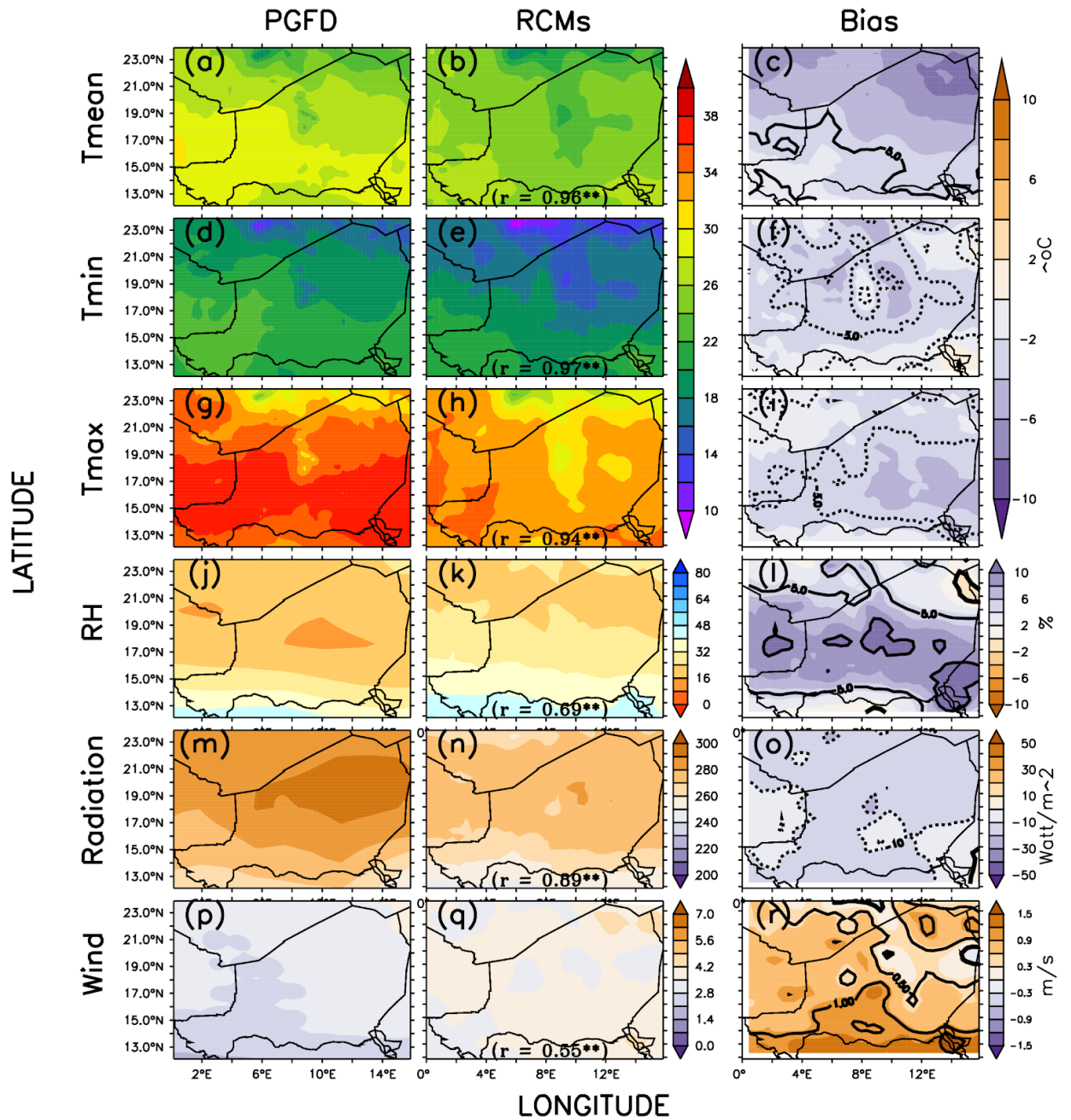


Figure 4.8: Spatial Distribution of Climate Variables over Niger as Depicted by PGFD and CORDEX RCMs Ensemble Mean in Reference period (1971-2000).

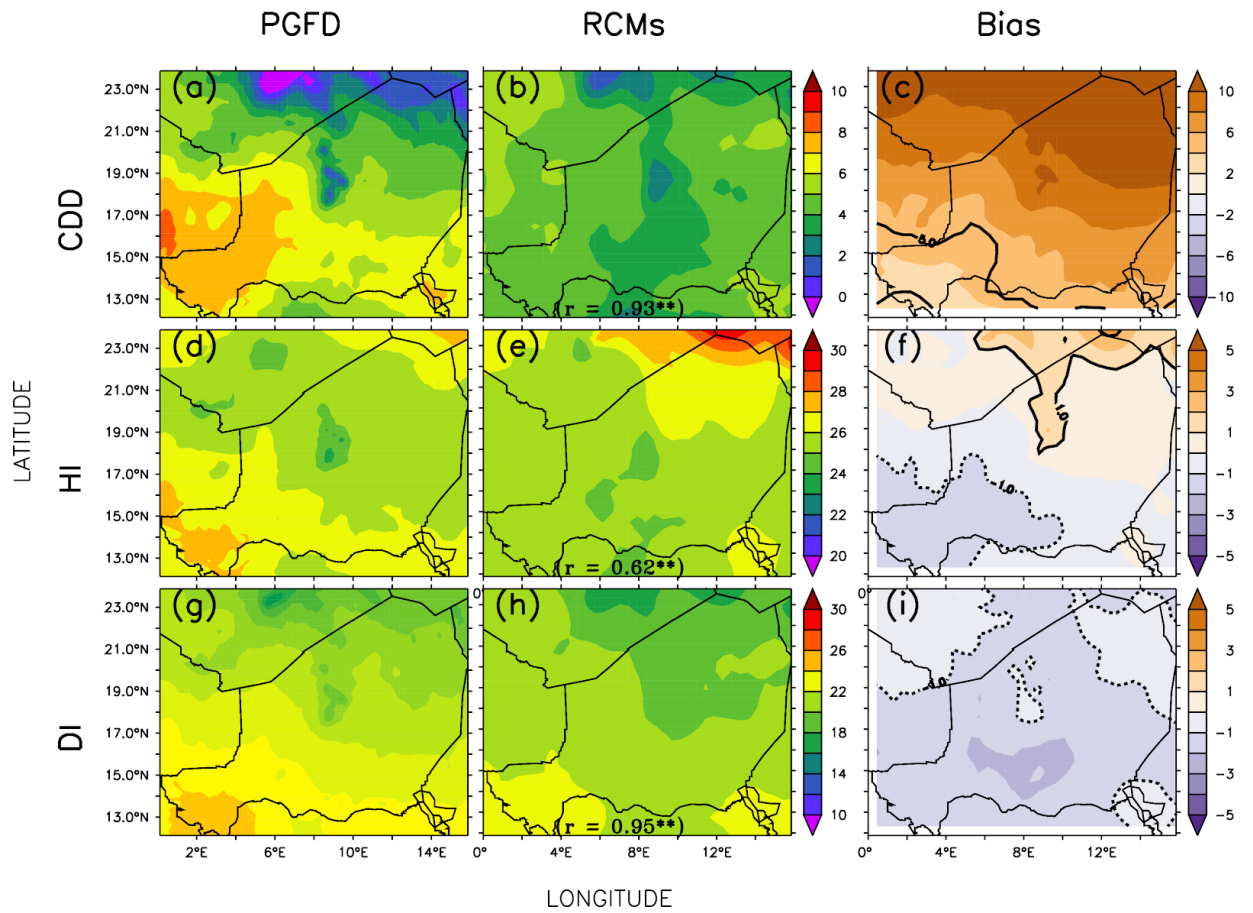


Figure 4.9: Spatial Distribution of Climate Variables over Niger as Depicted by PGFD and CORDEX RCMs Ensemble Mean in Reference period (1971-2000).

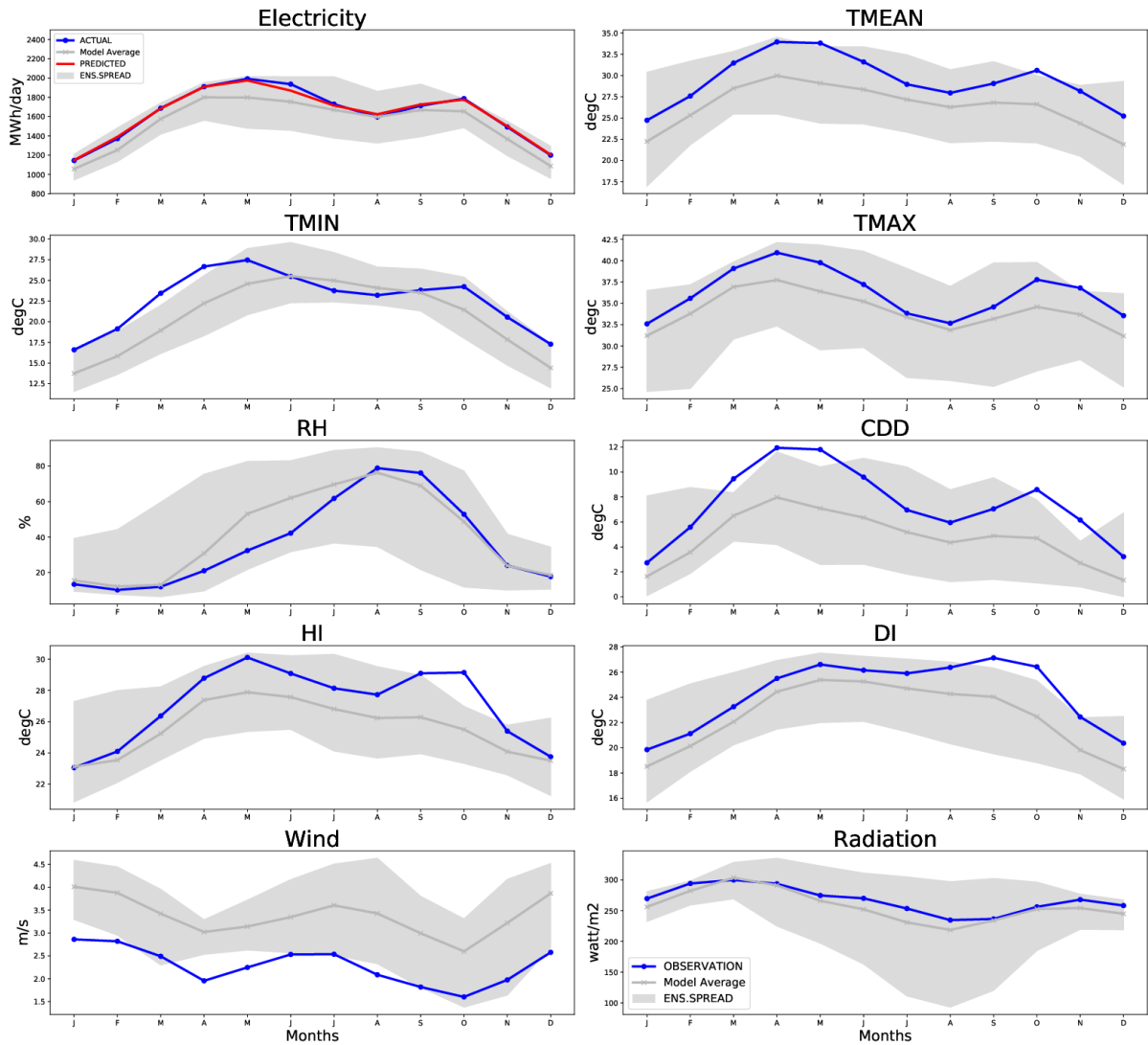


Figure 4.10: Annual Cycle of Daily Energy Demand and the Relevant Climate Variables Used to Build the Multiple Linear Regression Model in Niamey as Depicted by Observation and CORDEX RCMs

4.5 Future Projection of Daily Electricity Demand and Different Predictors

4.5.1 Mean Changes in Daily Electricity Demand and Relevant Predictors at specific Global Warming Levels

The CORDEX ensemble mean projects an increase of daily electricity demand over the entire country for all the GWLs (Figure 4.11a-d). However, the magnitude of the increase varies across the country and grows with increasing of GWLs. For instance, at GWL1.5, the changes are rather homogenous (between 4 and 8% increase in DED) over the entire country. In addition, the changes are robust (i.e. statistically significant at 99% confidence level). However, at GWL2.0, the increase in DED varies across the country, from 4 to 8% in the central part of the country to 8-12% in the remaining part of the country. Compared with changes at GWL1.5, an additional increase (up to 3%) in DED is observed over most part of the country. Conversely, a further increase in warming level beyond 2° will enhance the DED over the entire country, such that, at GWL3.0, most part of the country becomes hotspots of increase in DED due to climate change. This suggests that failing to keep the global warming level below or at 2° (level set by the Paris agreement) may have serious consequences on DED over the entire country. Indeed, an additional increase (up to 9.5% compared to GWL1.5) could be observed over most part of the country, with the highest increase around Niamey. The increase in DED over the entire country is robust (i.e. statistically significant at 99% confidence level) at all the GWLs. These findings are consistent with the conclusions of several studies which suggested that climate change will increase the electricity consumption in tropical countries (*Santamouris et al., 2015; Scapin et al., 2015; Huang and Hwang, 2016; Ang et al., 2017* among others). Moreover, Figure 4.11 shows that the projected changes in DED are consistent with the changes in CDD, and RH variables. For instance, the increase in DED may be attributed to the increase of CDD

and the decrease of RH. This is expected since high CDD will require more DED for cooling purposes while high RH reduce the demand. In fact, Figure 4.11 e-h indicates that the spatial correlation between the changes in DED and CDD is very high (>0.9) and significant (99% confidence level) at all the GWLs. Moreover, the increase in CDD is in agreement with the result of *Klutse et al. (2018)* who found an increase of temperature over the region as a result of climate change. Finally, the changes in DED are also in agreement with the changes of RH because of the fact that the humidity and DED are negatively correlated (Figure 4.4). So a decrease in relative humidity will lead to an increase in DED, which is observed in Figure 4.11a-d. Nonetheless, for both of SR and WSP, the projected changes are not consistent with changes observed in DED. For instance, one might have expected a decrease in SR result in a decrease in DED, because of the positive relationship between DED and SR (Figure 4.4). But the reverse is the case. This might be due to the fact that the impacts of the other climate variables (CDD, and RH) overwhelm those of SR on DED. Indeed, the absolute spatial correlation between DED and the radiation is weak ($r<0.3$) and not significant. Similarly, an increase in wind speed could also have resulted to a decrease of DED because of the negative relationship between DED and wind (Figure 4.4), but this is not the case. This can also be explained by the fact the wind has weak influence on electricity demand. The spatial correlation between wind and DED is weak ($r<0.3$) and not statistically significant.

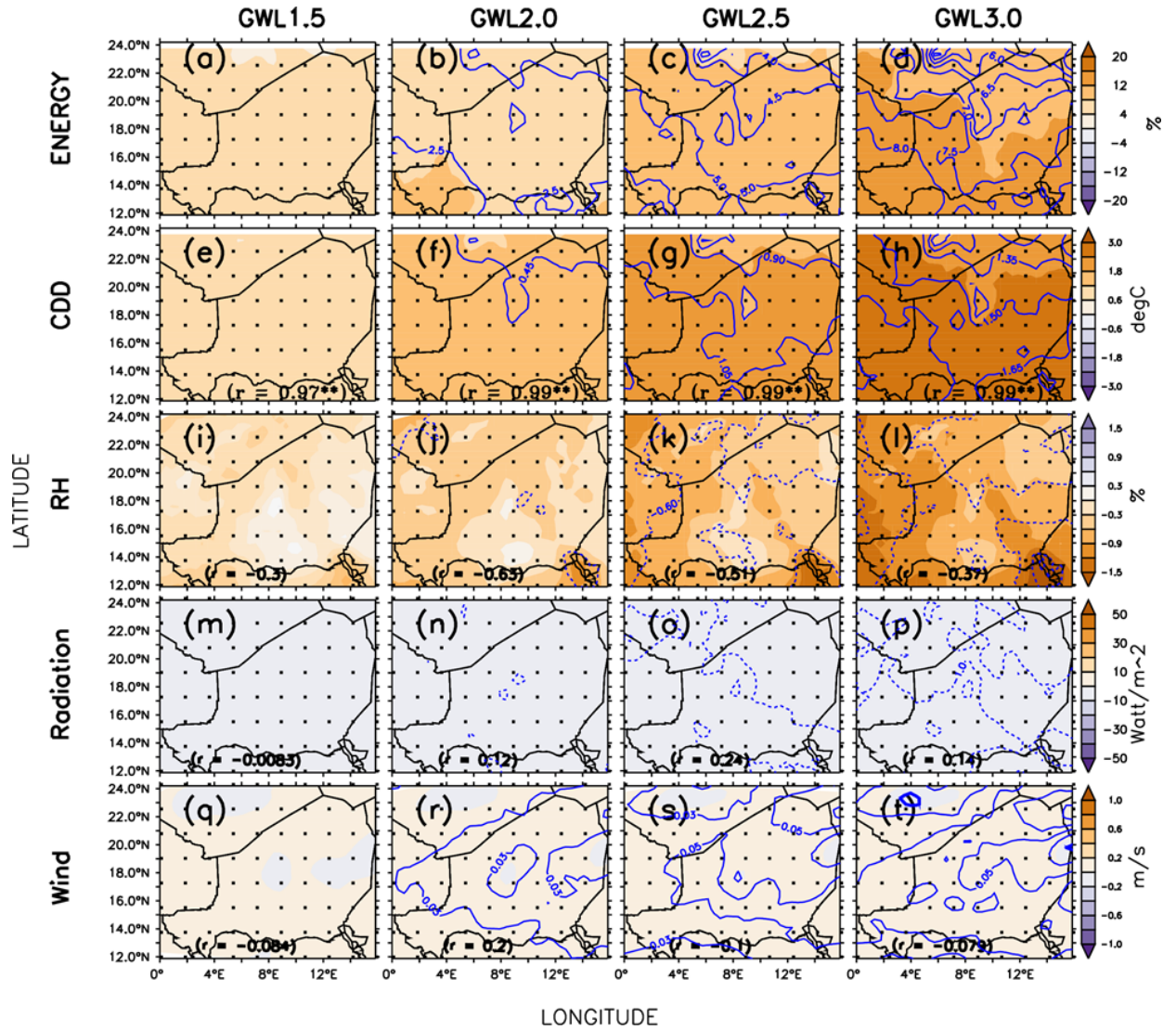


Figure 4.11: Projected Changes in DED (panel: a-d), CDD (e-h), RH (i-l), Radiation (m-p), and Wind (q-t) at different global Warming Level (GWL1.5, GWL2.0, GWL2.5, and GWL3.0).

The level of agreement among the models on the projections (a measure of robustness in the projected changes in the electricity demand over Niger), depends on the GWLs and the various variables (Figure 4.12). In general, agreement among simulations is better for the projections of Tmax, DED, CDD, and HI than RH, Radiation and Wind projections. For instance, almost all the simulations agree on the projections of the Tmax, DED, CDD, and HI for all the GWLs. This indicates that the projections of DED, CDD, and HI are robust at all the GWLs. The ensemble median of DED indicates an increase of about 5%, 7%, 12% and 15% for GWL1.5, GWL2.0, GWL2.5, and GWL3.0 respectively. The least agreement among the simulations is observed for the Radiation where the simulations do not agree on the projections of these variables for any of the GWLs. Nevertheless, the ensemble median of radiation indicates a decrease for this variable, with the magnitude of the decrease increasing with global warming level. However, for the RH and WSP, more than 75% of the simulations agree on the projections at GWL2.5 and GWL3.0. Hence, this indicates that changes in both RH and WSP are only robust for the warming level above 2°. It may also be noted that for all the variables, the spread among simulations increases with increasing global warming (Figure 4. 12).

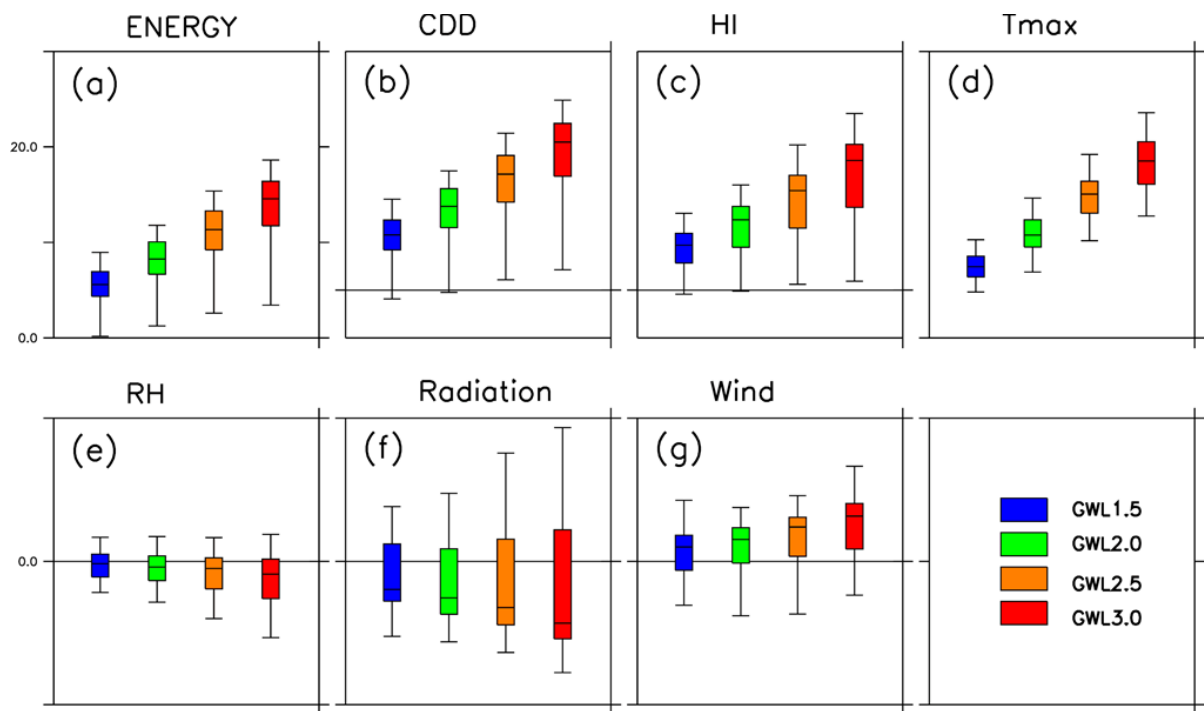


Figure 4.12: Projected changes in a-) DED, b-) CDD, c-) HI, d-) Tmax, e-) RH, f-) Radiation, and g-) Wind at specific GWLs in Niger

4.5.2 Seasonal Changes in DED, CDD and HI

The projected changes of Daily energy demand (DED), Cooling Degree days (CDD), and Heat Index (HI), and Discomfort Index (DI) are sensitive to seasons and Global Warming considered (Figure 4.13, 4.14, 15 and 4.16). For instance, the changes in DED varies with seasons and increasing GWLs. Looking at Figure 4.13, a general increase in DED can be observed over the entire country and the magnitude of the increase varies across the country with the GWLs and seasons. For instance, the magnitude of increase is much more important for March-May (MAM) and June-August (JJA) than that of December-February (DJF). For example, at GWL1.5, the ensemble median is projecting around 8% increase in DED in MAM and JJA while for DJF season, it projects an increase of about 1% in DED. These values go up under GWL3.0 and reach about 18% for MAM and JJA and about 5% for DJF. This is expected since, during DJF season, less energy is consumed because of relative cold weather observed in this season while in MAM, and JJA seasons more energy is required for cooling purposes. However, the robustness of the changes is better in DJF than the other season and the least robustness is observed for September-November (SON). Nevertheless, for all the seasons, at least 85% of simulations project that climate change will increase the DED at all the GWLs though the magnitudes of the increase vary with the seasons. Note that for all the seasons, the magnitude of increase grows with increasing GWLs.

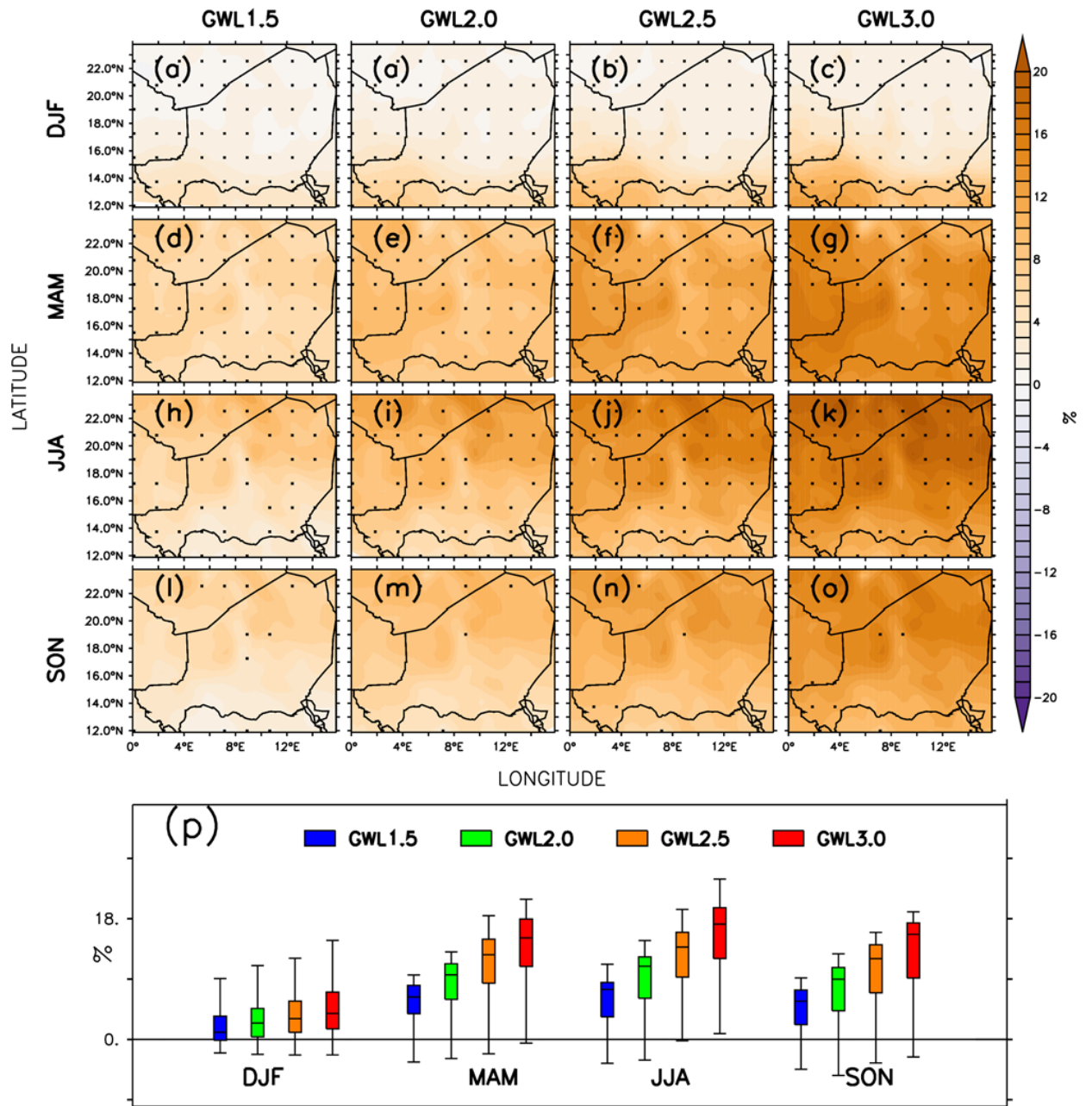


Figure 4.13: Projected changes of DED at different GWL for different seasons: DJF: December-February, MAM: March-May, JJA: June-August and SON: September-November.

Also, an increase in CDD is projected over the entire country for all the seasons with the magnitude of the increase growing with increasing GWLs (Figure 4.14). For instance, a general increase in CDD is observed over the entire country with the ensemble median growing with increase of GWLs. Indeed, at GWL1.5, the ensemble median indicates an increase of about 0.2°C, which grows to about 0.3 °C at GWL2.0, and 1 °C at GWL3.0 for DJF. Despite the fact that almost all the projections agree on the directions of change, the projections are not robust (statistically significant at 99% confidence level) for this season. However, for the season MAM, significant increase in CDD is projected as a result of climate change, with the magnitude of increase increasing with GWLs. The ensemble median indicates respectively an increase of about 1, 1.5, 2, and 2.5 increase in CDD for GWL1.5, GWL2.0, GWL2.5, and GWL3.0. It is also worth noting that the changes are statistically significant. The same pattern of changes can be observed for the two other seasons, JJA and SON, but with different magnitudes. Indeed, high magnitude of increase can be observed for JJA compared to MAM while for SON the magnitude of increase is lower than that of MAM.

Hence, the global warming predicts major changes in cooling degree days over Niger for all the seasons. Owing to the fact that the CDD is derived from the mean temperature, it can be safely concluded that these results are consistent with the previous studies, which have also projected an increase of temperature over west Africa (*Klutse et al., 2018, IPCC, 2013*).

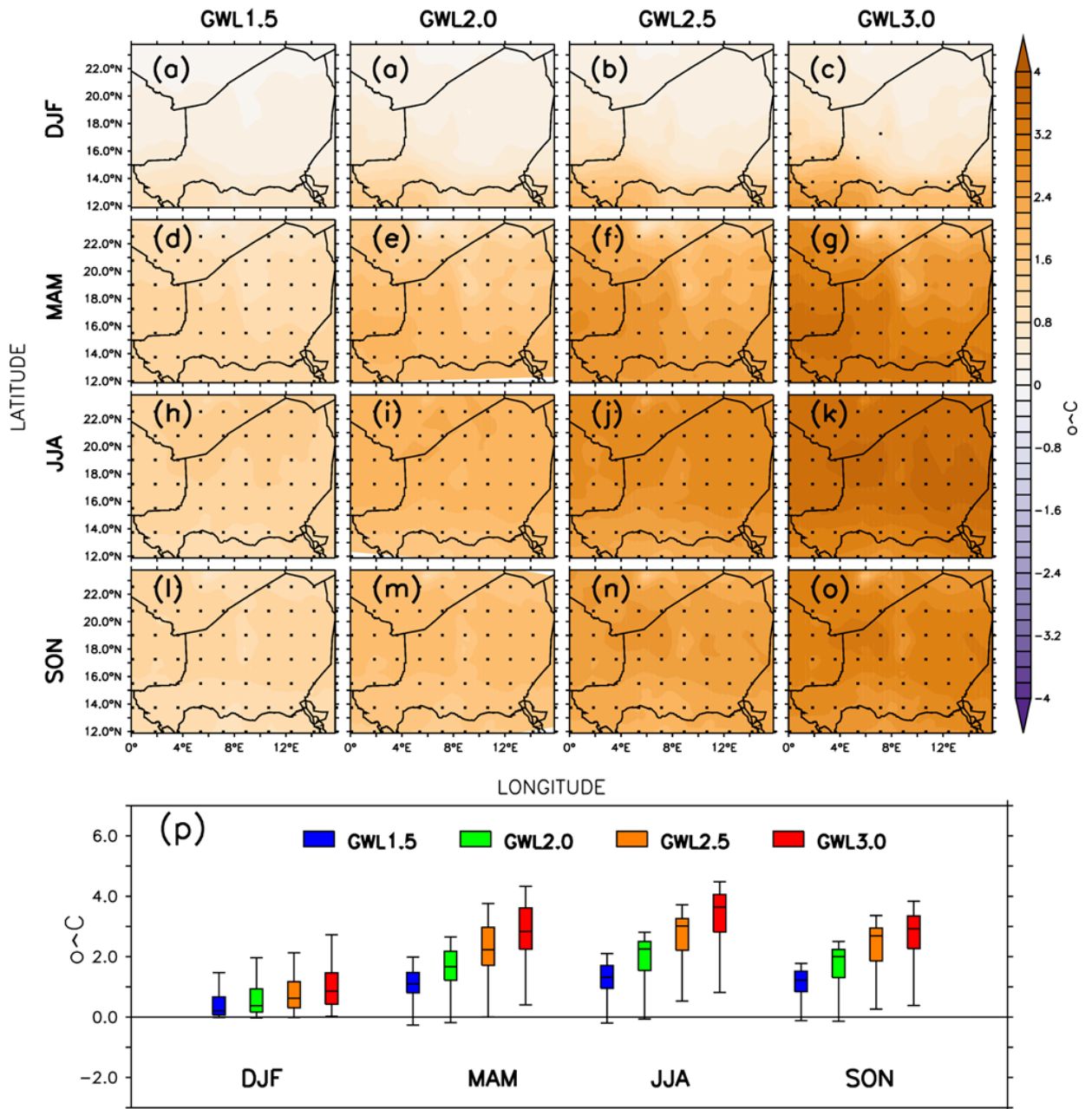


Figure 4.14: Projected changes of CDD at different GWL for different seasons: DJF: December-February, MAM: March-May, JJA: June-August and SON: September-November.

Figure 4.15 presents the projected changes of HI over Niger for different seasons and at different GWLs. However, the magnitude and direction of changes depends on GWLs and seasons considered. For instance, for DJF, a general decrease is observed over most part of the country, with the magnitude of the decrease growing with the increasing of GWLs. The ensemble median indicates a decrease of -0.5 for GWL1.5 and -1 for GWL3.0. The decrease in HI is robust for all the GWLs. Unlike DJF, a general increase is observed for the other seasons (MAM, JJA, and SON). For example, a general increase in HI is observed for the MAM season, with the magnitude of the increase growing with increasing GWLs. The ensemble median shows an increase of about +0.5, 1, 1.25 and 1.5 for the GWL1.5, GWL2.0, GWL2.5, and GWL3.0 respectively. The increase in HI is robust (statistically significant at 99% confidence level). For the JJA, a significant increase of HI is also observed over the entire country with the magnitude of the increase growing with increasing GWLs. The ensemble median projects an increase of 1, 1.5, 2 and 2.5 of increase in HI for GWL1.5, GWL2.0, GWL2.5, and GWL3.0 respectively. The inter-quartile simulations spread also indicates that most of the simulations (at least 99%) project an increase of HI, suggesting that all simulations agree on the direction of change.

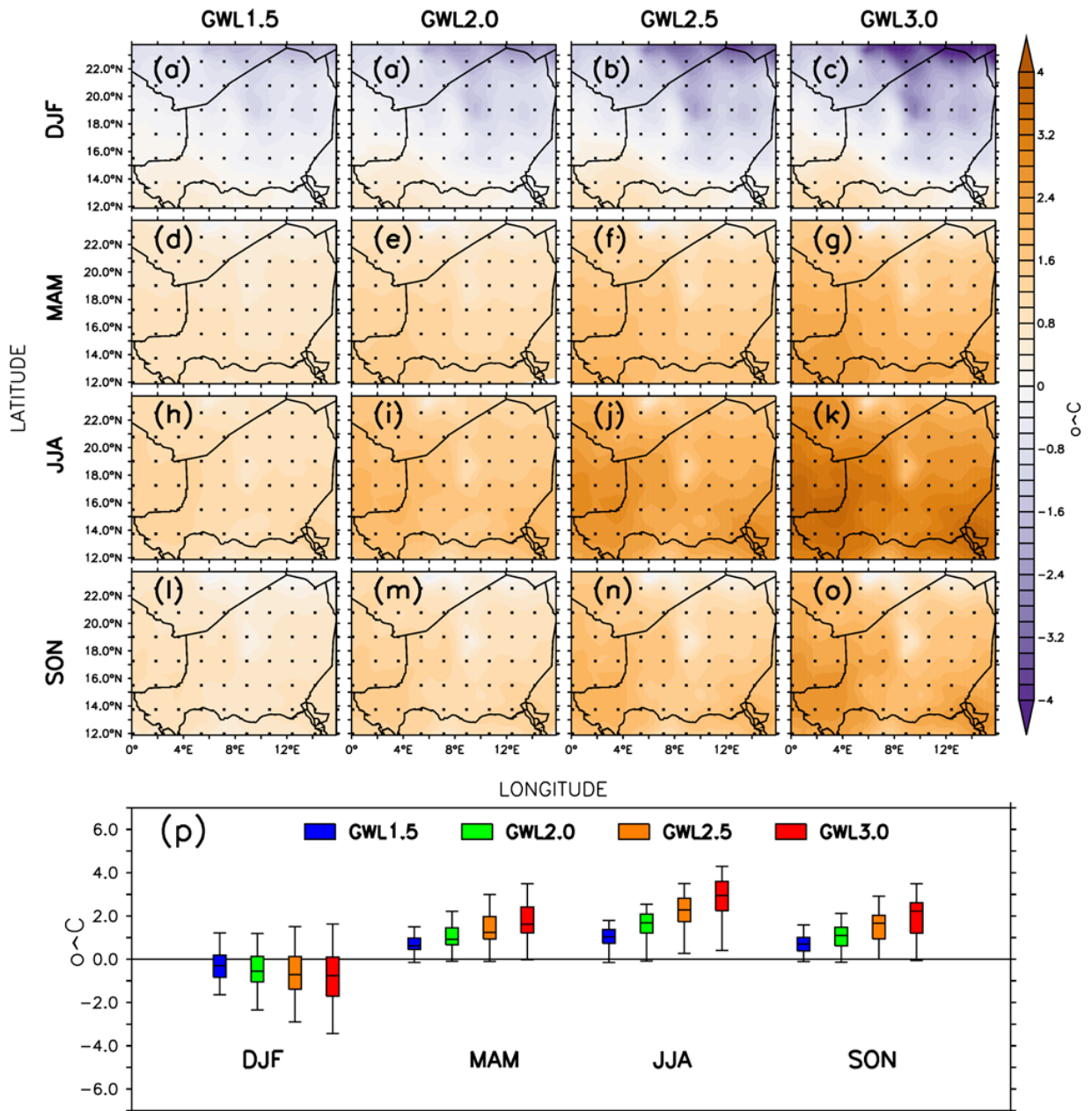


Figure 4.15: Projected Changes of HI at Different GWL for Different Seasons: DJF: December-February, MAM: March-May, JJA: June-August and SON: September-November.

The RCMs ensemble mean projects an increase of Discomfort Index (DI) for all the seasons at all the GWLs (Figure 4.16). However, the magnitude of the increase differs from one season to another and grows with the increasing GWL. In fact, for DJF, a general increase of DI is observed over the entire country with the magnitude of the increase grows with increasing GWLs. At GWL1.5, the changes are rather homogenous (about 1 °C) in most part of the country and the ensemble median indicates an increase of 0.75°C. The changes are robust (statistically significant at 99% confidence level). At GWL2.0, the DI increase by about 1.2°C over most part of the country with an ensemble median of about 1.4 °C. The changes are also robust. A warming beyond 2 °C will lead to more increase in DI such that at GWL3.0, a maximum increase of about 1.8 °C will be resulted. The ensemble median also features an increase of 1.8 °C. Similar changes are also observed for the other seasons (MAM, JJA, and SON). However, higher increase of DI is observed for JJA compared DJF season. Indeed, at GWL3.0, the RCMs ensemble mean features an increase of up to 3 °C. Moreover, the inter-quartile simulations spread also indicates that most of the simulations (at least 99%) project an increase of DI, suggesting that all simulations agree on the direction of change.

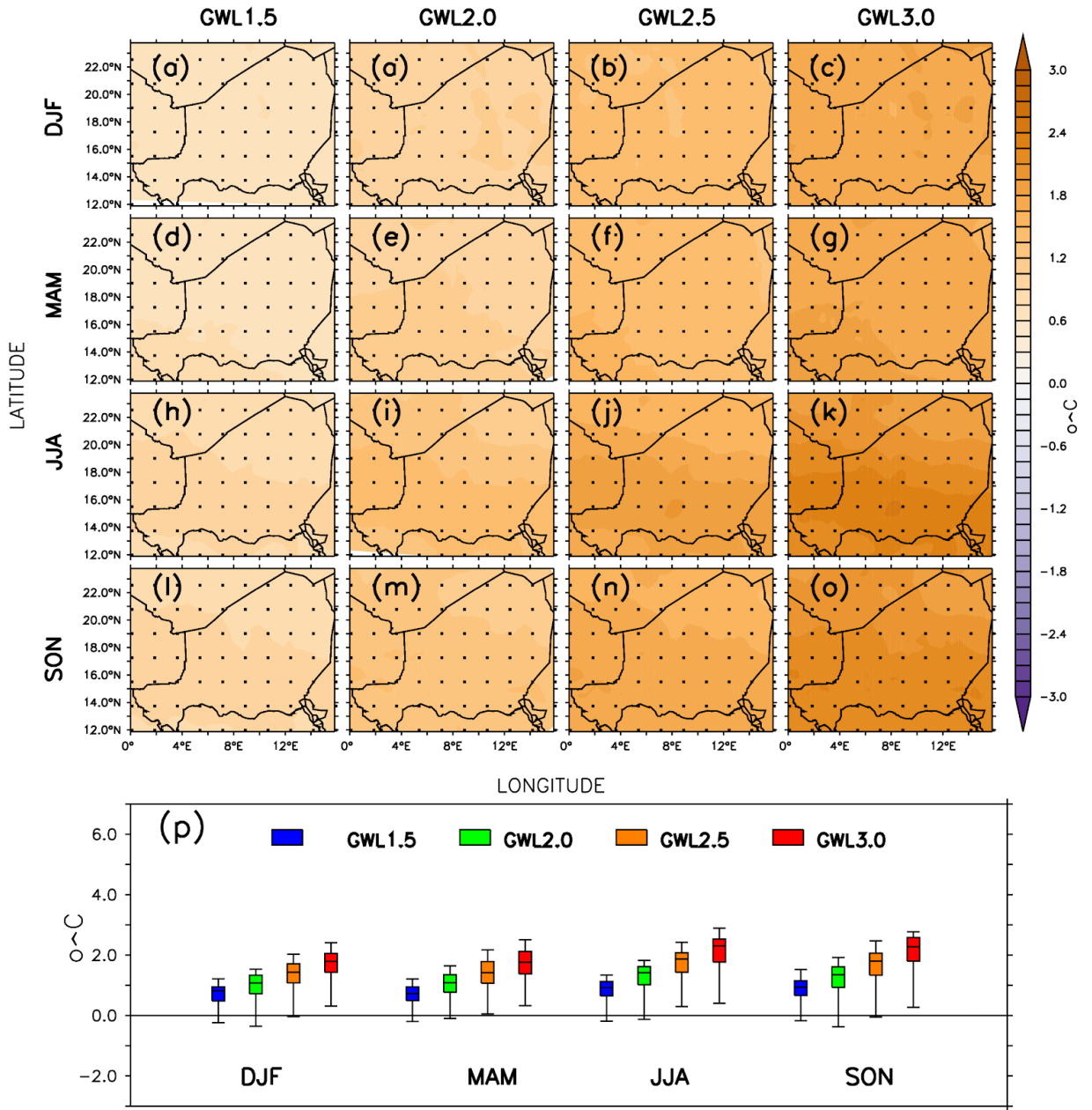


Figure 4.16: Projected changes in Discomfort Index at different Global Warming Levels for different seasons: DJF: December-February, MAM: March-May, JJA: June-August and SON: September-November.

4.5.3 Temporal Pattern of Changes in Predictors

The trend of changes in electricity predictors (Tmean, Tmax, Tmin, CDD, HI, DI, RH, Radiation and WSP) relative to the 1971-2000 reference period and expressed in percentage terms were averaged over Niger and presented in Figure 4.16. These predictors are projected to increase except for radiation where a slight decrease is observed in the 21st century under both RCP4.5 and RCP8.5 scenarios. However, the magnitude of the increase depends on both the predictor and the climate change scenario. Indeed, the CDD is projected to increase by more than 100% and 50% for the RCP8.5 and RCP4.5 respectively at the end of the century (Figure 4.16). Consequently, the electricity demand will significantly increase at the end of the century because of the very strong relationship between the CDD and electricity demand. The mean temperature is also projected to increase respectively by about 10% and 20% under RCP4.5 and RCP8.5 scenarios by the end of century. A moderate increase is also observed for both HI (about 5% increase under RCP4.5 and 10% under RCP8.5) and DI (about 2% increase under RCP4.5 and 8% increase under RCP8.5), and Tmin (1% increase under RCP4.5 and 2.5% under RCP8.5) at the end of the century. Finally, a very low change of SR and WSP can also be observed under the two RCP scenarios. In fact, the RCMs ensemble mean project a quasi-stationary evolution of solar radiation at the end of this century though the tendency shows a slight decrease for both RCPs. However, the slope is too low (< 0.1) to talk about any significant change. For the WSP, a slight increase is observed at the end of the century for both RCPs (about 1% increase under RCP4.5 and 2% under RCP8.5) (Figure 4.17 (i)).

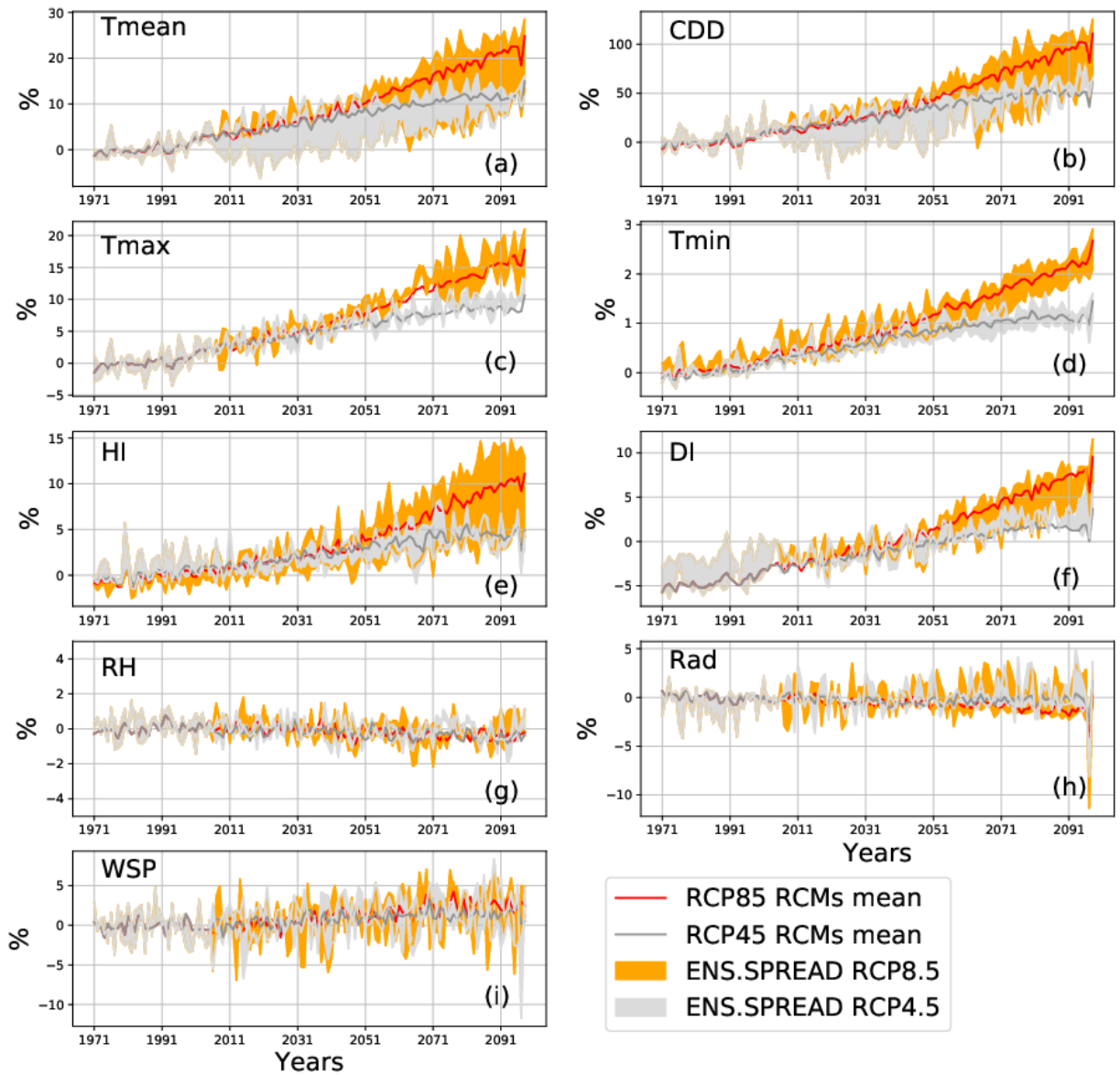


Figure 4.17: Long-Term Time Series Evolution of Electricity Predictors Displayed as Anomalies from the Reference Period (1971-2000) and Averaged Over the Entire Country (Niger)

4.5.4 Projected Changes in near (2021-2050) and far (2070-2099) future

The broad scale pattern of changes of Daily energy demand are different for the two RCPs as well as the period considered, with RCP8.5 exhibiting larger magnitude of increase than the RCP4.5 (Figure 4.18). For instance, under RCP4.5, a total increase in DED is observed over the Western part of the country (4 to 6% increase for the near Future and 8 to 10% for far future) while under RCP8.5, one can observe an increase in DED of more than 20% for far future.

In addition, the agreement between RCMs simulations on projected changes is better for far future than that of near future. For instance, for both RCP8.5 and RCP4.5, the projected changes of DED are not robust (statistically significant at 99% confidence level) for near future (2020-2049) over the Western part of the country while for the far future (2070-2099), the RCMs simulations indicate that the projected changes in DED are robust over the entire country. However, at least 75% of the simulations agree that the DED will increase under both RCP and for the two-time period considered.

It is also worth noting the spatial distribution of changes in DED across the country differs from one RCP to the other as well as the period considered. Indeed, the pattern of changes of DED are spatially more heterogeneous for the far future under RCP8.5.

Note that since variation in the simulated data solely results from day to day climate variables mainly CDD, Radiation, humidity and wind, the resulting changes are completely climate induced.

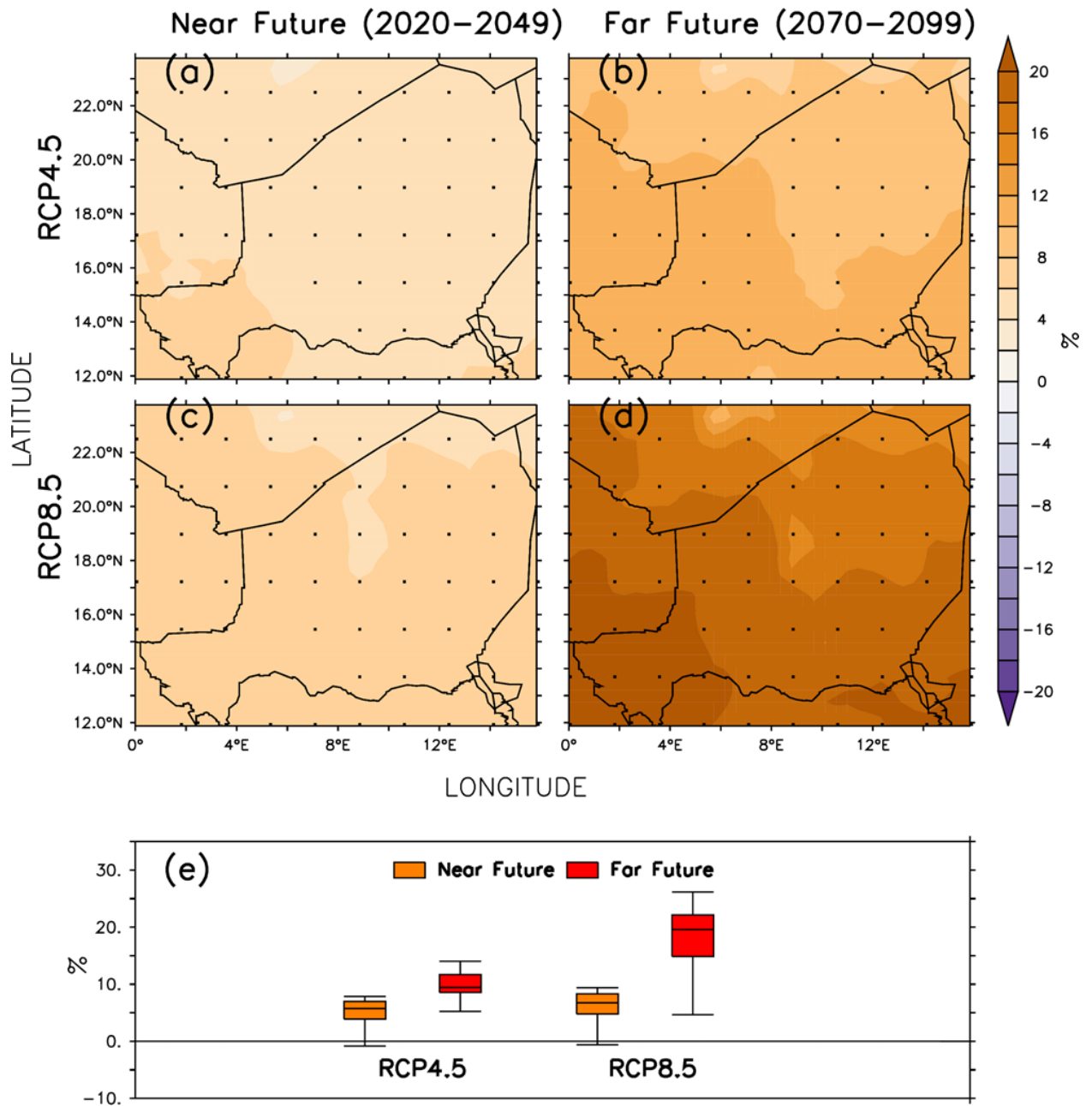


Figure 4.18: Projected changes in Daily Energy Demand expressed in Percentage (%) With Respect to the Reference Period 1971-2000 and Averaged over Two Time Periods as simulated by the RCMs for the Two RCP Scenarios.

Both RCPs project an increase in Cooling Degree-Days with the magnitude of the changes varies across the country and the period considered (Figure 4.19). For instance, under RCP4.5, an increase of CDD (0.8 to 1.2°C for near future and 2 to 2.4 °C for far future) is observed over the Western part of the country. However, the spatial extent of the changes differs from one period to the other. Indeed, for the near future, the hotspot of changes covers a smaller area compared to that of far future period. Also the spatial pattern of changes is more heterogeneous for the far future compared to that of near future. On the other hand, under RCP8.5, an increase of CDD (0.8 to 1.2 °C for the near future and up to 4 °C for far future) can be observed with the hotspot of increase located around the Western part of the country. Similarly, the spatial extent of the hotspot varies with the period considered. Indeed, for the near future period, the changes in CDD seem to be homogeneous compared to that of the far future where the hotspot is located over the western part. Hence, the impacts of climate change differ with the RCP scenario considered as well as the period used to quantify it. These changes in CDD are consistent with various climate change studies, which also projected an increase of Cooling Degree Days for both RCPs. Furthermore, looking at the impacts of climate change on HI, a general increase can also be observed, with the magnitude of changes varies across the country and the period considered. For instance, under RCP4.5, the highest increase located in the western part shows an absolute increase of HI of about 0.8 to 1.2 °C for near future and 1.2 to 1.6 °C for far future. On the other hand, an absolute increase can be observed over the hotspot of about 4 °C under RCP8.5 and for the far future period. However, the spatial pattern is more heterogeneous for RCP8.5 than that of RCP4.5. Also, note that the agreement among the simulations is better for RCP8.5 than that of RCP4.5 though for both RCPs, 99% of the simulations project an increase of heat index (HI).

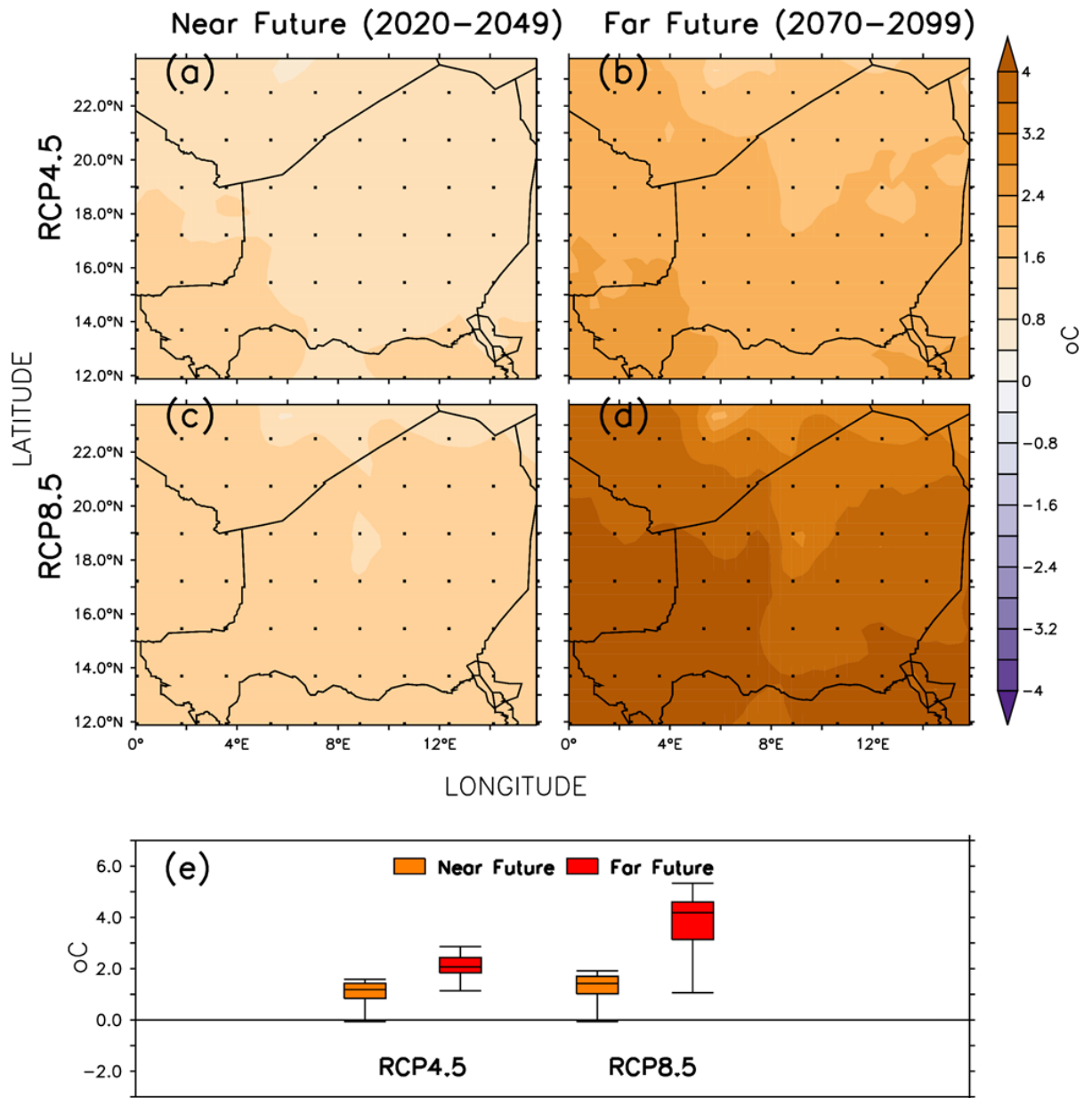


Figure 4.19: Projected changes in Daily CDD with Respect to the Reference Period 1971-2000 and Averaged Over Two Time Periods as Simulated by the CORDEX RCMs for the two RCP scenarios.

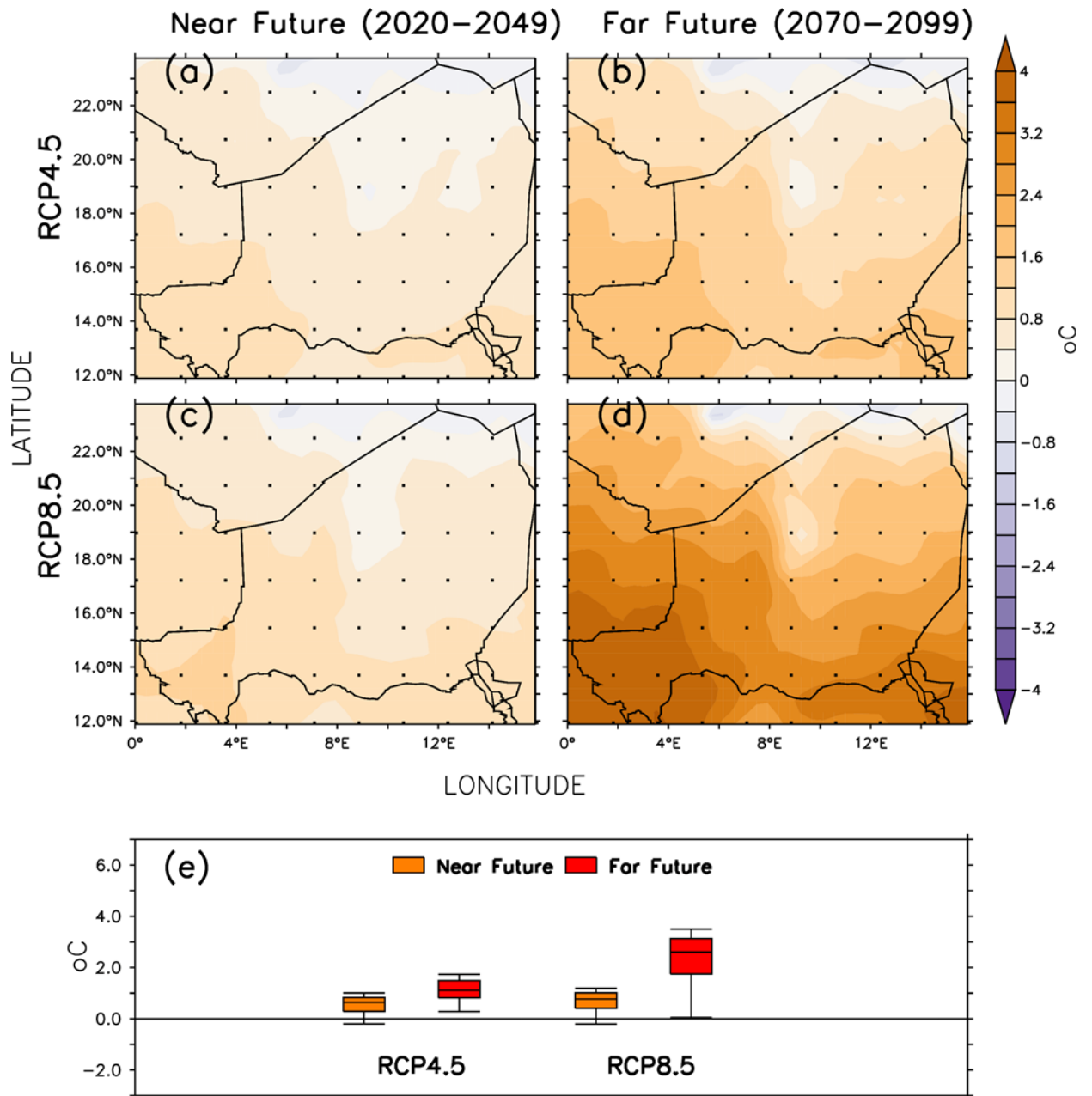


Figure 4.20: Projected Changes of HI with Respect to the Reference Period 1971-2000 and Averaged Over Two Time Periods as Simulated by the CORDEX RCMs for the two RCP scenarios.

Finally, the RCMs ensemble mean also project an increase of Discomfort Index (DI), with the magnitude increase varies across the country and grows with the time horizon (Figure 4.21). For instance, under RCP4.5, the highest increase located in the western part shows an absolute increase of DI of about 0.8 to 1.2 °C for near future and 1.2 to 1.8 °C for far future. On the other hand, an absolute increase can also be observed under RCP8.5 over the South of about 0.8 to 1.2 °C for near future and 3 °C for the far future period. However, the spatial pattern is more heterogeneous at RCP8.5 than that of RCP4.5. Also, note that the agreement among the simulations is better for far future period than that of near future period though for both RCPs, 99% of the simulations project an increase of DI. In addition, the changes for near future are quite the same for both RCPs except the fact that under RCP8.5, the increase in DI covers larger area than RCP4.5.

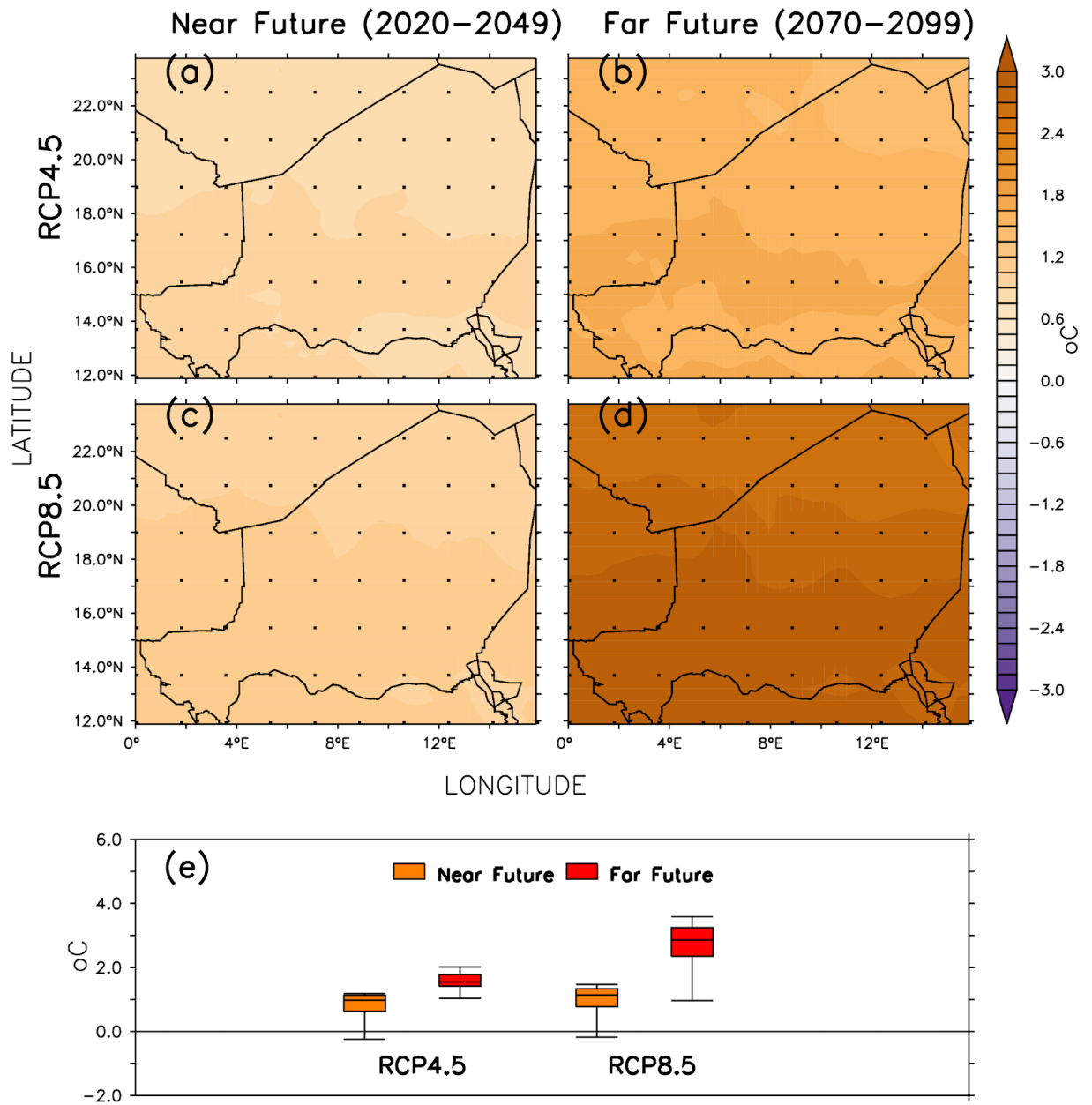


Figure 4.21: Projected Changes of DI with Respect to the Reference Period 1971-2000 and Averaged Over Two Time Periods as Simulated by the CORDEX RCMs for the two RCP scenarios.

4.6 Influence of Extreme Heat and Heat waves on Electricity Demand

In addition to mean changes in electricity demand, it is important to look at extraordinarily high demand either due to extreme temperature (hot days, and warm nights) or heatwaves, which is particularly relevant for network reliability. For this purpose, a closer look of extreme temperatures and heat waves on peak demand will be considered in this section.

4.6.1 Influence of Extreme Temperatures on Peak Electricity Demand

To investigate the impact of extreme heat on electricity demand, the frequency distribution of electricity load higher than 110MW (90th percentile of demand during the study period) as well as the frequency distribution of temperature higher than 40, DI higher than 29 °C, and HI higher than 39 °C are calculated and compared. Results are presented in Figure 4.22. High extreme temperatures are responsible for extreme heat and discomfort indices resulting to extreme electricity demand (Figure 4.22). For instance, high frequencies of Temperature, DI and HI in March, April, May, June and October are followed by high frequencies of electricity demand in the same months while lower frequencies of these variables in January, February, July, September, November and December are also followed by low frequencies of electricity load for these months. This suggest high relationship between the frequency distribution of electricity load and these variables (Temperature, DI, and HI). Indeed, the correlation between the frequency distribution of electricity load and the frequency distribution of these climate variables are very high ($r>0.8$).

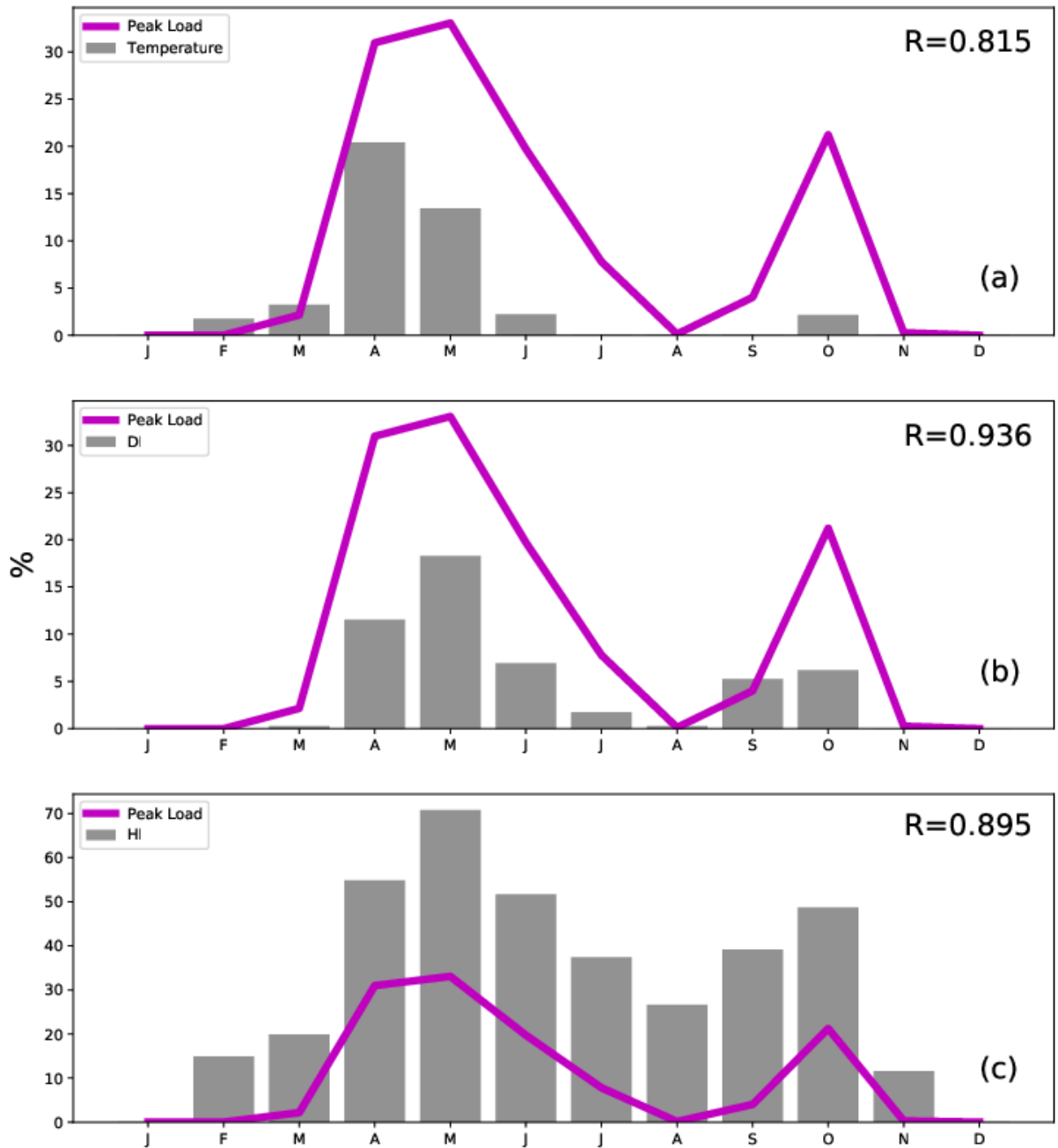


Figure 4.22: Frequency Distribution in (%) of days Peak Load > E90 (90th Percentile of Electricity Load) with (a) $T > 40$, (b) > 29 , and (c) > 39 . R Denotes the Correlation Between the Extreme Load and Extreme Heat Indices

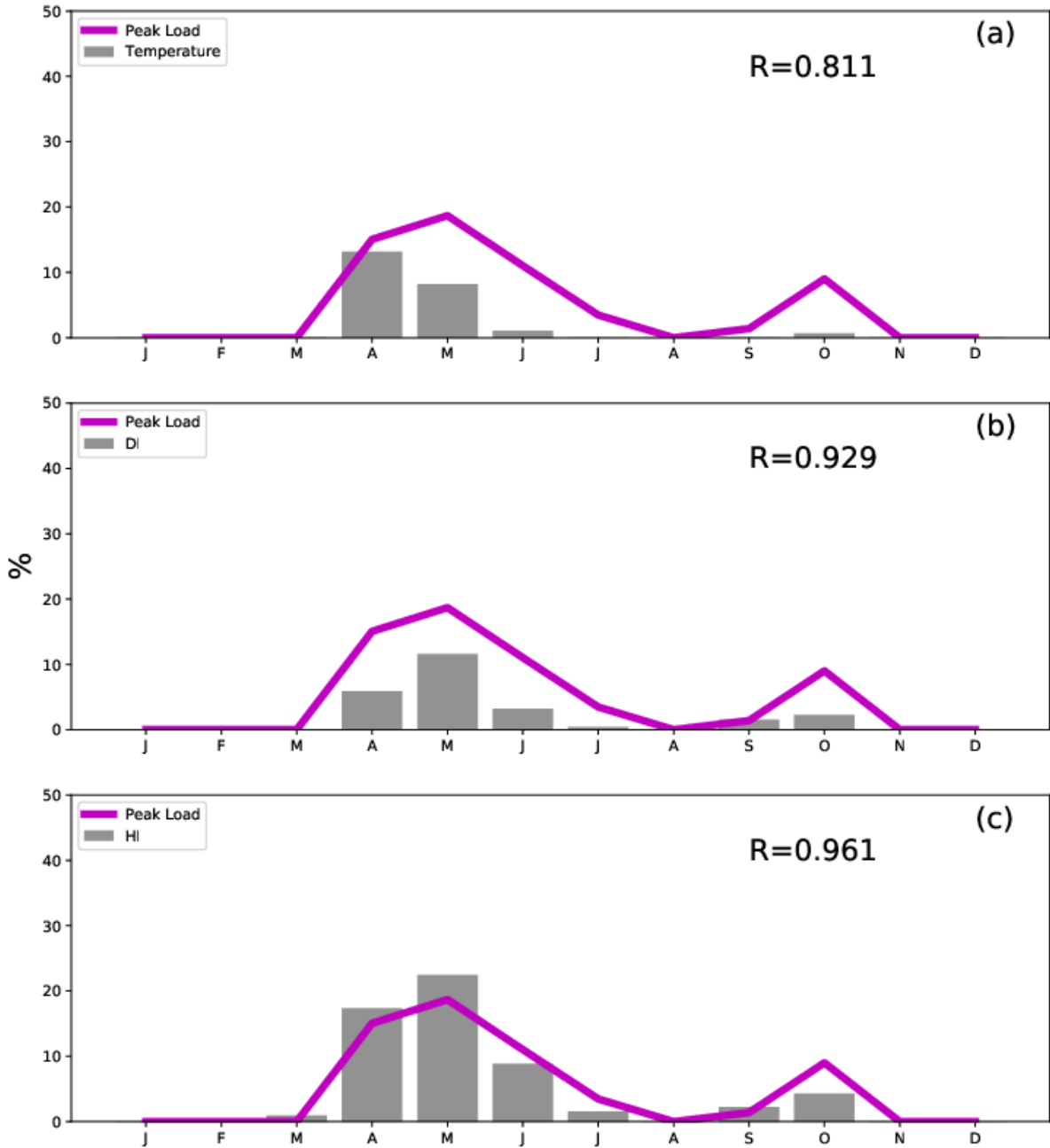


Figure 4.23: Heatwave Events Distribution in (%) of at least three successive days where Peak Load > E90 (90th percentile of electricity load) with (a) $T > 40$, (b) > 29 , and (c) > 39 . R Denotes the Correlation Between the Extreme Load and Extreme Heat Indices

Furthermore, to examine the impact of heatwaves (HW) on electricity load, the frequency distribution of heatwaves events (HWN is defined as consecutive three days where either the temperature or the HI, or the DI is greater than a given threshold) as well as the frequency distribution of at least three days where the electricity load is greater than 110MW are calculated and compared. Figure 4.23 shows that high frequency distribution of heatwaves events (HWN) are followed by high frequency distribution of extreme electricity load; suggesting strong relationship between HWN and extreme electricity load. For instance, the correlation between the extreme load and HWN is very high (>0.8).

4.6.2 Projected Changes of Climate Change on Heat Waves Characteristics

RCMs ensemble mean project an increase of heatwave days (HWF), Heatwaves number (HWN) and heatwave duration (HWD) over the entire country at all the GWLs with the magnitude of the increase varying across the country and grows with increasing GWLs (Figure 4.24 & 4.25). For instance, at GWL1.5, the RCMs ensemble mean projects an increase of HWF in the range of (0-10 days) in the southern part and (20-30 days) in the Northern part of the country. These values gradually grow with increasing GWLs and reach under GWL3.0 50-60 days in the South and 80-100 days in the North. Similar pattern of changes can also be observed for the heatwave number and duration. For example, at GWL1.5, an increase of HWN (0-3 events in South and up to 10 events in North) and HWD (2-2.5 days/events in South and 2.5-3.5 days/events in North) can also be observed. These values grow with increasing GWLs and reach for HWN (12-15/events/year in South and 20-25 events/year in the North) and for HWD (3-3.5 days/event in the South and 3.5-4.5 in the North). Note that all the simulations agree on the direction of the change, indicating the

robustness of the projections. These projections are consistent with projected temperature changes in West Africa (*Nikulin et al., 2018; Klutse et al., 2018*) and agree with some previous studies (*Patricola & Cook (2010)* and *Vizy and Cook (2012)*). Indeed, *Vizy and Cook (2010)* also project an increase of HWF North of 8N with the largest increase (80-120 days per year) occurring over the western Sahel between 12N and 18N. Similarly, *Patricola and Cook (2010)* project the largest increase of heatwaves days (up to 160 days/year) over the Sahel region. However, these previous studies feature slightly higher values of increase of HWN compared to RCMs ensemble mean projections. This might be due to the fact that, in this study an ensemble of CORDEX RCMs is used to carried out this study and also the study has been carried out by considering a specific warming target. Nevertheless, both studies show an increase of heat waves characteristics.

Since the extreme electricity load is highly influenced by both extreme heat and heat waves, this implies that climate change will significantly impact the peak load. Hence, for the issues of network reliability, the power sector should take anticipated measures to reduce the potential impacts of climate change on the energy sector.

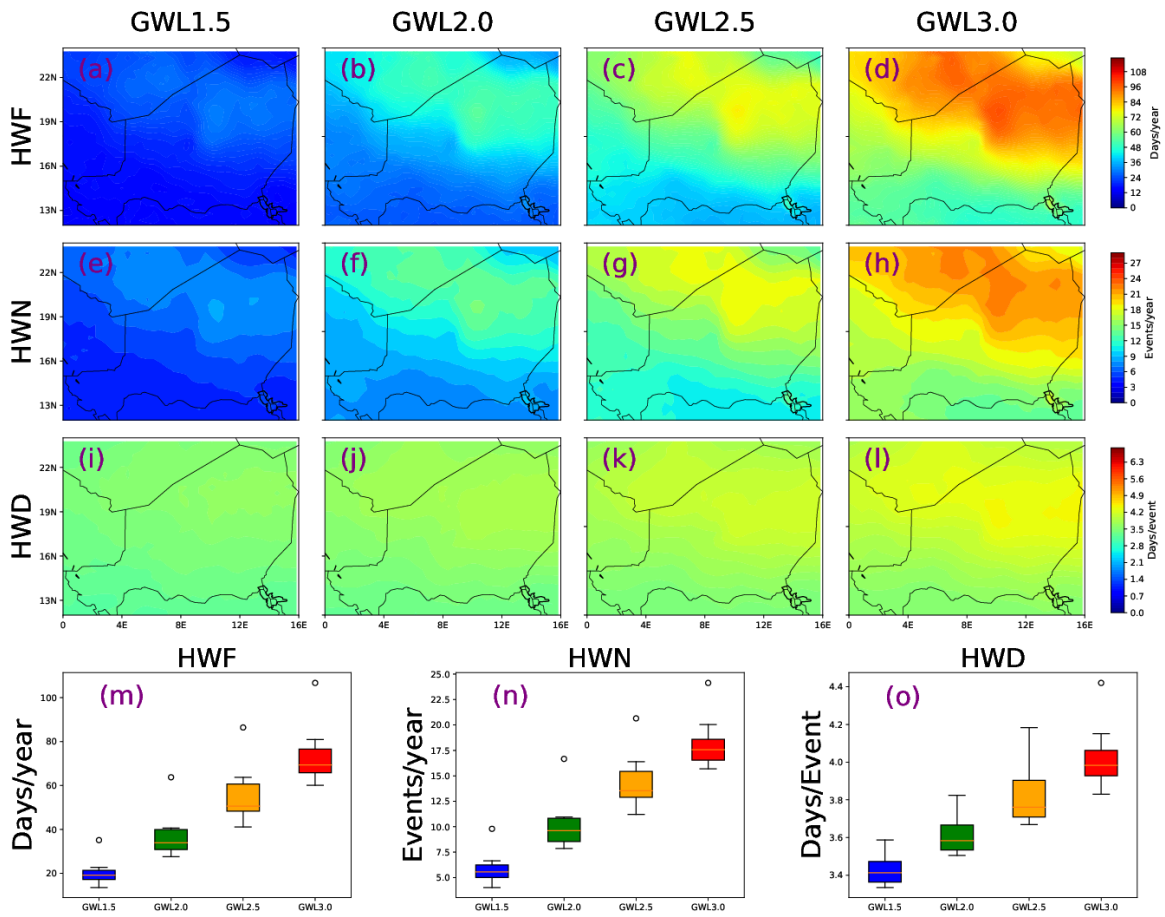


Figure 4.24: Projected Changes in Heat Waves Frequency (a-d), Heat Waves Number (HWN; e-h), and Heat Waves Duration (HWD; i-l). The Boxplots ((m)-(o)) Indicate the Agreement Among the RCMs Simulation using Tmax

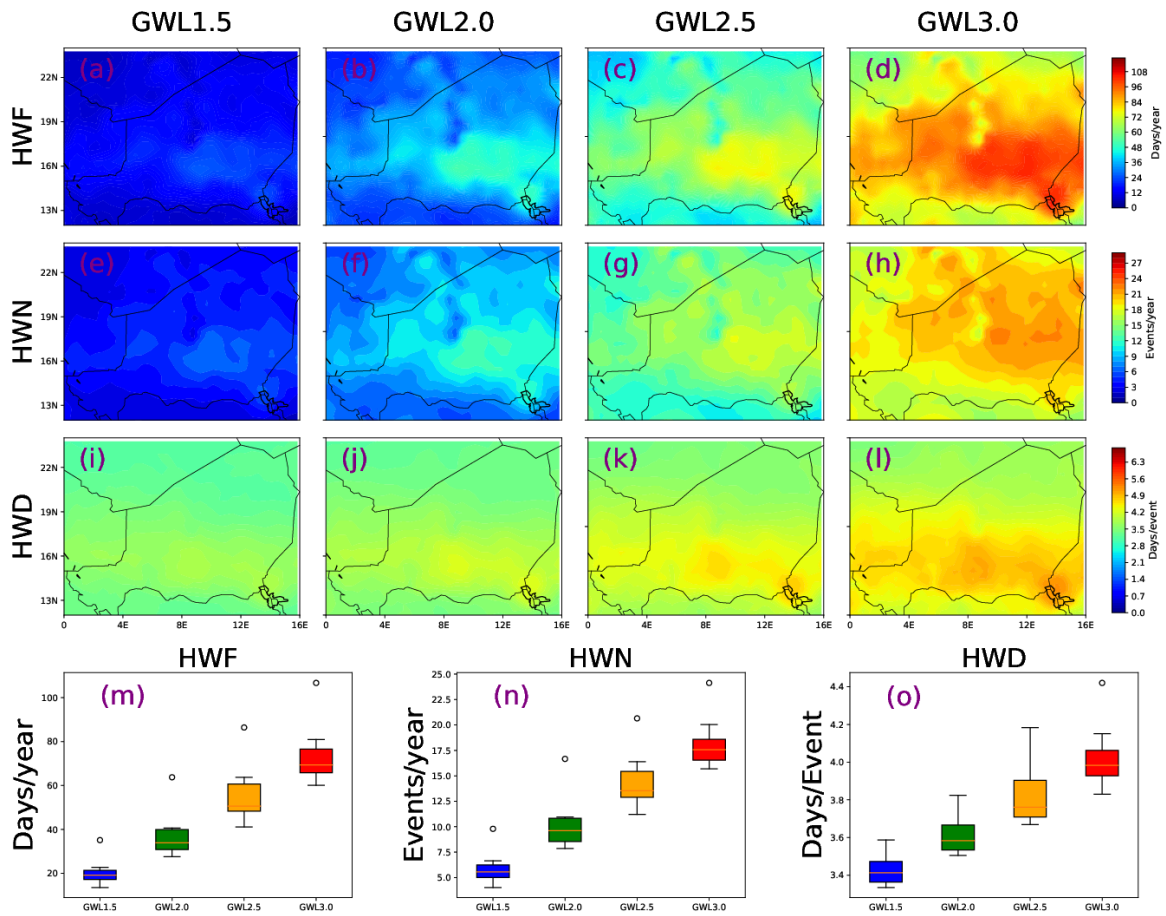


Figure 4.25::Projected Changes in Heat Waves Frequency (a-d), Heat Waves Number (HWN; (e)-(h), and Heat Waves Duration (HWD; (i)-(l)). The Boxplots ((m)-(o)) Indicate the Agreement Among the RCMs Simulation Using Excess Heat Factor (EHF).

CHAPTER FIVE

CONCLUSIONS AND RECOMMENDATIONS

5.1 CONCLUSIONS

As part of the efforts to understand and model the impact of climate change and variability on the energy sector over West Africa, this study investigated the potential impacts of climate change on electricity demand at specific Global Warming Levels (GWL1.5, GWL2.0, GWL2.5, and GWL3.0) in Niger. The study applies 14 Regional Climate Models that have participated in the CORDEX project to predict the impact of climate change on electricity demand. For each relevant climate variable, first the performance of RCMs in simulating the present climate is evaluated, and then the projected future changes at specific Global Warming Levels are presented before discussing the impacts of climate change on electricity demand.

The first research question was to examine the sensitivity of electricity demand to climate variables in Niger. To achieve this, the Wavelet Transform Coherence (WTC) and Phase Analysis (PA) were utilized. Results show that there is a coupling between electricity demand and climate variables mainly temperature and Cooling Degree Days (CDD) for the period 64-365 days; suggesting high seasonal relationship between electricity demand and these variables. Furthermore, the PA shows that both temperature and CDD are positively correlated with the electricity demand. Also, the arrows indicated that both temperature and CDD are leading the electricity demand. Moreover, positive correlation is found between Heat Index (HI) and electricity demand for the period 256-365 days. The radiation and electricity are also coupled for the period 64-256 days with in phase relationship; hence

suggesting positive correlation between radiation and electricity demand. In addition, the PA indicates that the radiation is leading the electricity demand. However, for relative Humidity and electricity demand, a strong coherence is also identified in the period around 256 days with anti-phase relationship. This indicates negative correlation between humidity and electricity demand. In other words, high humidity values will lead to low electricity demand. This is usually observed in July and August where a dip in electricity demand is observed as a result of high relative humidity. Finally, the WTC and PA indicated that the electricity demand and WSP are also coupled for the period around 256 days with anti-phase relationship suggesting also negative correlation between the WSP and the electricity demand. However, the influence of WSP is very weak compared to the other variables. In summary, it can be concluded that the electricity demand is sensitive to climate variables at different periods.

The second research question is to determine the historical relationship between the electricity demand and relevant climate variables. To achieve this, the trend (due to socio-economic development) and seasonality (due to holidays effect) were removed from the demand data in order to isolate only the influence of climate variables. Then, the Principal Component Analysis (PCA) was applied to the de-trended electricity demand and climate variables to identify the climate variables that are highly correlated with the electricity demand. Hence, the electricity demand model was developed using Multiple Linear Regression and Artificial Neural Networks (ANN) techniques. 80% of the data was used to train the model while 20% were used for validation. The research shows that both MLR and ANN are good in predicting the electricity demand in Niger. Indeed, the correlation between the actual values and forecasted values are very high ($r > 0.9$). This suggests the ability of

the selected climate variables in predicting the electricity demand in Niger. Furthermore, the resulted model indicated that the CDD is the most influential variables that affect the electricity demand. Indeed, 1°C increase in CDD will result 79.22 MWh/day increase in electricity demand. Moreover, the residual plots analysis showed that the models comply with the basics assumption of regression models (homogeneity of the variance, and the residuals follow normal distribution)

The third research question was to assess the ability of the CORDEX RCMs in simulating the observed climate of the relevant climate variables. To achieve this, the selected climate variables used to build the electricity model were evaluated by comparing the RCMs data to the Princeton Global Forecasting Data (PGFD). The RCMs ensemble mean provided realistic simulations of all the climate variables used in this study, but with some biases. They generally underestimate the temperatures (Tmean, Tmax, and Tmin), and radiation and overestimate the WSP and RH especially over the Northern part of the country. Furthermore, the RCMs also overestimate the CDD, underestimate the HI and DI compared to the PGFD. However, the RCMs are able to depict the annual cycle of all the variables mentioned above.

Finally, the fourth research question was to predict the potential impacts of climate change on energy demand as well as the relevant climate variables used to build the regression models. To achieve this, the climate data from the reference period was subtracted from the that of GWL period. The research found that the CORDEX RCMs project significant increases in daily electricity demand (DED), CDD, temperature, Heat Index, Discomfort Index and Wind Speed and decreases in radiation and relative humidity at all the GWLs

under both RCP4.5 and RCP8.5 scenarios. The changes in DED are consistent with those of CDD and RH. The simulations agree on the projections of DED as well as HI, DI, CDD. Conversely, there is no agreement among simulations for radiation at any of the GWLs. However, more than 75% of the simulations agree on the projections of WSP and RH at GWL2.5 and GWL3.0. The highest increase in DED is projected in MAM and JJA season while the lowest increase is projected in DJF.

Furthermore, the research also addresses projected changes of heatwaves characteristics (HWF, HWN, and HWD). The RCMs project an increase of heatwave frequency (HWF), heatwaves number (HWN), and heatwaves duration (HWD) with the highest increase over the Northern part of the country at all the GWLs. Since, there is high correspondence between heatwaves and extreme load demand; This suggests potential driven extreme load demand as a result of climate change.

5.2 RECOMMENDATIONS

As in any research activity, this research was carried out with some limitation which should be taken into account when interpreting the results. Hence, to provide more robust information for policymakers, this study can be improved in many ways. First, besides the factors related to climate, other factors such as population and GDP change, energy efficiency policy, consumer's behavior, urbanization among others may also determine the electricity demand in future. For instance, climate influences the electricity demand through the response of people to weather (*Valor et al., 2001*). Hence, depending on the weather conditions, people will increase or decrease the demand. Therefore, including these factors could improve the results of this study. Secondly, the current study used an aggregated

electricity demand including the residential, commercial and industrial sectors since the disaggregated data was not available. So future work may also look on the impacts of global warming on different sectors. This will provide more information regarding the impacts of climate change on individual sectors. Thirdly, conducting biases corrections on GCMs and RCMs simulations may further reduce the disagreement among the RCMs for the projections of radiation, WSP and RH, and thereby improve the results. Such considerations will make the results more relevant for policy makers in the energy sector. Nevertheless, the present study has demonstrated the capability of the CORDEX RCMs in reproducing the climate variables used in this study and quantified the potential impacts of climate change on electricity demand in Niger. This will help the policy makers in the energy sector to integrate the impacts of climate into their national electricity forecasting systems.

REFERENCES

- Abiodun, B. J. Makhanya N., Petja B., Abatan A. A., and Ogotunde G. P. (2018). *Future projection of droughts over major river basins in Southern Africa at specific global warming levels.*
- Abiodun, B. J., Lawal, K. A., Salami, A. T., and Abatan, A. A. (2013). Potential influences of global warming on future climate and extreme events in Nigeria. *Regional Environmental Change*, 13(3), 477–491. <https://doi.org/10.1007/s10113-012-0381-7>
- Abiodun, B. J., Pal, J. S., Afiesimama, E. A., Gutowski, W. J., and Adedoyin, A. (2008). Simulation of West African monsoon using RegCM3 Part II: Impacts of deforestation and desertification. *Theoretical and Applied Climatology*, 93(3–4), 245–261. <https://doi.org/10.1007/s00704-007-0333-1>
- Ahmed, T., Muttaqi, K. M., and Agalgaonkar, A. P. (2012). Climate change impacts on electricity demand in the State of New South Wales , Australia. *Applied Energy*, 98, 376–383. <https://doi.org/10.1016/j.apenergy.2012.03.059>
- Akbari, A., Org, E., and Akbari, H. (2005). *Title Energy Saving Potentials and Air Quality Benefits of Urban Heat Island Mitigation Permalink* <https://escholarship.org/uc/item/4qs5f42s> Publication Date Energy Saving Potentials and Air Quality Benefits of Urban Heat Island Mitigation 1. Retrieved from <http://heatland.lbl.gov/>
- Akil, Y. S., Syafaruddin, Waris, T., and Lateko A.A.H. (2014). *The Influence of Meteorological Parameters under Tropical Condition on Electricity Demand Characteristic : Indonesia Case Study.* 383–387.

- Ang, B. W., Wang, H., and Ma, X. (2017). Climatic influence on electricity consumption: The case of Singapore and Hong Kong. *Energy*, 127, 534–543. <https://doi.org/10.1016/j.energy.2017.04.005>
- Apadula, F., Bassini, A., Elli, A., and Scapin, S. (2012). Relationships between meteorological variables and monthly electricity demand. *Applied Energy*, 98, 346–356. <https://doi.org/10.1016/j.apenergy.2012.03.053>
- Arima, Y., Ooka, R., Kikumoto, H., and Yamanaka, T. (2016). Effect of climate change on building cooling loads in Tokyo in the summers of the 2030s using dynamically downscaled GCM data. *Energy and Buildings*, 114. <https://doi.org/10.1016/j.enbuild.2015.08.019>
- Badescu, V., and Zamfir, E. (1999). Degree-days, degree-hours and ambient temperature bin data from monthly-average temperatures (Romania). *Energy Conversion and Management*, 40(8), 885–900. [https://doi.org/10.1016/S0196-8904\(98\)00148-4](https://doi.org/10.1016/S0196-8904(98)00148-4)
- Braun, M. R., Altan, H., and Beck, S. B. M. (2014). Using regression analysis to predict the future energy consumption of a supermarket in the UK. *Applied Energy*, 130, 305–313. <https://doi.org/10.1016/j.apenergy.2014.05.062>
- Cartalis, C., Synodinou, A., Proedrou, M., Tsangrassoulis, A., and Santamouris, M. (2001). Modifications in energy demand in urban areas as a result of climate changes: An assessment for the southeast Mediterranean region. *Energy Conversion and Management*, 42(14), 1647–1656. [https://doi.org/10.1016/S0196-8904\(00\)00156-4](https://doi.org/10.1016/S0196-8904(00)00156-4)
- Cellura, M., Guarino, F., Longo, S., and Tumminia, G. (2018). Climate change and the building sector: Modelling and energy implications to an office building in southern

- Europe. *Energy for Sustainable Development*, 45(2018), 46–65.
<https://doi.org/10.1016/j.esd.2018.05.001>
- Chan, A. L. S. (2011). Developing future hourly weather files for studying the impact of climate change on building energy performance in Hong Kong. *Energy and Buildings*, 43(10), 2860–2868. <https://doi.org/10.1016/j.enbuild.2011.07.003>
- Chen, C. Sen, Chen, Y. L., Liu, C. L., Lin, P. L., and Chen, W. C. (2007). Statistics of heavy rainfall occurrences in Taiwan. *Weather and Forecasting*, 22(5), 981–1002.
<https://doi.org/10.1175/WAF1033.1>
- Christenson, M., Manz, H., and Gyalistras, D. (2006). Climate warming impact on degree-days and building energy demand in Switzerland. *Energy Conversion and Management*, 47(6), 671–686. <https://doi.org/10.1016/j.enconman.2005.06.009>
- Colombo, A. F., Etkin, D., and Karney, B. W. (1999). Climate variability and the frequency of extreme temperature events for nine sites across Canada: Implications for power usage. *Journal of Climate*, 12(8 PART 2), 2490–2502. [https://doi.org/10.1175/1520-0442\(1999\)012<2490:CVATFO>2.0.CO;2](https://doi.org/10.1175/1520-0442(1999)012<2490:CVATFO>2.0.CO;2)
- Cornforth, R. (2012). Overview of the West African Monsoon 2011. *Weather*, 67(3), 59–65. <https://doi.org/10.1002/wea.1896>
- Crawley, D. B. (2007). Estimating the impacts of climate change and urbanization on building performance. *IBPSA 2007 - International Building Performance Simulation Association 2007*, 1493, 1115–1122. <https://doi.org/10.1080/19401490802182079>
- Damm, A., Köberl, J., Prettenthaler, F., Rogler, N., & Töglhofer, C. (2017). Impacts of +2 °C global warming on electricity demand in Europe. *Climate Services*, 7, 12–30.

<https://doi.org/10.1016/j.cliser.2016.07.001>

Dirks, J. A., Gorrissen, W. J., Hathaway, J. H., Skorski, D. C., Scott, M. J., Pulsipher, T.

C., Huang M., Liu Y., and Rice, J. S. (2015). Impacts of climate change on energy consumption and peak demand in buildings: A detailed regional approach. *Energy*, 79(C), 20–32. <https://doi.org/10.1016/j.energy.2014.08.081>

Dong, B., Cao, C., and Lee, S. E. (2005). Applying support vector machines to predict building energy consumption in tropical region. *Energy and Buildings*, 37(5), 545–553. <https://doi.org/10.1016/j.enbuild.2004.09.009>

ECREEE, and ECOWAS Centre for Renewable Energy and Energy Efficiency (ECREEE).

(2015). *ECOWAS Renewable Energy Policy* (p. 82). p. 82. Retrieved from http://www.ecreee.org/sites/default/files/documents/ecowas_renewable_energy_policy.pdf

Ekonomou, L. (2010). Greek long-term energy consumption prediction using artificial neural networks. *Energy*, 35(2), 512–517. <https://doi.org/10.1016/j.energy.2009.10.018>

Energy Networks. (2019). Heatwaves and Electricity Supply. *Fact Sheet*, (Jan).

FAO (Food and Agriculture Organization). 2014. FAOSTAT: Emissions—land use. Accessed May 2014. http://faostat3.fao.org/faostat-gateway/go/to/download/G2/*E.

Fearnside, P. M. (2002). Greenhouse gas emissions from a hydroelectric reservoir (Brazil's Tucuruídam) and the energy policy implications. *Water, Air, and Soil Pollution*, 133(1–4), 69–96. <https://doi.org/10.1023/A:1012971715668>

- Fu, Y., Li, Z., Zhang, H., and Xu, P. (2015). Using Support Vector Machine to Predict Next Day Electricity Load of Public Buildings with Sub-metering Devices. *Procedia Engineering*, 121, 1016–1022. <https://doi.org/10.1016/j.proeng.2015.09.097>
- Fung, W. Y., K. S. Lam, W. T. Hung, S. W. Pang, and Y. L. Lee. 2006. “Impact of Urban Temperature on Energy Consumption of Hong Kong.” *Energy* 31 (14): 2287–2301. <https://doi.org/10.1016/j.energy.2005.12.009>
- Giannakopoulos, C., Hadjinicolaou, P., Zerefos, C., and Demosthenous, G. (2009). Changing energy requirements in the Mediterranean under changing climatic conditions. *Energies*, 2(4), 805–815. <https://doi.org/10.3390/en20400805>
- Giannakopoulos, C., and Psiloglou, B. E. (2006). Trends in energy load demand for Athens, Greece: Weather and non-weather related factors. *Climate Research*, 31(1), 97–108. <https://doi.org/10.3354/cr031097>
- Giannini, A., Saravanan, R., and Chang, P. (2003). Oceanic Forcing of Sahel Rainfall on Interannual to Interdecadal Time Scales. *Science*, 302(5647), 1027–1030. <https://doi.org/10.1126/science.1089357>
- Griggs, D. J., and Noguer, M. (2002). *Climate change 2001: The scientific basis . Contribution of Working Group I to the Third Assessment Report of the Intergovernmental Panel on Climate Change*. 57(August), 2001–2003.
- Guan, H., Beecham, S., Xu, H., and Ingleton, G. (2017). Incorporating residual temperature and specific humidity in predicting weather-dependent warm-season electricity consumption. *Environmental Research Letters*, 12(2). <https://doi.org/10.1088/1748-9326/aa57a9>

- Hekkenberg, M., Moll, H. C., and Uiterkamp, A. J. M. S. (2009). Dynamic temperature dependence patterns in future energy demand models in the context of climate change. *Energy*, 34(11), 1797–1806. <https://doi.org/10.1016/j.energy.2009.07.037>
- Huang, B., Hwang, M. J., and Yang, C. W. (2007). *Causal relationship between energy consumption and GDP growth revisited: A dynamic panel data approach* ☆. 7. <https://doi.org/10.1016/j.ecolecon.2007.11.006>
- Huang, J., and Gurney, K. R. (2016). The variation of climate change impact on building energy consumption to building type and spatiotemporal scale. *Energy*, 111, 137–153. <https://doi.org/10.1016/j.energy.2016.05.118>
- Huang, K. T., and Hwang, R. L. (2016). Future trends of residential building cooling energy and passive adaptation measures to counteract climate change: The case of Taiwan. *Applied Energy*, 184, 1230–1240. <https://doi.org/10.1016/j.apenergy.2015.11.008>
- Hulme, M. (2016). after the Paris Agreement. *Nature Publishing Group*, 1–2. <https://doi.org/10.1038/nclimate2939>
- Huo, H., Wang, M., Zhang, X., He, K., Gong, H., Jiang, K., Jin Y., Shi Y., and Yu, X. (2012). Projection of energy use and greenhouse gas emissions by motor vehicles in China: Policy options and impacts. *Energy Policy*, 43, 37–48. <https://doi.org/10.1016/j.enpol.2011.09.065>
- IEA, 2014. “Electricity Access in Africa - 2012.” http://www.worldenergyoutlook.org/media/weowebbsite/africa/Africa_Energy_Outlook_2014_Electricity_database.xlsx.

- International Energy Agency (IEA). 2017. "Energy Access Outlook 2017: From Poverty to Prosperity." *Oecd »Iea* 94 (March): 144. <https://doi.org/10.1787/9789264285569-en>.
- Impact, L., and Wave, M. H. (2015). *Long-Term Impact of Moscow Heat Wave and Wildfires on Mortality*. 26(2), 2014–2015. <https://doi.org/10.1097/EDE.0000000000000251>
- Invidiata, A., and Ghisi, E. (2016). Impact of climate change on heating and cooling energy demand in houses in Brazil. *Energy and Buildings*, 130, 20–32. <https://doi.org/10.1016/j.enbuild.2016.07.067>
- IPCC, 2013. (2013). Summary for Policymakers. In: Climate Change 2013: The Physical Science Basis. Contribution of Working Group I to the Fifth Assessment Report of the Intergovernmental Panel on Climate Change. *CEUR Workshop Proceedings*. <https://doi.org/10.1017/CBO9781107415324.015>
- Isaac, M., and van Vuuren, D. P. (2009). Modeling global residential sector energy demand for heating and air conditioning in the context of climate change. *Energy Policy*, 37(2), 507–521. <https://doi.org/10.1016/j.enpol.2008.09.051>
- Jain, R. K., Smith, K. M., Culligan, P. J., and Taylor, J. E. (2014). Forecasting energy consumption of multi-family residential buildings using support vector regression: Investigating the impact of temporal and spatial monitoring granularity on performance accuracy. *Applied Energy*, 123(November), 168–178. <https://doi.org/10.1016/j.apenergy.2014.02.057>
- Jentsch, M. F., Bahaj, A. B. S., and James, P. A. B. (2008). Climate change future proofing of buildings-Generation and assessment of building simulation weather files. *Energy*

- and Buildings*, 40(12), 2148–2168. <https://doi.org/10.1016/j.enbuild.2008.06.005>
- Jovanović, S., Savić, S., Bojić, M., Djordjević, Z., and Nikolić, D. (2015). The impact of the mean daily air temperature change on electricity consumption. *Energy*, 88, 604–609. <https://doi.org/10.1016/j.energy.2015.06.001>
- Jylhä, K., Jokisalo, J., Ruosteenoja, K., Pilli-Sihvola, K., Kalamees, T., Seitola, T., Mäkelä H. M., Hyvönen R., Laapas M. and Drebs, A. (2015). Energy demand for the heating and cooling of residential houses in Finland in a changing climate. *Energy and Buildings*, 99, 104–116. <https://doi.org/10.1016/j.enbuild.2015.04.001>
- Kadiolu, M., Şen, Z., and Gültekin, L. (2001). Variations and trends in turkish seasonal heating and cooling degree-days. *Climatic Change*, 49(1–2), 209–223. <https://doi.org/10.1023/A:1010637209766>
- Kalkstein, L. S., and Davis, R. E. (1989). Weather and Human Mortality: An Evaluation of Demographic and Interregional Responses in the United States. *Annals of the Association of American Geographers*, 79(1), 44–64. <https://doi.org/10.1111/j.1467-8306.1989.tb00249.x>
- Kaufmann, R. K., Gopal, S., Tang, X., Raciti, S. M., Lyons, P. E., Geron, N., and Craig, F. (2013). Revisiting the weather effect on energy consumption : Implications for the impact of climate change. *Energy Policy*, 62, 1377–1384. <https://doi.org/10.1016/j.enpol.2013.07.056>
- Kavaklioglu, K. (2011). Modeling and prediction of Turkey ’ s electricity consumption using Support Vector Regression. *Applied Energy*, 88(1), 368–375. <https://doi.org/10.1016/j.apenergy.2010.07.021>

- Kavaklioglu, K., Ceylan, H., Kemal, H., and Ersel, O. (2009). Modeling and prediction of Turkey ' s electricity consumption using Artificial Neural Networks. *Energy Conversion and Management*, 50(11), 2719–2727. <https://doi.org/10.1016/j.enconman.2009.06.016>
- Klutse, N. A. B., Ajayi, V. O., Gbobaniyi, E. O., Egbebiyi, T. S., Kouadio, K., Nkrumah, F., Quagraine A. K., Olusegun C., Diasso U., Abiodun B. J., Lawal K., Nikulin G., Lennard C. and Dosio, A. (2018). Potential impact of 1.5 °c and 2 °c global warming on consecutive dry and wet days over West Africa. *Environmental Research Letters*, 13(5). <https://doi.org/10.1088/1748-9326/aab37b>
- Klutse, N. A. B., Sylla, M. B., Diallo, I., Sarr, A., Dosio, A., Diedhiou, A., Kamga A., Lamptey B., Ali A., Gbobaniyi E. O., Owusu K., Lennard C., Hewitson B., Nikulin G., Panitz H. and Büchner, M. (2016). Daily characteristics of West African summer monsoon precipitation in CORDEX simulations. *Theoretical and Applied Climatology*, 123(1–2), 369–386. <https://doi.org/10.1007/s00704-014-1352-3>
- Kolokotroni, M., Davies, M., Croxford, B., Bhuiyan, S., and Mavrogianni, A. (2010). A validated methodology for the prediction of heating and cooling energy demand for buildings within the Urban Heat Island: Case-study of London. *Solar Energy*, 84(12), 2246–2255. <https://doi.org/10.1016/j.solener.2010.08.002>
- Lam, J. C., Wan, K. K. W., Liu, D., and Tsang, C. L. (2010). Multiple regression models for energy use in air-conditioned office buildings in different climates. *Energy Conversion and Management*, 51(12), 2692–2697. <https://doi.org/10.1016/j.enconman.2010.06.004>

- Lebel, T., and Ali, A. (2009). Recent trends in the Central and Western Sahel rainfall regime (1990-2007). *Journal of Hydrology*, 375(1–2), 52–64. <https://doi.org/10.1016/j.jhydrol.2008.11.030>
- Li, Q., Meng, Q., Cai, J., Yoshino, H., and Mochida, A. (2009). Applying support vector machine to predict hourly cooling load in the building. *Applied Energy*, 86(10), 2249–2256. <https://doi.org/10.1016/j.apenergy.2008.11.035>
- Losada, T., Rodríguez-Fonseca, B., Janicot, S., Gervois, S., Chauvin, F., and Ruti, P. (2010). A multi-model approach to the Atlantic Equatorial mode: Impact on the West African monsoon. *Climate Dynamics*, 35(1), 29–43. <https://doi.org/10.1007/s00382-009-0625-5>
- Lotsch, A., Friedl, M. A., Anderson, B. T., and Tucker, C. J. (2003). Coupled vegetation-precipitation variability observed from satellite and climate records. *Geophysical Research Letters*, 30(14), 8–11. <https://doi.org/10.1029/2003GL017506>
- Lu, W. C. (2017). Greenhouse gas emissions, energy consumption and economic growth: A panel cointegration analysis for 16 Asian countries. *International Journal of Environmental Research and Public Health*, 14(11). <https://doi.org/10.3390/ijerph14111436>
- Ma, Z., Ye, C., Li, H., and Ma, W. (2018). Applying support vector machines to predict building energy consumption in China. *Energy Procedia*, 152, 780–786. <https://doi.org/10.1016/j.egypro.2018.09.245>
- Maure, G., Pinto, I., Ndebele-Murisa, M., Muthige, M., Lennard, C., Nikulin, G., Dosio A. and Meque, A. (2018). The southern African climate under 1.5 °c and 2 °c of global

- warming as simulated by CORDEX regional climate models. *Environmental Research Letters*, 13(6). <https://doi.org/10.1088/1748-9326/aab190>
- Miller, N. L., Hayhoe, K., Jin, J., and Auffhammer, M. (2008). Climate, extreme heat, and electricity demand in California. *Journal of Applied Meteorology and Climatology*, 47(6), 1834–1844. <https://doi.org/10.1175/2007JAMC1480.1>
- Moral-Carcedo J., and Vincens-Ocero J. 2005. “Modelling the Non-Linear Response of Spanish Electricity Demand to Temperature Variations” 27: 477–94. <https://doi.org/10.1016/j.eneco.2005.01.003>.
- Moustris, K. P., Nastos, P. T., Bartzokas, A., Larissi, I. K., Zacharia, P. T., and Paliatsos, A. G. (2015). Energy consumption based on heating/cooling degree days within the urban environment of Athens, Greece. *Theoretical and Applied Climatology*, 122(3–4), 517–529. <https://doi.org/10.1007/s00704-014-1308-7>
- Nairn, J., and Fawcett, R. (2013). Defining heatwaves: heatwave defined as a heat-impact event servicing all community and business sectors in Australia. In *CAWCR technical report*. <https://doi.org/551.5250994>
- Nikulin G., Lennard, C., Dosio A., Kjellström E., Chen, Y., Hänsler A., Kupiainen M., Laprise R., Mariotti L., Maule C. F., Meijgaard E. V., Panitz H., Scinocca J. F., and Somot S. (2018). *The effects of 1.5 and 2 degrees of global warming on Africa in the CORDEX ensemble OPEN ACCESS The effects of 1.5 and 2 degrees of global warming on Africa in the CORDEX ensemble*.
- Oğcu, G., Demirel, O. F., and Zaim, S. (2012). Forecasting Electricity Consumption with Neural Networks and Support Vector Regression. *Procedia - Social and Behavioral*

Sciences, 58, 1576–1585. <https://doi.org/10.1016/j.sbspro.2012.09.1144>

Paeth, H., Fink, A. H., Pohle, S., Keis, F., Mächel, H., and Samimi, C. (2011). Meteorological characteristics and potential causes of the 2007 flood in sub-Saharan Africa. *International Journal of Climatology*, 31(13), 1908–1926. <https://doi.org/10.1002/joc.2199>

Pao, H. T., Yu, H. C., and Yang, Y. H. (2011). Modeling the CO₂ emissions, energy use, and economic growth in Russia. *Energy*, 36(8), 5094–5100. <https://doi.org/10.1016/j.energy.2011.06.004>

Papakostas, K., Mavromatis, T., and Kyriakis, N. (2010). Impact of the ambient temperature rise on the energy consumption for heating and cooling in residential buildings of Greece. *Renewable Energy*, 35(7), 1376–1379. <https://doi.org/10.1016/j.renene.2009.11.012>

Pardo, A., Meneu, V., and Valor, E. (2002). Temperature and seasonality influences on Spanish electricity load. *Energy Economics*, 24(1), 55–70. [https://doi.org/10.1016/S0140-9883\(01\)00082-2](https://doi.org/10.1016/S0140-9883(01)00082-2)

Patricola, C. M., and Cook, Æ. K. H. (2010). *Northern African climate at the end of the twenty-first century : an integrated application of regional and global climate models*. 193–212. <https://doi.org/10.1007/s00382-009-0623-7>

Perkins, S. E., Alexander, L. V., and Nairn, J. R. (2012). Increasing frequency, intensity and duration of observed global heatwaves and warm spells. *Geophysical Research Letters*, 39(20), 1–5. <https://doi.org/10.1029/2012GL053361>

Peterson, T. C., Taylor, M. A., Demeritte, R., Duncombe, D. L., Burton, S., Thompson, F.,

- Porter A., Mercedes M., Villegas E., Fils R. S., Tank A. K., Albert M., Warner R., Joyette A., Mills W., Alexander L., and Gleason, B. (2002). Recent changes in climate extremes in the Caribbean region. *Journal of Geophysical Research Atmospheres*, *107*(21), 1–9. <https://doi.org/10.1029/2002JD002251>
- Ravinesh, D. K., and Chung, C. D. J. (2016). Projection of heat wave mortality related to climate change in Korea. *Natural Hazards*, *80*(1), 623–637. <https://doi.org/10.1007/s11069-015-1987-0>
- Robert, A., and Kummert, M. (2012). Designing net-zero energy buildings for the future climate, not for the past. *Building and Environment*, *55*, 150–158. <https://doi.org/10.1016/j.buildenv.2011.12.014>
- Rodríguez-Fonseca, B., Janicot, S., Mohino, E., Losada, T., Bader, J., Caminade, C., Chauvin F., Fontaine B., Garcia-Serrano J., Gervois S., Joly M., Polo I., Ruti P., Roucou P., and Voldoire, A. (2011). Interannual and decadal SST-forced responses of the West African monsoon. *Atmospheric Science Letters*, *12*(1), 67–74. <https://doi.org/10.1002/asl.308>
- Rogelj, J., Elzen, M. Den, Höhne, N., Fransen, T., Fekete, H., Winkler, H., Schaeffer R., Riahi, K., Sha, F., and Meinshausen M. (2016). Paris Agreement climate proposals need a boost to keep warming well below 2 ° C. 1–10. <https://doi.org/10.1038/nature18307>
- Roux, C., Schalbart, P., Assoumou, E., and Peuportier, B. (2016). Integrating climate change and energy mix scenarios in LCA of buildings and districts. *Applied Energy*, *184*, 619–629. <https://doi.org/10.1016/j.apenergy.2016.10.043>

- Russo, S., Dosio, A., Graversen, R. G., Sillmann, J., Carrao, H., Dunbar, M. B., Singleton A., Montagna P., Barbola P., and Vogt, J. V. (2014). Magnitude of extreme heat waves in present climate and their projection in a warming world. *Journal of Geophysical Research Atmospheres*, 119(22), 12500–12512. <https://doi.org/10.1002/2014JD022098>
- Sailor, D. J., and Pavlova, A. A. (2003). Air conditioning market saturation and long-term response of residential cooling energy demand to climate change. *Energy*, 28(9), 941–951. [https://doi.org/10.1016/S0360-5442\(03\)00033-1](https://doi.org/10.1016/S0360-5442(03)00033-1)
- Salifou, G. (2015). *The Energy Sector of Niger: Perspectives and Opportunities*. 16. https://doi.org/https://energycharter.org/fileadmin/DocumentsMedia/Occasional/Niger_Energy_Sector.pdf
- Santamouris, M., Cartalis, C., Synnefa, A., and Kolokotsa, D. (2015). On the impact of urban heat island and global warming on the power demand and electricity consumption of buildings—A review. *Energy and Buildings*, 98, 119–124. <https://doi.org/10.1016/j.enbuild.2014.09.052>
- Sarr, B. (2012). Present and future climate change in the semi-arid region of West Africa: A crucial input for practical adaptation in agriculture. *Atmospheric Science Letters*, 13(2), 108–112. <https://doi.org/10.1002/asl.368>
- Sawadogo, W., Abiodun, B. J., and Okogbue, E. C. (2019). Projected changes in wind energy potential over West Africa under the global warming of 1.5 °C and above. *Theoretical and Applied Climatology*, (2015). <https://doi.org/10.1007/s00704-019-02826-8>

- Scapin, S., Apadula, F., Brunetti, M., and Maugeri, M. (2015). *High-resolution temperature fields to evaluate the response of Italian electricity demand to meteorological variables: an example of climate service for the energy sector*.
<https://doi.org/10.1007/s00704-015-1536-5>
- Schleussner, C., Rogelj, J., Schaeffer, M., Lissner, T., Licker, R., Fischer, E. M., Knutti R., Levermann A., Frieler K., and Hare, W. (2016). Science and policy characteristics of the Paris Agreement temperature goal. *Nature Publishing Group*, (July).
<https://doi.org/10.1038/nclimate3096>
- Semmler, T., Mcgrath, R., Steele-Dunne, S., Hanafin, J., Nolana, P., and Wanga, S. (2010). Influence of climate change on heating and cooling energy demand in Ireland. *International Journal of Climatology*, 30(10), 1502–1511.
<https://doi.org/10.1002/joc.1997>
- Sheffield, J., Goteti, G., and Wood, E. F. (2006). Development of a 50-year high-resolution global dataset of meteorological forcings for land surface modeling. *Journal of Climate*, 19(13), 3088–3111. <https://doi.org/10.1175/JCLI3790.1>
- Shen, P. (2017). Impacts of climate change on U.S. building energy use by using downscaled hourly future weather data. *Energy and Buildings*, 134, 61–70.
<https://doi.org/10.1016/j.enbuild.2016.09.028>
- Shen, P., and Lior, N. (2018). Vulnerability to climate change impacts of present renewable energy systems designed for achieving net-zero energy buildings Vulnerability to climate change impacts of present renewable energy systems designed for achieving net-zero energy buildings. *Energy*, 114(June), 1288–1305.

<https://doi.org/10.1016/j.energy.2016.07.078>

Shi, Y., Zhang, D. F., Xu, Y., and Zhou, B. T. (2018). Changes of heating and cooling degree days over China in response to global warming of 1.5 °C, 2 °C, 3 °C and 4 °C. *Advances in Climate Change Research*, 9(3), 192–200.
<https://doi.org/10.1016/j.accre.2018.06.003>

Shourav, M. S. A., Shahid, S., Singh, B., Mohsenipour, M., Chung, E. S., and Wang, X. J. (2018). Potential Impact of Climate Change on Residential Energy Consumption in Dhaka City. *Environmental Modeling and Assessment*, 23(2), 131–140.
<https://doi.org/10.1007/s10666-017-9571-5>

Sivak, M. (2008). Where to live in the United States: Combined energy demand for heating and cooling in the 50 largest metropolitan areas. *Cities*, 25(6), 396–398.
<https://doi.org/10.1016/j.cities.2008.09.001>

Son, J., Lee, J., Anderson, G. B., and Bell, M. L. (2012). *The Impact of Heat Waves on Mortality in Seven Major Cities in Korea*. 566(4), 566–572.

Song, X., and Ye, C. (2017). Climate Change Adaptation Pathways for Residential Buildings in Southern China. *Energy Procedia*, 105, 3062–3067.
<https://doi.org/10.1016/j.egypro.2017.03.635>

Soytas, U., Sari, R., and Ewing, B. T. (2007). Energy consumption, income, and carbon emissions in the United States. *Ecological Economics*, 62(3–4), 482–489.
<https://doi.org/10.1016/j.ecolecon.2006.07.009>

- Spinoni, J., Vogt, J. V., Barbosa, P., Dosio, A., McCormick, N., Bigano, A., and Füssel, H. M. (2018). Changes of heating and cooling degree-days in Europe from 1981 to 2100. *International Journal of Climatology*, 38(December 2017), e191–e208. <https://doi.org/10.1002/joc.5362>
- Sylla, M. B., Giorgi, F., Coppola, E., and Mariotti, L. (2013). Uncertainties in daily rainfall over Africa: Assessment of gridded observation products and evaluation of a regional climate model simulation. *International Journal of Climatology*, 33(7), 1805–1817. <https://doi.org/10.1002/joc.3551>
- Taseska, V., Markovska, N., and Callaway, J. M. (2012). Evaluation of climate change impacts on energy demand. *Energy*, 48(1), 88–95. <https://doi.org/10.1016/j.energy.2012.06.053>
- Taylor, C. M., Lambin, E. F., Stephenne, N., Harding, R. J., and Essery, R. L. H. (2002). The influence of land use change on climate in the Sahel. *Journal of Climate*, 15(24), 3615–3629. [https://doi.org/10.1175/1520-0442\(2002\)015<3615:TIOLUC>2.0.CO;2](https://doi.org/10.1175/1520-0442(2002)015<3615:TIOLUC>2.0.CO;2)
- Valor, E., Meneu, V., and Caselles, V. (2001). Daily Air Temperature and Electricity Load in Spain. *Journal of Applied Meteorology*, 40(8), 1413–1421. [https://doi.org/10.1175/1520-0450\(2001\)040<1413:DATAEL>2.0.CO;2](https://doi.org/10.1175/1520-0450(2001)040<1413:DATAEL>2.0.CO;2)
- Van Vliet, O., Brouwer, A. S., Kuramochi, T., Van Den Broek, M., and Faaij, A. (2011). Energy use, cost and CO2 emissions of electric cars. *Journal of Power Sources*, 196(4), 2298–2310. <https://doi.org/10.1016/j.jpowsour.2010.09.119>
- Vizy, E. K., & Cook, K. H. (2012). Mid-twenty-first-century changes in extreme events over northern and tropical Africa. *Journal of Climate*, 25(17), 5748–5767.

<https://doi.org/10.1175/JCLI-D-11-00693.1>

Wan, K. K. W., Li, D. H. W., Pan, W., and Lam, J. C. (2012). Impact of climate change on building energy use in different climate zones and mitigation and adaptation implications. *Applied Energy*, 97, 274–282. <https://doi.org/10.1016/j.apenergy.2011.11.048>

Wang, L., Liu, X., and Brown, H. (2017). Prediction of the impacts of climate change on energy consumption for a medium-size office building with two climate models. *Energy and Buildings*, 157, 218–226. <https://doi.org/10.1016/j.enbuild.2017.01.007>

Wang, Q., Wu, S., Zeng, Y., and Wu, B. (2016). Exploring the relationship between urbanization, energy consumption, and CO₂ emissions in different provinces of China. *Renewable and Sustainable Energy Reviews*, 54, 1563–1579. <https://doi.org/10.1016/J.RSER.2015.10.090>

Wang, X., Chen, D., and Ren, Z. (2010). Assessment of climate change impact on residential building heating and cooling energy requirement in Australia. *Building and Environment*, 45(7), 1663–1682. <https://doi.org/10.1016/j.buildenv.2010.01.022>

WRI (World Resources Institute). 2014. Climate Analysis Indicators Tool (CAIT) 2.0: WRI's climate data explorer. Accessed May 2014. <http://cait.wri.org>

Xu, P., Huang, Y. J., Miller, N., Schlegel, N., and Shen, P. (2012). Impacts of climate change on building heating and cooling energy patterns in California. *Energy*, 44(1), 792–804. <https://doi.org/10.1016/j.energy.2012.05.013>

Yi-Ling, H., Hai-Zhen, M., Guang-Tao, D., and Jun, S. (2014). Influences of Urban Temperature on the Electricity Consumption of Shanghai. *Advances in Climate*

Change Research, 5(2), 74–80. <https://doi.org/10.3724/sp.j.1248.2014.074>

You, Q., Kang, S., Aguilar, E., Pepin, N., Flugel, W. A., Yan, Y., Xu Y., Zhang Y., and Huang, J. (2011). Changes in daily climate extremes in China and their connection to the large scale atmospheric circulation during 1961-2003. *Climate Dynamics*, 36(11–12), 2399–2417. <https://doi.org/10.1007/s00382-009-0735-0>

Zhang, J., Yang, X., Shen, F., Li, Y., Xiao, H., and Qi, H. (2012). *Energy Procedia Principal Component Analysis of Electricity Consumption Factors in China*. <https://doi.org/10.1016/j.egypro.2012.01.292>

Zhou, Y., Clarke, L., Eom, J., Kyle, P., Patel, P., Kim, S. H., Dirks J., Jensen E., Liu Y., Rice J., Schmidt L., and Seiple, T. (2014). Modeling the effect of climate change on U.S. state-level buildings energy demands in an integrated assessment framework. *Applied Energy*, 113, 1077–1088. <https://doi.org/10.1016/j.apenergy.2013.08.034>

Zhou, Y., Eom, J., and Clarke, L. (2013). The effect of global climate change, population distribution, and climate mitigation on building energy use in the U.S. and China. *Climatic Change*, 119(3–4), 979–992. <https://doi.org/10.1007/s10584-013-0772-x>

APPENDICES

PUBLICATIONS FROM THE THESIS

Titles	Status
1- Wavelet Analysis of Daily Energy Demand and Weather Variables Journal of Energy, Hindawi https://doi.org/10.1155/2019/4974107	Published
2- Potential impacts of Global Warming on Electricity Demand in Niger Rev Theoretical and Applied Climatology, Springer Manuscript Number: TAAC-D-19-00154	Under Rev
3- Influence of Climate variables on electricity demand in Niamey Journal of Energy, Elsevier Manuscript Number: EGY-D-19-06705	Under Rev